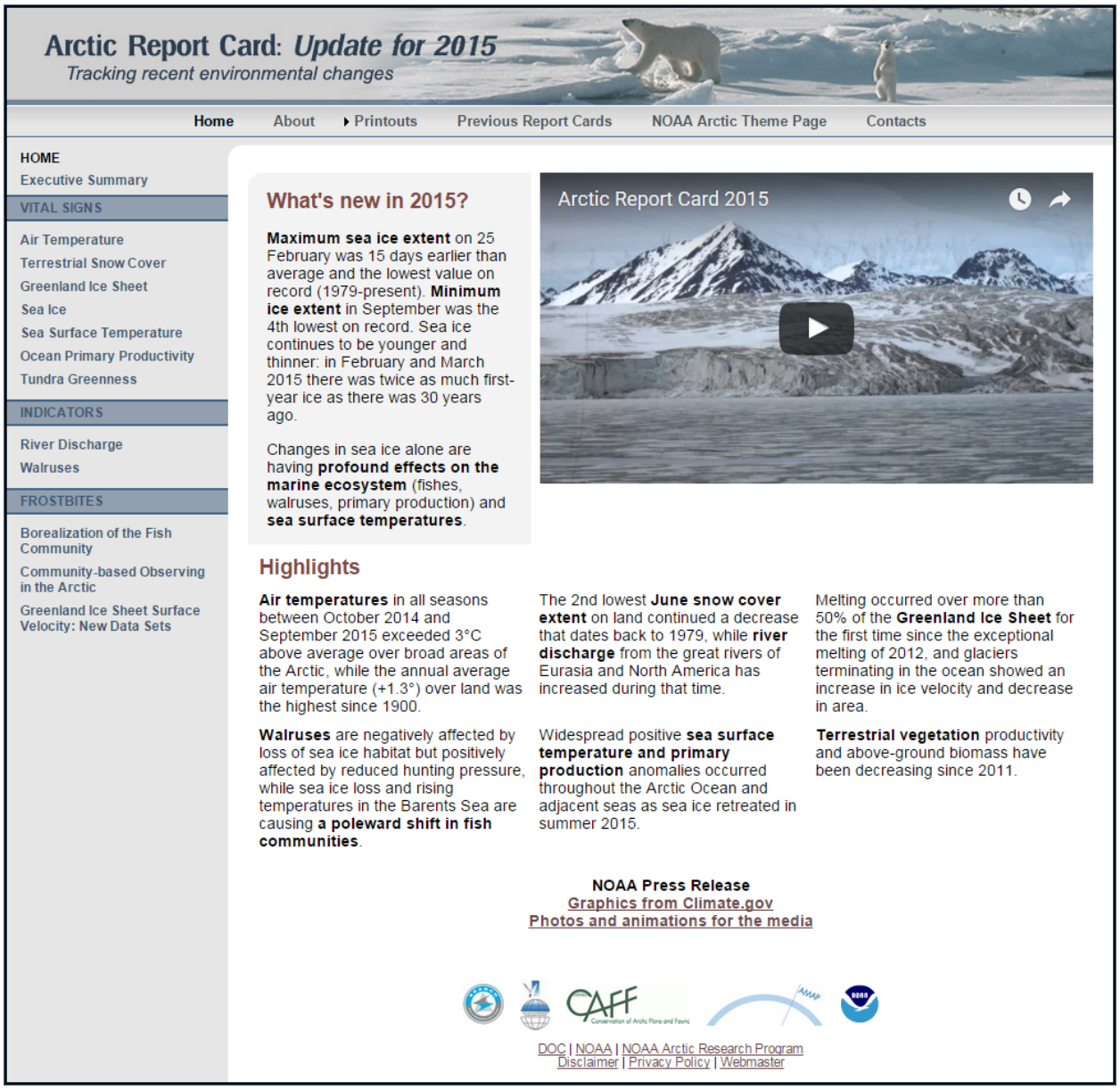

December 2015

www.arctic.noaa.gov/reportcard

Citing the complete report:
M. O. Jeffries, J. Richter-Menge, and J. E. Overland, Eds., 2015: Arctic Report Card 2015, http://www.arctic.noaa.gov/reportcard.

Citing an essay (for example):
Derksen, C., R. Brown, L. Mudryk, and K. Luojus, 2015: Snow [in Arctic Report Card 2015], http://www.arctic.noaa.gov/reportcard.

Table of Contents

Authors and Affiliations

L. Alessa, Center for Resilient Communities, University of Idaho, Moscow, ID, USA; International Arctic Research Center, University of Alaska Fairbanks, Fairbanks, AK, USA; Department of Homeland Security Arctic Domain Awareness Center, Anchorage, AK, USA

M. M. Aschan, UiT, The Arctic University of Norway, Tromsø, Norway

D. Atkinson, University of Victoria, Department of Geography, Victoria, BC, Canada

U. S. Bhatt, Geophysical Institute, University of Alaska Fairbanks, Fairbanks, AK, USA

P. A. Bieniek, Geophysical Institute, University of Alaska Fairbanks, Fairbanks, AK, USA

N. T. Boelman, Lamont-Doherty Earth Observatory, Columbia University, Palisades, NY, USA

J. E. Box, Geological Survey of Denmark and Greenland, Copenhagen, Denmark

R. Brown, Climate Research Division, Environment Canada, Toronto, Canada

J. Cappelen, Danish Meteorological Institute, Copenhagen, Denmark

J. C. Comiso, Cryospheric Sciences Laboratory, NASA Goddard Space Flight Center, Greenbelt, MD, USA

L. W. Cooper, Chesapeake Biological Laboratory, University of Maryland Center for Environmental Science, Solomons, MD, USA

C. Derksen, Climate Research Division, Environment Canada, Toronto, Canada

A. V. Dolgov, Knipovich Polar Research Institute of Marine Fisheries and Oceanography, Murmansk, Russia

H. E. Epstein, Department of Environmental Sciences, University of Virginia, Charlottesville, VA, USA

S. Farrell, NOAA Earth System Science Interdisciplinary Center, University of Maryland, College Park, MD, USA

R. S. Fausto, Geological Survey of Denmark and Greenland, Copenhagen, Denmark

X. Fettweis, University of Liege, Liege, Belgium

B. C. Forbes, Arctic Centre, University of Lapland, Rovaniemi, Finland

D. Forbes, Geological Survey of Canada, Natural Resources Canada, Dartmouth, NS, Canada

M. Fossheim, Institute of Marine Research, Norway

K. E. Frey, Graduate School of Geography, Clark University, Worcester, Massachusetts, USA

S. Gerland, Norwegian Polar Institute, Fram Centre, Tromsø, Norway

R. R. Gradinger, Institute of Marine Research, Tromsø, Norway

J. M. Grebmeier, Chesapeake Biological Laboratory, University of Maryland Center for Environmental Science, Solomons, MD, USA

D. Griffith, Center for Resilient Communities, University of Idaho, Moscow, ID, USA

E. Hanna, Department of Geography, University of Sheffield, Sheffield, UK

K. Hansen, Danish Meteorological Institute, Copenhagen, Denmark

I. Hanssen-Bauer, Norwegian Meteorological Institute, Blindern, 0313 Oslo, Norway

S. Hendricks, Alfred Wegener Institute, Bremerhaven, Germany

R. M. Holmes, Woods Hole Research Center, Falmouth, MA, USA

R. B. Ingvaldsen, Institute of Marine Research, Norway

M. O. Jeffries, Office of Naval Research, Arlington, VA, USA

E. Johannesen, Institute of Marine Research, Norway

I. Joughin, Polar Science Center, Applied Physics Laboratory, University of Washington, Seattle, WA, USA

S. -J. Kim, Korea Polar Research Institute, Incheon, Republic of Korea

A. Kliskey, Center for Resilient Communities, University of Idaho, Moscow, ID, USA; International Arctic Research Center, University of Alaska Fairbanks, Fairbanks, AK, USA

K. M. Kovacs, Norwegian Polar Institute, Tromsø, Norway

P. Lemons, U.S. Fish and Wildlife Service, Anchorage, AK, USA

K. Luojus, Arctic Research Centre, Finnish Meteorological Institute, Helsinki, Finland

C. Lydersen, Norwegian Polar Institute, Tromsø, Norway

J. G. MacCracken, U.S. Fish and Wildlife Service, Anchorage, AK, USA

M. Macias-Fauria, School of Geography and the Environment, University Oxford, Oxford, UK

J. W. McClelland, University of Texas at Austin, Marine Science Institute, Port Aransas, TX, USA

W. Meier, NASA Goddard Space Flight Center, Greenbelt, MD, USA

T. Moon, Department of Geological Sciences, University of Oregon, Eugene, OR, USA

T. Mote, Department of Geography, University of Georgia, Athens, Georgia, USA

L. Mudryk, Department of Physics, University of Toronto, Canada

T. Mustonen, Snowchange Cooperative, Selkie, Finland

I. H. Myers-Smith, School of GeoSciences, University of Edinburgh, Edinburgh, UK

J. E. Overland, National Oceanic and Atmospheric Administration, Pacific Marine Environmental Laboratory, Seattle, WA, USA

D. Perovich, ERDC - CRREL, 72 Lyme Road, Hanover USA; Thayer School of Engineering, Dartmouth College, Hanover, NH, USA

J. Pinzon, Biospheric Science Branch, NASA Goddard Space Flight Center, Greenbelt, MD, USA

R. Primicerio, UiT, The Arctic University of Norway, Tromsø, Norway

A. Proshutinsky, Woods Hole Oceanographic Institution, Woods Hole, MA, USA

P. Pulsifer, National Snow and Ice Data Center, University of Colorado Boulder, Boulder, CO, USA

M. K. Raynolds, Institute of Arctic Biology, University of Alaska Fairbanks, Fairbanks, AK, USA

J. Richter-Menge, U.S. Army Corps of Engineers, Cold Regions Research and Engineering Laboratory, Hanover, NH, USA

A. I. Shiklomanov, University of New Hampshire, Durham, NH, USA; Shirshov Institute of Oceanology, Moscow, Russia

C. J. P. P. Smeets, Institute for Marine and Atmospheric Research Utrecht, Utrecht University, Utrecht, The Netherlands

S. K. Sweet, Lamont-Doherty Earth Observatory, Columbia University, Palisades, NY, USA

S. E. Tank, University of Alberta, Edmonton, AB, Canada

M. Tedesco, The City College of New York, New York, NY, USA; Lamont Doherty Earth Observatory of Columbia University, Palisades, NY, USA

R. L. Thoman, NOAA, National Weather Service, Fairbanks, AK, USA

M. -L. Timmermans, Yale University, New Haven, CT, USA

J. -É. Tremblay, Québec-Océan and Takuvik, Biology Department, Université Laval, Québec City, QC, Canada

M. Tretiakov, Arctic and Antarctic Research Institute, St. Petersburg, Russia

M. Tschudi, Aerospace Engineering Sciences, University of Colorado, Boulder, CO, USA

C. J. Tucker, Biospheric Science Branch, NASA Goddard Space Flight Center, Greenbelt, MD, USA

D. van As, Geological Survey of Denmark and Greenland, Copenhagen, Denmark

R. S. W. van de Wal, Institute for Marine and Atmospheric Research Utrecht, Utrecht University, Utrecht, The Netherlands

J. Wahr, Department of Physics & Cooperative Institute for Research in Environmental Sciences, University of Colorado, Boulder, CO, USA

D. A. Walker, Institute of Arctic Biology, University of Alaska Fairbanks, Fairbanks, AK, USA

J. E. Walsh, International Arctic Research Center, University of Alaska Fairbanks, Fairbanks, AK, USA

M. Wang, Joint Institute for the Study of the Atmosphere and Ocean, University of Washington, Seattle, WA, USA

Executive Summary

M. O. Jeffries[1], J. Richter-Menge[2], J. E. Overland[3]

[1]Office of Naval Research, Arlington, VA, USA
[2]U.S. Army Corps of Engineers, Cold Regions Research and Engineering Laboratory, Hanover, NH, USA
[3]National Oceanic and Atmospheric Administration, Pacific Marine Environmental Laboratory, Seattle, WA, USA

December 7, 2015

The Arctic Report Card (www.arctic.noaa.gov/reportcard/) considers a range of environmental observations throughout the Arctic, and is updated annually. As in previous years, the 2015 update to the Arctic Report Card highlights the changes that continue to occur in both the physical and biological components of the Arctic environmental system.

The average annual surface air temperature anomaly (+1.3°C relative to the 1981-2010 baseline) over land north of 60°N between October 2014 and September 2015 was the highest in the observational record beginning in 1900. This represents a 2.9°C increase since the beginning of the 20th Century. Average air temperature anomalies in all seasons between October 2014 and September 2015 were generally positive throughout the Arctic, with extensive regions exceeding +3°C relative to the 1981-2010 baseline. Strong connections between the Arctic and mid-latitude regions occurred (1) from November 2014 through June 2015, causing anomalously warm conditions in the Pacific Arctic region due to southerly air flow into and across Alaska, and (2) from February through April 2015, causing anomalously cold conditions from north-eastern North America to southwest Greenland due to northerly air flow.

In 2014, the most recent year with a complete data set, the combined discharge of the eight largest Arctic rivers (2487 km^3 from the Pechora, S. Dvina, Ob', Yenisey, Lena, Kolyma [Eurasia], Yukon and Mackenzie [North America]) was 10% greater than the average discharge during 1980-1989. Since 1976, discharge of the Eurasian and North American rivers has increased 3.1% and 2.6% per decade, respectively. For the first seven months of 2015, the combined discharge for the six largest Eurasian Arctic rivers shows that peak discharge was 10% greater and five days earlier than the 1980-1989 average for those months.

Arctic snow cover extent (SCE, for land areas north of 60°N) anomalies in May and June 2015 were below the long-term average for 1981-2010, a continuation of consistent early spring snow melt during the past decade. June SCE in both the North American and Eurasian sectors of the Arctic was the 2nd lowest in the satellite record (1967-present). The rate of June SCE reductions since 1979 (the start of the passive microwave satellite era) is 18% per decade. Since 2011, the rate of June snow cover loss has exceeded the rate of September sea ice loss (-13.4% per decade).

Minimum sea ice extent in September 2015 was 29% less than the average for 1981-2010 and the fourth lowest value in the satellite record (1979-2015). Earlier in the year, the lowest ever maximum ice extent in the satellite record was 7% less than the average for 1981-2010. Occurring on 25 February, it was also the second earliest in the record and 15 days earlier than average (12 March). In February and March 2015, the oldest ice (>4 years) and first-year ice made up 3% and 70%, respectively of the pack ice compared to values of 20% and 35%, respectively, in 1985.

Sea ice retreat is believed to be the most pervasive threat to ice-associated marine mammals, including walruses. In the Pacific Arctic, vast walrus herds are now hauling out on land rather than on sea ice as it retreats far to the north over the deep Arctic Ocean. This is raising concern about the energetics of females and young animals that must now make feeding trips from coastal haul-outs to areas of high prey abundance (180 km one-way), rather than utilizing nearby ice edges as they did in the past. Walrus populations are also affected by hunting. In the case of Svalbard in the Atlantic Arctic, a hunting ban from 1952 to 2012 allowed the walrus population to recover even as ocean and air temperatures increased and sea ice and walrus carrying capacity declined.

As sea ice retreat becomes more extensive in summer and previously ice-covered water is exposed to more solar radiation, sea surface temperature (SST) and upper ocean temperatures are increasing throughout much of the Arctic Ocean and adjacent seas. The Chukchi Sea northwest of Alaska and eastern Baffin Bay off west Greenland have the largest warming trends: ~0.5°C per decade since 1982. In August 2015, SST was up to 4°C higher than the 1982-2010 average in eastern Baffin Bay and the Kara Sea north of central Eurasia.

Increasing ocean primary productivity (conversion of CO_2 to organic material) is being observed as summer sea ice extent declines. In 2015, there were widespread positive primary productivity anomalies throughout the Arctic Ocean and adjacent ice-affected seas, from 0.7% to 21% above the 2003-2014 average in Hudson Bay and the Barents Sea, respectively. For the period 2003-2015 there are statistically significant primary productivity trends in the eastern (Eurasian) Arctic, Barents Sea, Greenland Sea, and North Atlantic; the steepest trends are in the eastern Arctic (19.26 g C/m^2/yr/dec, a 41.9% increase) and the Barents Sea (17.98 g C/m^2/yr/dec, a 30.2% increase).

On land, satellite observations since 1982 of peak tundra greenness, a measure of vegetation productivity and strongly correlated with above-ground biomass, show a consistent decline since 2011. In 2014, the most recent year with a complete data set, maximum greenness (MaxNDVI) in the Eurasian Arctic and for the Arctic as a whole was below the 1982-2014 average, while greenness over the entire growing season (TI-NDVI) had the lowest value in the Eurasian record and the second lowest in the North American record. For the entire period of record (1982-2014), linear trends in MaxNDVI continue to show general circumpolar increases in tundra greenness. However, since 1982 the tundra in northwestern Russia, the Yukon Delta region of western Alaska, and the far northern Canadian Arctic Archipelago has become less green (also referred to as "browning"). Linear trends in TI-NDVI for 1982-2014 also show "browning" in these regions.

Ice on land, as represented by the Greenland Ice Sheet, experienced extensive melting again in 2015; melting occurred over more than 50% of the ice sheet for the first time since the exceptional melting of 2012 and exceeded the 1981-2010 average on 50 of 92 days (54%). Melt season duration was as much as 30-40 days longer than average in western, northwestern and northeastern Greenland, but close to or below average elsewhere on the ice sheet. Average albedo in 2015 was below the 2000-2009 average in northwest Greenland and above average in southwest Greenland. Ice mass loss of 186 Gt over the entire ice sheet between April 2014 and April 2015 was 22% below the average mass loss of 238 Gt for 2002-2015, but was 6.4 times higher than the 29 Gt loss of the preceding 2013-2014 season. Between the end of the 2014 melt season and the end of the 2015 melt season, 22 of the 45 widest and fastest-flowing marine-terminating glaciers had retreated, but the advance of 9 relatively wide glaciers resulted in a low annual net area loss of 16.5 km^2. This is the lowest annual net area loss in the 16-year

period of observations (1999-2015) and 7.7 times lower than the annual average area change trend of -127 km^2.

In summary, there are many signals indicating that environmental system components throughout the Arctic continue to be influenced by long-term upward trends in air temperature, modulated by natural variability in regional and seasonal anomalies.

Editors' Acknowledgments

Financial support for the Arctic Report Card is provided by the Arctic Research Program in the NOAA Climate Program Office, and in-kind support is provided by the Office of Naval Research. We thank our respective organizations - the Office of Naval Research, the U.S. Army Corps of Engineers - Cold Regions Research and Engineering Laboratory, and the NOAA Pacific Marine Environmental Laboratory - for their continued support, and the Editorial Advisory Board for its advice and assistance with identifying topics and authors for Indicators and Frostbites essays. The 12 contributions to Arctic Report Card 2015 represent the collective effort of an international team of 72 researchers in 11 countries. Independent peer-review of Arctic Report Card 2015 was facilitated by the Arctic Monitoring and Assessment Program (AMAP) of the Arctic Council.

Surface Air Temperature

J. Overland[1], E. Hanna[2], I. Hanssen-Bauer[3], S. -J. Kim[4], J. E. Walsh[5], M. Wang[6], U. S. Bhatt[7], R. L. Thoman[8]

[1]NOAA/PMEL, Seattle, WA, USA
[2]Department of Geography, University of Sheffield, Sheffield, UK
[3]Norwegian Meteorological Institute, Blindern, 0313 Oslo, Norway
[4]Korea Polar Research Institute, Incheon, Republic of Korea
[5]International Arctic Research Center, University of Alaska Fairbanks, Fairbanks, AK, USA
[6]Joint Institute for the Study of the Atmosphere and Ocean, University of Washington, Seattle, WA, USA
[7]Geophysical Institute, University of Alaska Fairbanks, Fairbanks, AK, USA
[8]NOAA, National Weather Service, Fairbanks, AK, USA

November 17, 2015

Highlights

- Average annual surface air temperature anomaly (+1.3°C) over land north of 60°N for October 2014-September 2015 was the highest in the observational record beginning in 1900; this represents a 2.9°C increase since the beginning of the 20th Century.
- Average air temperature anomalies in all seasons between October 2014 and September 2015 were generally positive throughout the Arctic, with extensive regions exceeding +3°C relative to a 1981-2010 baseline.
- Anomalously warm conditions from November 2014 through June 2015 in Alaska were caused by weather patterns that advected warm mid-latitude air northward from the northeast Pacific Ocean. Anomalously warm Arctic conditions during spring (April, May, June) 2015 across central Eurasia were also due to southerly winds.
- Strong connections between the Arctic and the mid-latitudes were also seen in late winter-early spring (February-April) 2015, when cold air advected south-eastward from the central Arctic resulted in major negative temperature anomalies over eastern North America.

Arctic air temperatures are both an indicator and a driver of regional and global changes. Although there are year-to-year and regional differences in air temperatures due to natural random variability, the magnitude and Arctic-wide character of the long-term temperature increase is a major indicator of global warming (Overland 2009). Here we report on the spatial and temporal variability of Arctic air temperatures during the period October 2014 through September 2015, the 12-month period since the end of the previous reporting period (Overland et al. 2014).

Mean Annual Land Surface Temperature

The mean annual surface air temperature anomaly (+1.3°C relative to the 1981-2010 mean value) for October 2014-September 2015 for land stations north of 60°N is the highest value in the record starting in 1900 (**Fig. 1.1**). This is an increase of 2.3°C since the 1970s and 2.9°C since the beginning of the 20th century. The global rate of temperature increase has slowed in the last decade (Kosaka and Xie 2013), but Arctic air temperatures have continued to increase. Currently, the Arctic is warming at more than twice the rate of lower latitudes (**Fig. 1.1**).

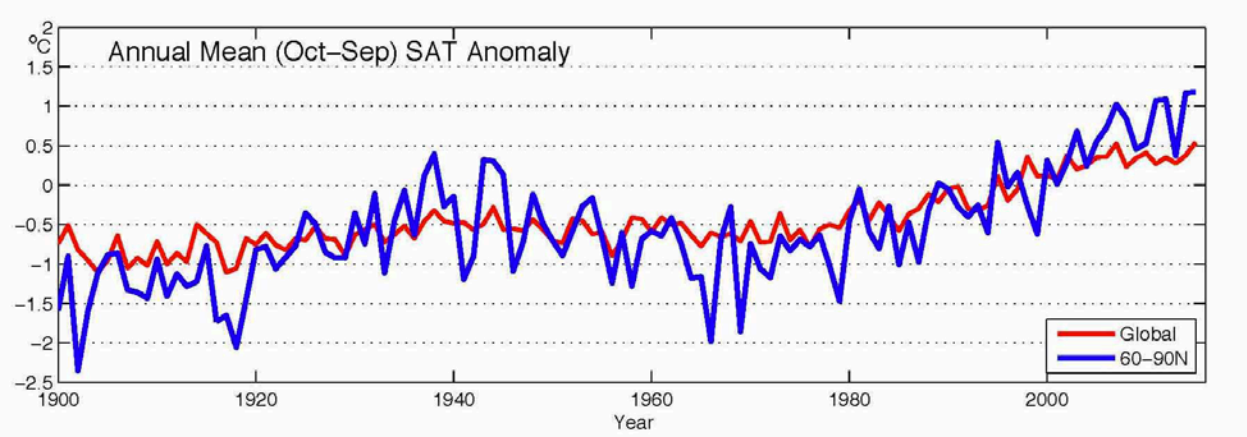

Fig. 1.1. Arctic (land stations north of 60°N) and global mean annual land surface air temperature (SAT) anomalies (in °C) for the period 1900-2015 relative to the 1981-2010 mean value. Note that there were few stations in the Arctic, particularly in northern Canada, before 1940. The data are from the CRUTEM4 dataset, which is available at www.cru.uea.ac.uk/cru/data/temperature/.

The greater rate of Arctic temperature increase than the global increase is referred to as Arctic Amplification. Mechanisms for Arctic Amplification include: reduced summer albedo due to sea ice and snow cover loss; the decrease of total cloudiness in summer and increase in winter; the additional heat generated by newly sea-ice free ocean areas that are maintained later into the autumn; and the lower rate of heat loss to space in the Arctic relative to the sub-tropics due to lowered mean temperatures (Serreze and Barry 2011; Makshtas et al. 2011; Pithan and Mauritsen 2014).

Seasonal Surface Air Temperature Variation

Seasonal air temperature variations are divided into autumn 2014 (October, November, December [OND]), and winter (January, February, March [JFM]), spring (April, May, June [AMJ]) and summer (July, August, September [JAS]) of 2015. All seasons show extensive positive temperature anomalies across the central Arctic with many regional seasonal temperature anomalies greater than +3°C, relative to a 1981-2010 baseline (**Fig. 1.2**).

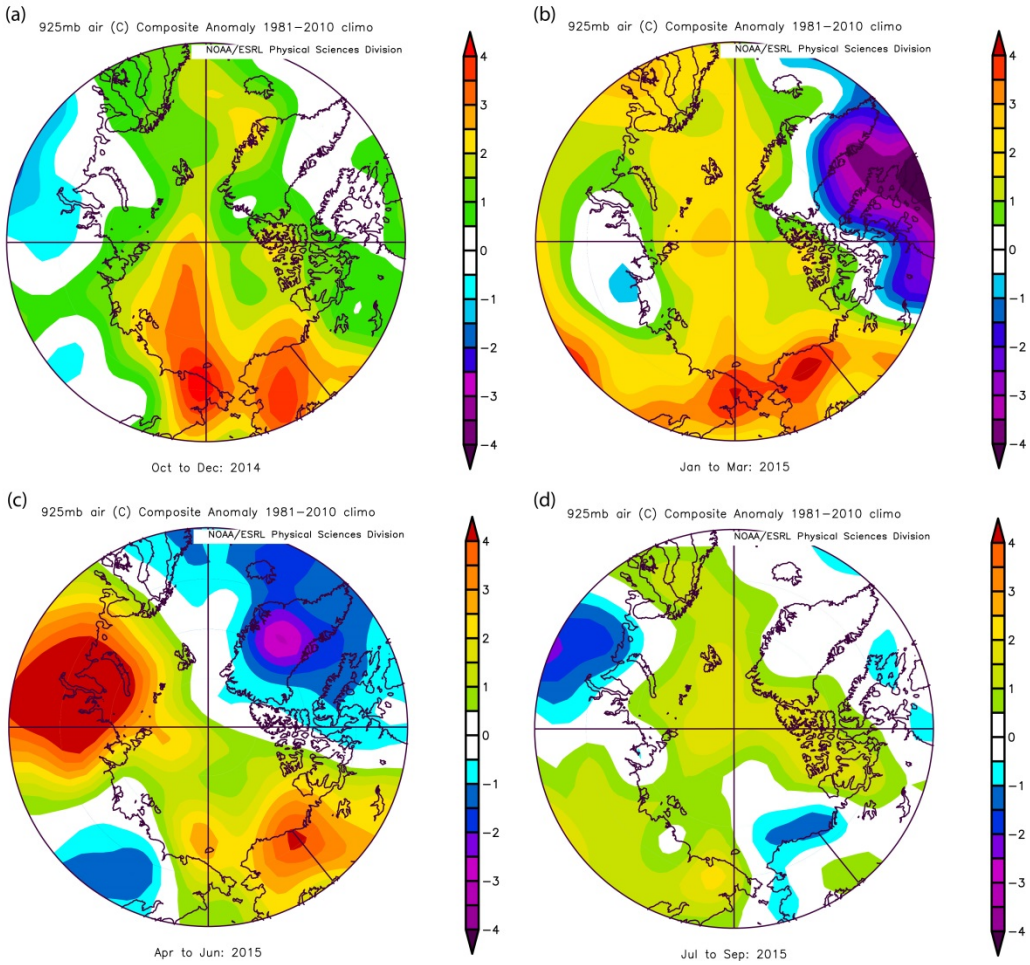

Fig. 1.2. Seasonal anomaly patterns for near surface air temperatures (in °C) relative to the baseline period 1981-2010 in (a, top left) autumn 2014, (b, top right) winter 2015, (c, bottom left) spring 2015 and (d, bottom right) summer 2015. Temperatures are from slightly above the surface layer (at 925 mb level) to emphasize large spatial patterns rather than local features. Data for this and the following figures are from NOAA/ESRL, Boulder, CO, at http://www.esrl.noaa.gov/psd/.

Autumn 2014 (OND). A broad swath of warm temperature anomalies stretched across the Arctic, extending from the Pacific to the Atlantic sectors (**Fig. 1.2a**). The warmest temperature anomalies, centered on Alaska and far eastern Siberia, were due to advection of warm air from the south (for more information, see the section below on *Arctic and Mid-latitudes Connections*).

Winter 2015 (JFM). As in fall 2014 (**Fig. 1.2a**), warm temperature anomalies continued to extend across the Arctic, from the Pacific sector to the Atlantic sector. The warmest temperature anomalies, again, were centered on Alaska and far eastern Siberia, including the Chukchi and East Siberian seas (**Fig. 1.2b**). In Svalbard, in the Atlantic sector northeast of Greenland, winter temperatures were typically 3-4°C above the 1981-2010 average. In contrast, a cold temperature anomaly of minus 2-3°C extended from southwest Greenland to eastern Canada (**Fig. 1.2b**), and into the eastern United States. Temperature anomalies for coastal Greenland locations are summarized in **Table 3.1** in the essay on the *Greenland Ice Sheet* (Tedesco et al. 2015). The Svalbard and Greenland/eastern Canada warm and cold anomalies, respectively, are described further in the section below on *Arctic and Mid-latitudes Connections*.

Although there is an Arctic-wide long-term pattern of temperature increases, regional differences can be manifest in any given season based on random variability of the atmospheric circulation. Such a contrast is seen between the high temperature anomalies over the Chukchi and East Siberian seas with the substantial cold anomalies over eastern North America (Overland et al. 2011; Kug et al. 2015).

Spring 2015 (AMJ). A broad swath of warm temperature anomalies continued to stretch across the Arctic, with a continuing warm anomaly over Alaska (**Fig. 1c**). However, unlike the fall 2014 and winter 2015 patterns (**Figs. 1.2a** and **1.2b**), the spring pattern saw a shift to a very warm anomaly (+4°C) over central Eurasia (**Fig. 1.2c**), where there were strongly negative snow cover extent anomalies (see the essay on *Terrestrial Snow Cover*). In contrast, a significant cold anomaly (-3°C) was centered over Greenland (**Fig. 1.2c**). In contrast to Greenland, spring temperatures in Svalbard were typically 2-2.5°C above the 1981-2010 average, as Svalbard was located on the margin of the broad swath of positive temperature anomalies that extended from Alaska to Eurasia (**Fig. 1.2c**).

Summer 2015 (JAS). A warm temperature anomaly over much of the Arctic Ocean, with the exception of a moderately cold anomaly over the Beaufort Sea north of Alaska, characterized summer 2015 (**Fig. 1.2d**). Particularly cold anomalies occurred over western Eurasia. As noted in the essay on the *Greenland Ice Sheet*, a new record August low temperature of -39.6°C occurred on August 28 at Summit (elevation 3,216 m in the centre of the ice sheet), while summer temperatures at most coastal locations were above average (Tedesco et al. 2015). The role of atmospheric circulation associated with a negative North Atlantic Oscillation on Greenland air temperatures and ice sheet melting is described in the essay on the *Greenland Ice Sheet*. Similar to coastal Greenland locations, in Svalbard the average summer 2015 temperature was 1-2°C above the 1981-2010 average, and was the highest ever recorded in the composite Longyearbyen-Svalbard Airport record that dates back to 1898 (Nordli et al. 2014).

Arctic and Mid-latitudes Connections

As noted in the previous section, Alaska was anomalously warm in fall 2014, and winter and spring 2015 (**Figs. 1.2a**, **1.2b** and **1.2c**). The persistent positive near surface air temperature anomalies in Alaska and extending into the Chukchi and Beaufort seas were associated with warm sea surface temperatures in the Gulf of Alaska and a pattern of geopotential height anomalies characterized by higher values along the Pacific coast of northwestern North America and lower values further offshore (**Fig. 1.3**). Winds follow the contours of geopotential heights clockwise around high values. Consequently, warm air over the northeast Pacific Ocean was advected into and across Alaska. Associated with the southerly winds, a downslope component of the wind on the north side of the Alaska Range and into Interior Alaska caused dry conditions and reinforced high temperatures. The warm and dry conditions in Interior Alaska during May and June contributed to the second worst fire season on record for those months, eclipsed only by 2004.

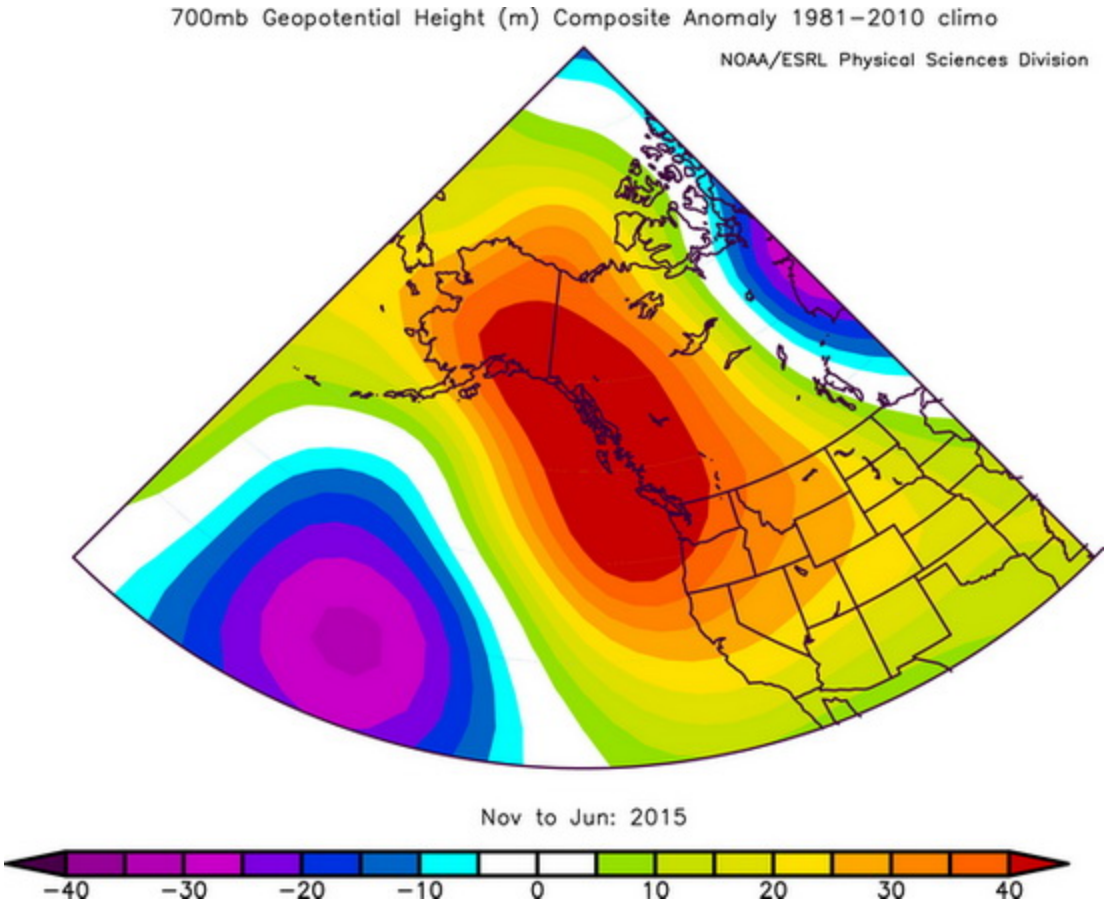

Fig. 1.3. Geopotential height (700 mb) anomalies from November 2014 to June 2015 over western North America and the eastern Pacific Ocean.

In contrast to the warm temperature anomaly in winter in Alaska (**Fig. 1.2c**) due to warm, southerly air flow (**Fig. 1.3**), the cold anomaly extending from eastern Canada to southwest Greenland (**Fig. 1b**) was caused by strong northerly air flow. This cold anomaly extended in to early spring. The cause of these relatively cold temperatures is illustrated by the winter (JFM) geopotential height field anomaly pattern (**Fig. 1.4**), which shows high values over northwestern North America and low values over eastern North America, Greenland and across the central Arctic Ocean to central Eurasia. As wind flows clockwise and counter-clockwise around high and low height centers, respectively, northerly winds on the west side of the trough between the two centers channeled cold air southward from the source region in the central Arctic into northeastern North America. This geopotential height anomaly pattern also explains the above average winter air temperatures in Svalbard due to warm air advection across western Eurasia and into the central Arctic Ocean (**Figs. 1.2b** and **1.2c**).

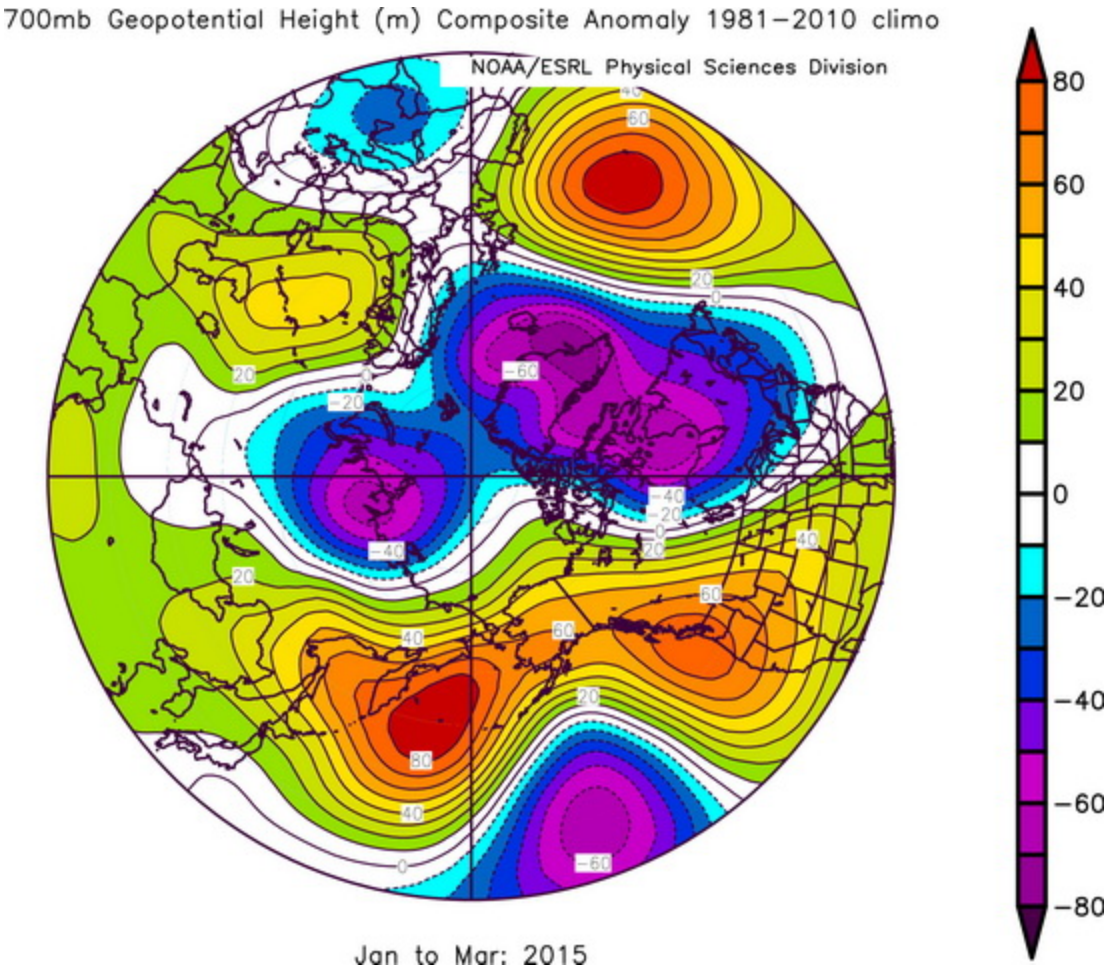

Fig. 1.4. Large geopotential height anomalies occurred over western and eastern North America and continued into the North Atlantic sector in winter 2015.

References

Kosaka, Y., and S.-P. Xie, 2013: Recent global-warming hiatus tied to equatorial Pacific surface cooling. *Nature*, 501, 403-407.

Kug, J.-S., J.-H. Jeong, Y.-S. Jang, B.-M. Kim, C. K. Folland, S.-K. Min, and S.-W. Son, 2015: Two distinct influences of Arctic warming on cold winters over North America and East Asia. *Nature Geoscience*, 8, DOI:10.1038/NGEO2517.

Makshtas A. P., I. I. Bolshakova, R. M. Gun, O. L. Jukova, N. E. Ivanov, and S. V. Shutilin, 2011: Climate of the Hydrometeorological Observatory Tiksi region. In *Meteorological and Geophysical Investigations*. Paulsen, 2011, 49-74.

Nordli, Ö, R. Przybylak, A. E. J. Ogilvie, and K. Isaksen, 2014: Long-term temperature trends and variability on Spitsbergen: the extended Svalbard Airport temperature series, 1898-2012. *Polar Res.*, 33, 21349.

Overland, J. E., 2009: The case for global warming in the Arctic. In *Influence of Climate Change on the Changing Arctic and Sub-Arctic Conditions*, J. C. J. Nihoul and A. G. Kostianoy (eds.), Springer, 13-23.

Overland, J. E., K. R. Wood, and M. Wang, 2011: Warm Arctic-cold continents: Impacts of the newly open Arctic Sea. *Polar Res.*, 30, 15787, doi: 10.3402/polar.v30i0.15787.

Overland, J. E., E. Hanna, I. Hanssen-Bauer, B.-M. Kim, S.-J. Kim, J. Walsh, M. Wang, and U. Bhatt, 2014: Air Temperature. In *Arctic Report Card: Update for 2014*, http://www.arctic.noaa.gov/report14/air_temperature.html.

Pithan, F. and T. Mauritsen, 2014: Arctic amplification dominated by temperature feedbacks in contemporary climate models. *Nature Geoscience*, doi: 10.1038/ngeo2071.

Serreze, M., and R. Barry, 2011: Processes and impacts of Arctic amplification: A research synthesis. *Global and Planetary Change*, 77, 85-96.

Tedesco, M., J. E. Box, J. Cappelen, R. S. Fausto, X. Fettweis, T. Mote, C. J. P. P. Smeets, D. van As, R. S. W. van de Wal, and J. Wahr, 2015: Greenland Ice Sheet. In *Arctic Report Card: Update for 2015*, www.arctic.noaa.gov/report15/greenland_ice_sheet.html.

Terrestrial Snow Cover

C. Derksen[1], R. Brown[1], L. Mudryk[2], K. Luojus[3]

[1]Climate Research Division, Environment Canada, Toronto, Canada
[2]Department of Physics, University of Toronto, Canada
[3]Arctic Research Centre, Finnish Meteorological Institute, Helsinki, Finland

November 17, 2015

Highlights

- Arctic SCE anomalies in May and June 2015 (for land areas north of 60°N) were below the long-term average (1981-2010), a continuation of consistent early spring snow melt during the past decade. June SCE in both the North American and Eurasian sectors of the Arctic was the 2nd lowest in the satellite record (1967-present).
- For the fifth time in the past six years (2009-2015), total Arctic SCE in June was below 3 million km^2, despite never falling below this threshold in the previous 43 years of the snow chart data record (1967-2008).
- The rate of June SCE reductions since 1979 (the start of the passive microwave satellite era used to monitor sea ice extent) is -17.2% per decade. Since 2011, the rate of June snow cover loss has exceeded the rate of September sea ice loss.

The Arctic (land areas north of 60°N) is always completely snow covered in winter, so it is the transition seasons of fall and spring that are significant when characterizing variability and change. The timing of spring snow melt is particularly important because the transition from highly reflective snow cover to the low albedo of snow-free ground is coupled with increasing solar radiation during the lengthening days of the high latitude spring. Strong snow-atmosphere feedbacks (including the well documented snow-albedo feedback), the energy sink induced by melting snow, and the strong thermal insulation effect of snow on the underlying soil all highlight the important role of variability and trends in Arctic snow cover extent (SCE) on the climate system and terrestrial ecosystems.

SCE anomalies (relative to the 1981-2010 reference period) for the 2015 Arctic spring (April, May, June) 2015 were computed separately for the North American and Eurasian sectors of the Arctic from the NOAA snow chart climate data record, maintained at Rutgers University (Estilow et al. 2015; http://climate.rutgers.edu/snowcover/). Consistent with nearly all spring seasons of the past decade, both May and June SCE anomalies were strongly negative in 2015 (**Fig. 2.1**); June SCE in both the North American and Eurasian sectors of the Arctic was the 2nd lowest in the snow chart record, which extends back to 1967.

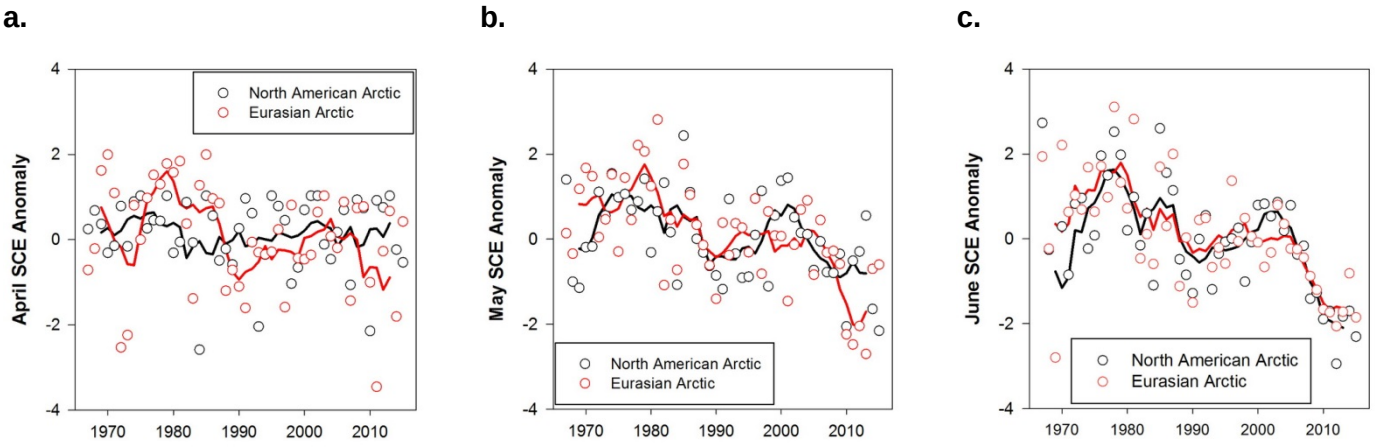

Fig. 2.1. Monthly snow cover extent (SCE) for Arctic land areas (>60°N) from the NOAA snow chart CDR for (a, left) April (b, center) May and (c, right) June from 1967 to 2015. Anomalies are relative to the average for 1981-2010 and standardized (each observation differenced from the mean and divided by the standard deviation and thus unitless). Solid black and red lines depict 5-year running means for North America and Eurasia, respectively.

There are complex interactions between regional variability in the onset of snow cover in the autumn, subsequent winter season snow accumulation patterns (which themselves are driven by the complex interplay of temperature and precipitation anomalies) and the continental scale spring SCE anomalies (**Fig. 2.1**). Snow cover duration (SCD) departures derived from the NOAA daily Interactive Multisensor Snow and Ice Mapping System (IMS) snow cover product (Helfrich et al. 2007) show earlier snow cover onset in the fall over much of the Arctic, for the 2014-2015 snow year (**Fig. 2.2a**). This is consistent with pre-melt snow depth anomalies (derived from the Canadian Meteorological Centre daily gridded global snow depth analysis; Brasnett 1999), which were largely positive over much of the Arctic land surface (+25.1% and +33.7%, respectively, for the North American and Eurasian sectors of the Arctic) (**Fig. 2.3b**). There was a notable east-west snow depth gradient across Eurasia with above average snow depth in eastern Siberia and below average snow depth across western Siberia and northern Europe. The North American Arctic was characterized by a more latitudinal gradient of deeper than normal snow depth north of the boreal tree line and shallower than normal snow depth across the boreal forest (**Figs. 2.3a** and **2.3b**). Note that the CMC results shown in **Fig. 3** mask out anomalies over high elevation areas (in the Canadian Arctic Archipelago, Baffin Island, coastal Alaska) known to be affected by an internal trend of higher winter snow depths since 2006 due to changes in the resolution of the precipitation forcing used as part of the CMC analysis.

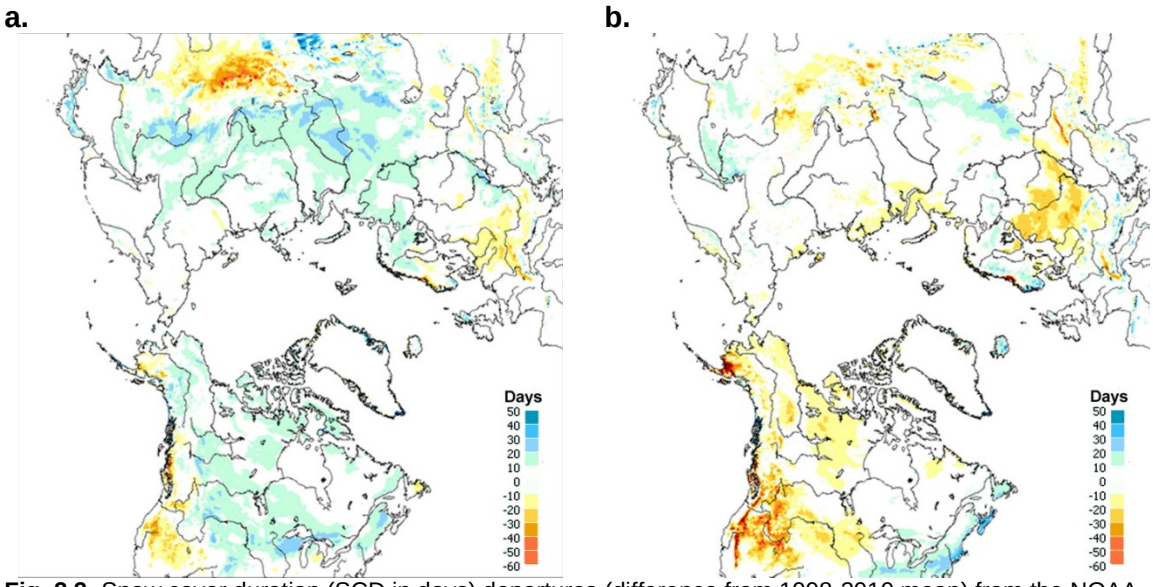

Fig. 2.2. Snow cover duration (SCD in days) departures (difference from 1998-2010 mean) from the NOAA IMS data record for the 2014-2015 snow year: (a, left) fall; and (b, right) spring.

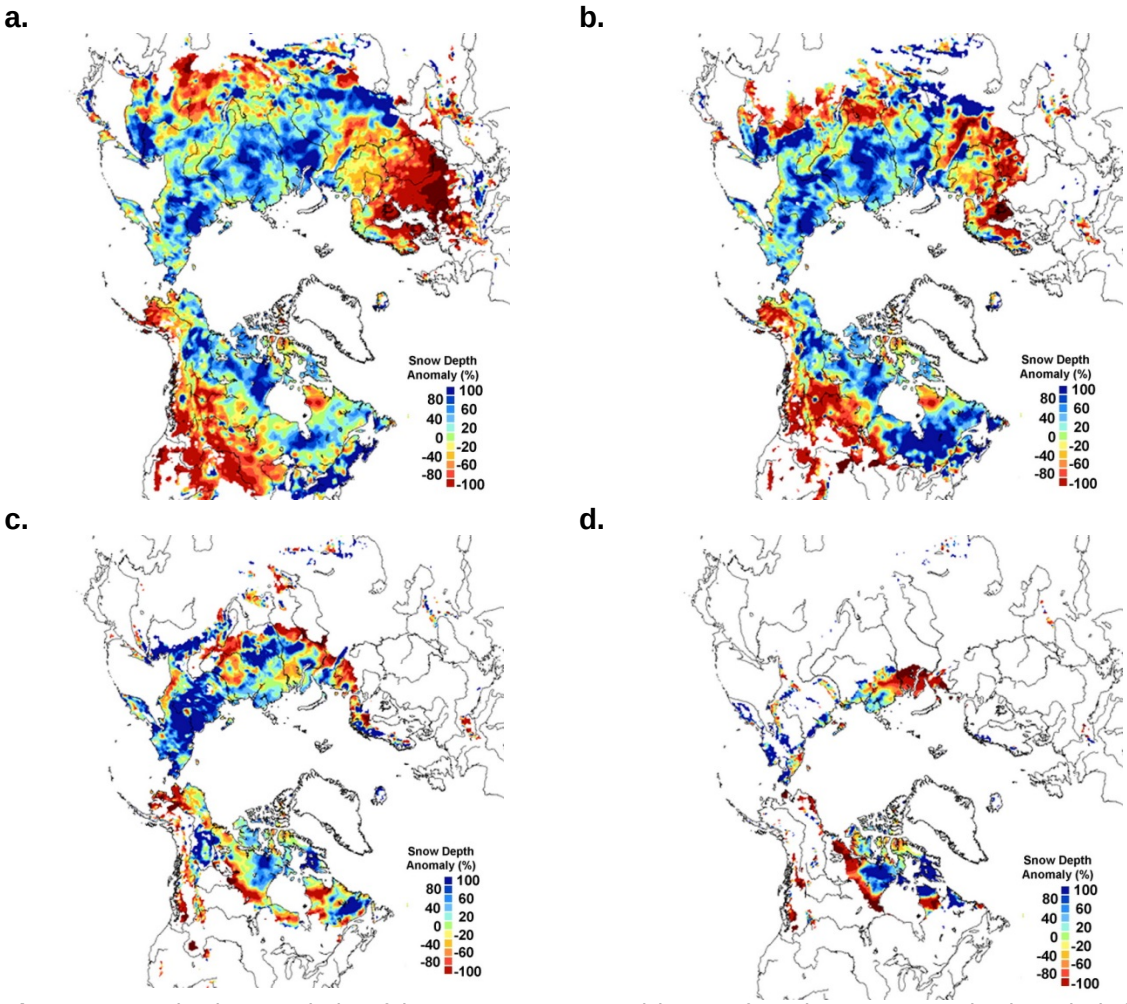

Fig. 2.3. Snow depth anomaly (% of the 1999-2010 average) in 2015 from the CMC snow depth analysis for (a, top left) March, (b, top right) April, (c, bottom left) May, and (d, bottom right) June.

Strong positive surface temperature anomalies over central Siberia, Alaska and the western Canadian Arctic in May (which persisted into June; see **Fig. 1.2c** in the essay on *Air Temperature*) were associated with rapid reductions in regional snow depth (**Figs. 2.3c** and **2.3d**) and earlier than normal snow melt in these regions (**Fig. 2.2b**), which drove the negative continental-scale SCE anomalies in May and June. For the fifth time in the past six years (2009-2015), Arctic SCE in June was below 3 million km^2 (**Fig. 2.4a**) despite never falling below this threshold in the previous 43 years of the snow chart data record (1967-2008). **Figure 2.4** shows the changing rate of SCE loss across the Arctic since 1998 via calculations over running time periods since 1979, the first year of the satellite passive microwave record used to track sea ice extent (calculations were made for 1979-1998, 1979-1999, 1979-2000, and so on). The April and May SCE reductions have remained relatively consistent year over year, ranging between -1% and -2% per decade (April) and -3% and -5% per decade (May). In contrast, since 2005, the rate of June SCE loss has increased from approximately -8% per decade (1979-2005) to -17% per decade (1979-2015). Since 2011, the rate of June snow cover loss has exceeded the rate of September sea ice loss.

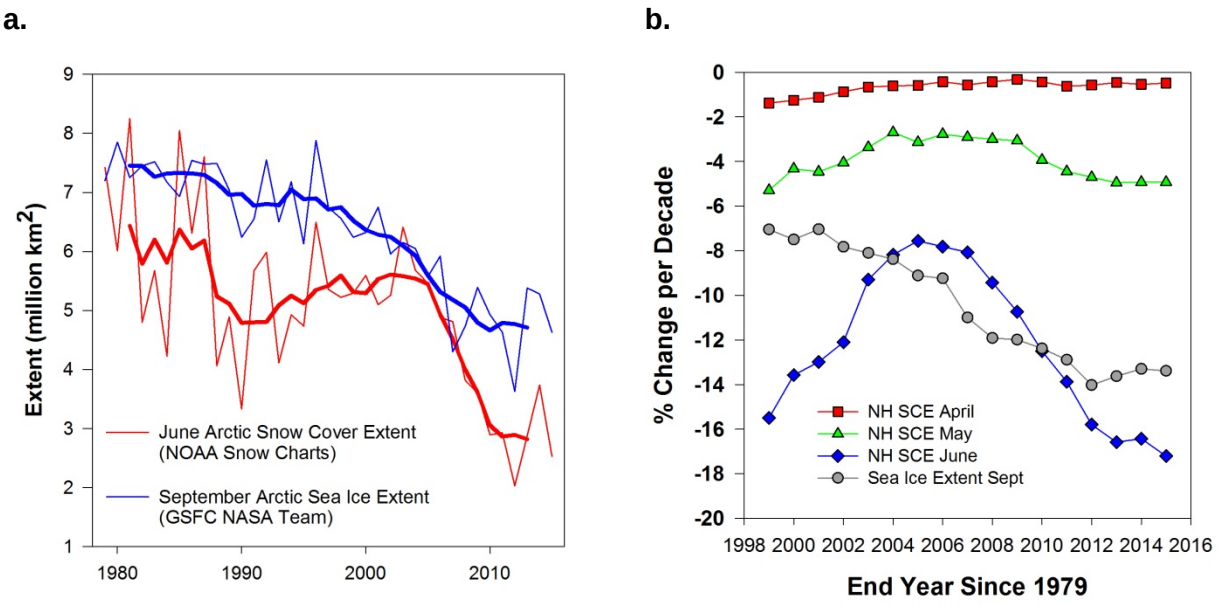

Fig. 2.4. (a, left) Northern Hemisphere (NH) June snow cover extent and September Arctic sea ice extent. Sea ice extent data for 1979-2014 are derived from the NASA Team algorithm (Cavalieri et al., 1996); ice extent estimates for 2015 are produced from real time data (Maslanik and Stroeve 1999). Bold red and blue lines are 5-year running means of the original snow and sea ice extent records, respectively. (b, right) % change per decade in spring snow cover extent and September sea ice extent for running time series starting in 1979 (1979-1998, 1979-1999, 1979-2000, and so on).

The 2015 spring melt season provided continued evidence of earlier snowmelt across the terrestrial Arctic. There is increased awareness of the impact of these changes on the cryosphere and the Arctic environment (Callaghan et al. 2013). There remains a need to better quantify and understand the impacts of variability and trends in high latitude snow cover in the fall season, given the potential remote impacts on the climate system (Cohen et al. 2014) but higher observational uncertainty during this time of year because of a short daylight period and increases in cloud cover that accompany snow cover onset (Brown and Derksen 2013).

References

Brasnett, B., 1999: A global analysis of snow depth for numerical weather prediction. *J. Appl. Meteorol.*, 38, 726-740.

Brown, R., and C. Derksen, 2013: Is Eurasian October snow cover extent increasing? *Env. Res. Lett.*, 8, 024006 doi:10.1088/1748-9326/8/2/024006.

Callaghan, T., M. Johansson, R. Brown, P. Groisman, N. Labba, V. Radionov, R. Barry, O. Bulygina, R. Essery, D Frolov, V. Golubev, T. Grenfell, M. Petrushina, V. Razuvaev, D. Robinson, P. Romanov, D. Shindell, A. Shmakin, S. Sokratov, S. Warren, D. Yang, 2011: The changing face of Arctic snow cover: A synthesis of observed and projected changes. *Ambio*, 40:17-31.

Cavalieri, D. J., C. L. Parkinson, P. Gloersen, and H. J. Zwally, 1996, updated yearly: Sea Ice Concentrations from Nimbus-7 SMMR and DMSP SSM/I-SSMIS Passive Microwave Data, Version 1 [1979-2014]. Boulder, Colorado USA. NASA National Snow and Ice Data Center Distributed Active Archive Center. http://dx.doi.org/10.5067/8GQ8LZQVL0VL.

Cohen, J., J. Furtado, J. Jones, M. Barlow, D. Whittleson, and D. Enekhabi, 2014: Linking Siberian Snow Cover to Precursors of Stratospheric Variability. J. Climate, 27: 5422-5432.

Estilow, T. W., A. H. Young, and D. A. Robinson, 2015: A long-term Northern Hemisphere snow cover extent data record for climate studies and monitoring. *Earth Sys. Sci. Data*, 7.1: 137-142.

Helfrich, S., D. McNamara, B. Ramsay, T. Baldwin, and T. Kasheta, 2007: Enhancements to, and forthcoming developments in the Interactive Multisensor Snow and Ice Mapping System (IMS). *Hydrol. Process.*, 21, 1576-1586.

Maslanik, J. and J. Stroeve, 1999, updated daily: Near-Real-Time DMSP SSMIS Daily Polar Gridded Sea Ice Concentrations, Version 1. [September 2015]. Boulder, Colorado USA. NASA National Snow and Ice Data Center Distributed Active Archive Center. http://dx.doi.org/10.5067/U8C09DWVX9LM.

Greenland Ice Sheet

M. Tedesco[1,2], J. E. Box[3], J. Cappelen[4], R. S. Fausto[3], X. Fettweis[5], K. Hansen[4], T. Mote[6], C. J. P. P. Smeets[7], D. van As[3], R. S. W. van de Wal[7], J. Wahr[8]

[1]The City College of New York, New York, NY, USA
[2]Lamont Doherty Earth Observatory of Columbia University, Palisades, NY, USA
[3]Geological Survey of Denmark and Greenland, Copenhagen, Denmark
[4]Danish Meteorological Institute, Copenhagen, Denmark
[5]University of Liege, Liege, Belgium
[6]Department of Geography, University of Georgia, Athens, Georgia, USA
[7]Institute for Marine and Atmospheric Research Utrecht,
Utrecht University, Utrecht, The Netherlands
[8]Department of Physics & Cooperative Institute for Research in Environmental Sciences,
University of Colorado, Boulder, CO, USA

December 7, 2015

In memoriam. This essay is dedicated to the memory of John Wahr[8] (June 1951 - November 2015) for his exceptional contribution to studying and promoting the understanding of the interactions between the solid layers of the Earth and the overlying atmosphere, oceans and ice sheets, and for his unique and outstanding human qualities.

Highlights

- Melt area in 2015 exceeded more than half of the ice sheet on July 4th for the first time since the exceptional melt events of July 2012, and was above the 1981-2010 average on 54.3% of days (50 of 92 days).
- The length of the melt season was as much as 30-40 days longer than average in the western, northwestern and northeastern regions, but close to and below average elsewhere on the ice sheet.
- Average summer albedo in 2015 was below the 2000-2009 average over the northwest and above the average over the southwest portion of the Greenland ice sheet. In July, albedo averaged over the entire ice sheet was lower than in 2013 and 2014, but higher than the lowest value on record observed in 2012.
- Ice mass loss of 186 Gt over the entire ice sheet between April 2014 and April 2015 was 22% below the average mass loss of 238 Gt for the 2002- 2015 period, but was 6.4 times higher than the 29 Gt loss of the preceding 2013-2014 season.
- The net area loss from marine-terminating glaciers during 2014-2015 was 16.5 km^2. This was the lowest annual net area loss of the period of observations (1999-2015) and 7.7 times lower than the annual average area change trend of -127 km^2.

Surface Melting

Estimates of the spatial extent of melting across the Greenland ice sheet in 2015, derived from spaceborne brightness temperatures recorded by the Special Sensor Microwave Imager/Sounder (SSMIS) passive microwave radiometer (e.g., Mote 2007; Tedesco 2007; Tedesco et al. 2013), show that melting occurred over more than half of the ice sheet for the first time since the exceptional melt events of July 2012 (Nghiem et al. 2012). The 2015 melt

extent exceeded two standard deviations above the 1981-2010 average, reaching a maximum of 52% of the ice sheet area on 4 July (**Fig. 3.1a**). For comparison, melt extent in 2014 reached a maximum of 39% of the ice sheet area and ~90% in 2012.

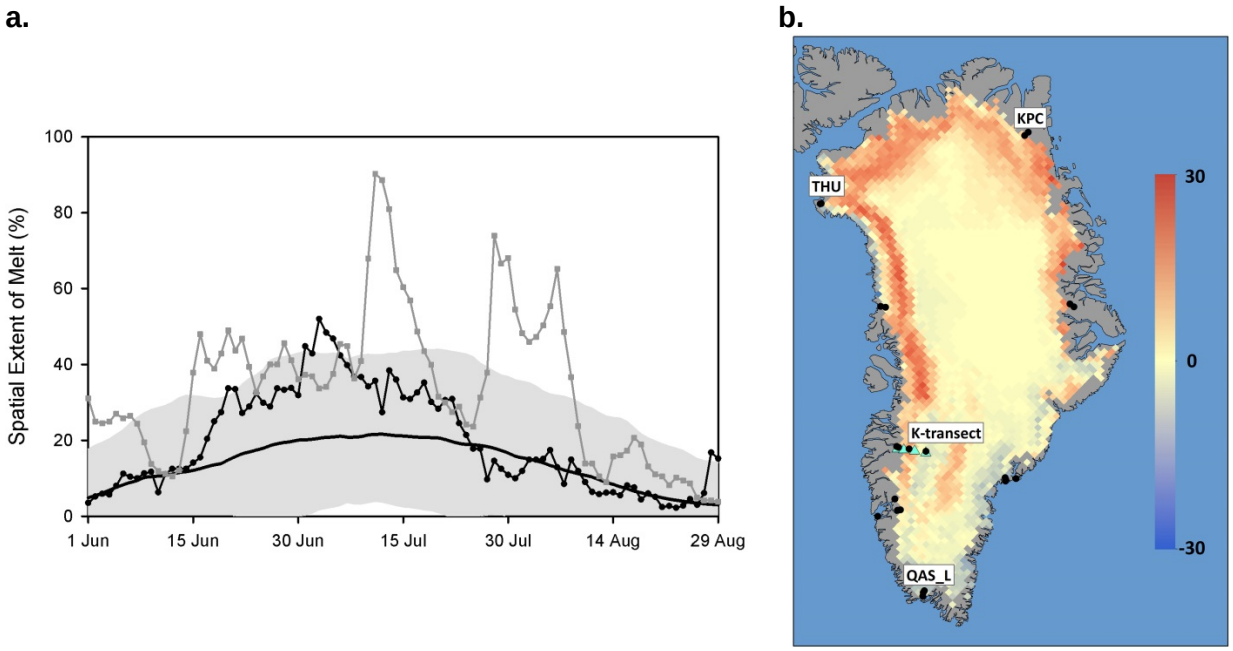

Fig. 3.1. (a) Daily spatial extent of melting from Special Sensor Microwave Imager/Sounder (SSMIS) as a percentage of the total ice sheet area during summer (JJA) 2015 (symbols), the 1981-2010 average spatial extent of melting (solid line) and ±2 standard deviations of the mean (shaded); (b) map of the anomaly (with respect to the 1981-2010 average) of the number of days when melting was detected in summer 2015. The black dots are PROMICE network stations (www.promice.dk), which include locations at Thule (THU), Kronprins Christian Land (KPC) and Qassimiut lobe (QAS_L). PROMICE and K-transect data are presented in the Surface Mass Balance section.

The number of melting days along the southwestern and southeastern margins of the ice sheet was close to or below the long-term average (**Fig. 3.1b**), with maximum negative anomalies (increased relative to the 1981-2010 average) being of the order of 5-10 days. In contrast, the number of melt days in the northeastern, western and northwestern regions, was up to 30-40 days above the 1981-2010 average and setting new records for meltwater production and runoff in the northwestern region (Tedesco et al. manuscript in preparation).

Surface Mass Balance

The surface mass balance for September 2014 through September 2015 measured along the southwestern portion of the ice sheet at the K-transect (**Fig. 3.1b**; van de Wal et al. 2005, 2012), was the third least negative since the beginning of the record in 1990; not since the 1991-1992 (when melting was low due to the Mount Pinatubo eruption) and 1995-1996 balance years has so little ice been lost (**Fig. 3.2a**). This is consistent with the negative anomalies detected by the SSMI/S along the southwestern portion of the ice sheet. Data from location S5 (~540 m a.s.l., 67.10°N, 50.09°W), in the ablation area, show that the melt season started approximately 15-20 days later than the 2008-2014 average, then decreased substantially near the end of July and remained low during August (**Fig. 3.2b**). At station S9 (~1500 m a.s.l. near the equilibrium line [the lowest altitude at which winter snow survives], 67.05°N, 48.25°W), melting ceased due to snowfall at the end of July and there was no melting during August (**Fig. 3.2c**).

a.

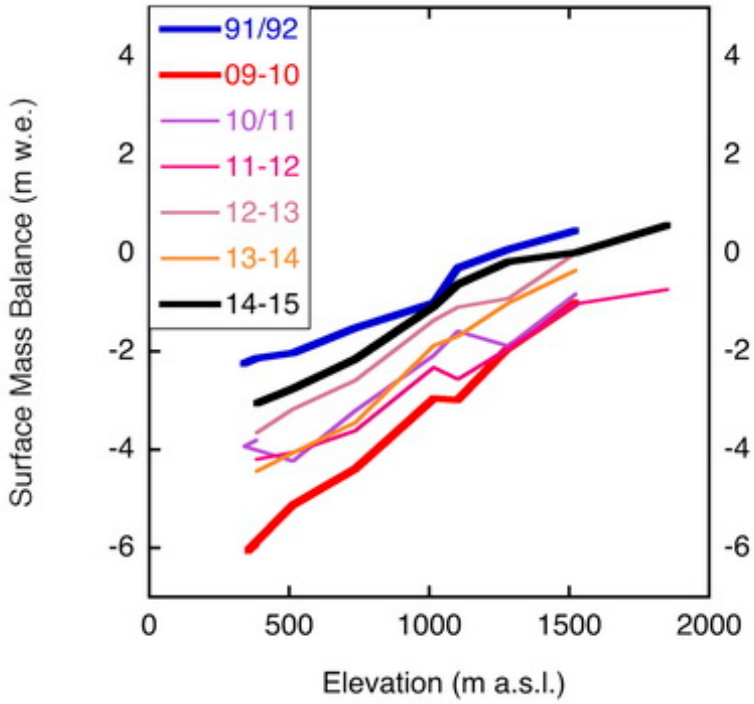
91/92
09-10
10/11
11-12
12-13
13-14
14-15
Surface Mass Balance (m w.e.)
4
2
0
-2
-4
-6
0
500
1000
1500
2000
Elevation (m a.s.l.)

b.

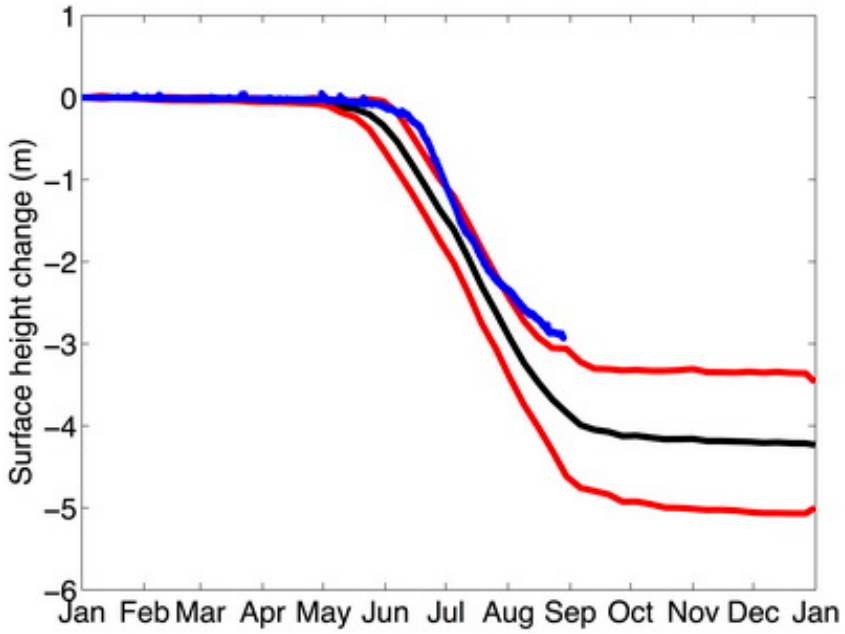
Surface height change (m)
1
0
−1
−2
−3
−4
−5
−6
Jan
Feb
Mar
Apr
May
Jun
Jul
Aug
Sep
Oct
Nov
Dec
Jan

c.

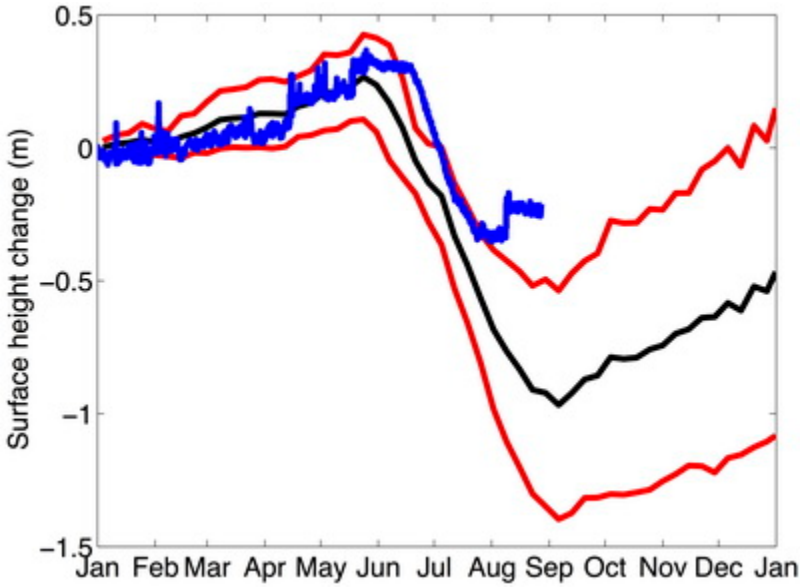

Fig. 3.2. (a, top) The surface mass balance as a function of elevation along the K-transect since balance year 2009-2010. (b, centre) Time series of surface height change at the S5 station at ~540 m a.s.l. on the K-transect. (c, bottom) Same as (b) but for the S9 station at ~1500 m a.s.l near the equilibrium line on the K-transect. In (b) and (c), the black line is the average for the period 2008-2015 and the red lines indicate 1 standard deviation of the average. Note that in (a), the 91-92 curve is for the period affected by the eruption of Mount Pinatubo, when surface melting was lowered dramatically.

Anomalously low melt in 2015 with respect to the 2008-2014 average at PROMICE network stations (van As et al. 2011; Fausto et al. 2012) is consistent with the K-transect. At all PROMICE stations (**Fig. 3.1b**), ablation in summer 2015 was relatively low with respect to the 2008-2014 observational period, except at the most northerly latitudes (Kronprins Christian Land, KPC, 80°N, 25°W; Thule, THU, 76°N, 68°W), where melt totals were slightly above average. The highest recorded melt in 2015, 5.1 m on the Qassimiut lobe (QAS_L station, 61°N, 47°W), was little more than half the record-setting 9.3 m at that site in 2010 (Fausto et al. 2012).

Albedo

Albedo, a measure of surface reflectivity, is the ratio of reflected solar radiation to total incoming solar radiation. A relatively low albedo promotes increased melting, with net solar radiation being the major driver of summer surface melt over Greenland. Average albedo in summer 2015, derived from data collected by the Moderate-resolution Imaging Spectroradiometer (MODIS, after Box et al. 2012), was below the 2000-2009 average in the northwestern region and above the average in the southwestern region (**Fig. 3.3a**). This is consistent with the negative surface mass balance and melting day anomalies measured over the same region. The 2000-2009 reference period is used here because MODIS observations began in 2000. The trend of mean summer albedo over the entire ice sheet for the period 2000-2015 is -5.5±0.4% (**Fig. 3.3b**).

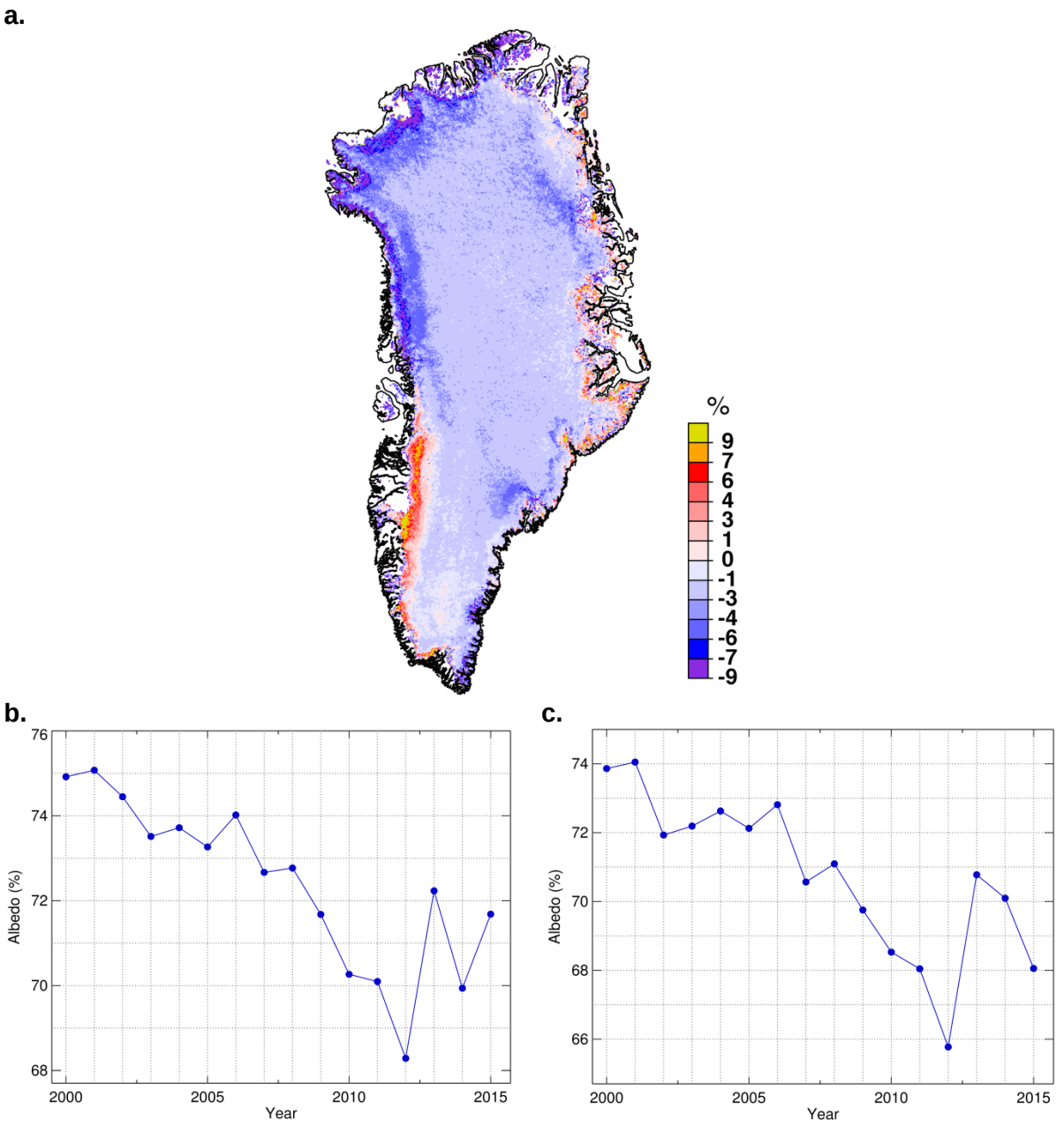

Fig. 3.3. (a, top) Greenland Ice Sheet surface albedo anomaly for summer (JJA) 2015 relative to the average for those months between 2000 and 2009. (b, lower left) Average July albedo of the entire ice sheet. (c, lower right) Average surface albedo of the entire ice sheet each summer (JJA) since 2000. The period 2000-2009 is used as reference to be consistent with previous Arctic Report Card albedo reports.

In July 2015, when extensive melting occurred (**Fig. 3.1a**), albedo averaged over the entire ice sheet was 68.1%, i.e., lower than the 2013 and 2014 values and higher than the lowest average July albedo of 65.8% recorded in 2012 (**Fig. 3.3c)**. Albedo in July 2015 was anomalously low (as much as 15-20% below average) along the northwestern ice sheet and along the west coast, where large positive melting days anomalies were observed (**Fig. 3.1b**). But, over the entire summer, the albedo anomaly along the west coast was positive. The summer mean albedo in 2015 was higher than the albedo recorded in 2014 and close to the value recorded in

2013 (**Fig. 3.3b**), mostly because of the relatively short melt season and early snowfall in August.

Total Ice Mass

GRACE satellite data (Velicogna and Wahr 2013) are used to estimate monthly changes in the total mass of the Greenland ice sheet (**Fig. 3.4**). Between mid-April 2014 and mid-April 2015, roughly corresponding to the period between the beginning of the two consecutive melt seasons, the 186 Gt of ice loss was 22% lower than the average April-to-April mass loss (238 Gt) during 2002-2015. For comparison, since GRACE measurements began in 2002, the smallest April-to-April mass loss was 29 Gt during 2013-2014 and the largest was 562 Gt during 2012-2013.

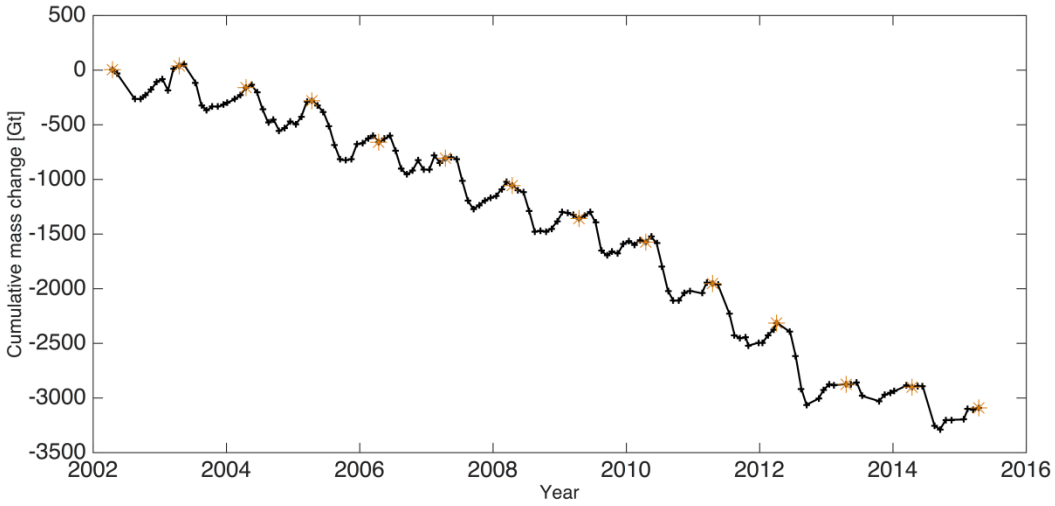

Fig. 3.4. Cumulative change in the total mass (in Gigatonnes, Gt) of the Greenland Ice Sheet between April 2002 and April 2015 estimated from GRACE measurements. Each symbol is an individual month and the orange asterisks denote April values for reference.

Marine-terminating Glaciers

Marine-terminating glaciers are the outlets via which the inland ice sheet discharges to the ocean. When in balance, the rate of iceberg calving (by area) is balanced by the seaward flow of the ice (see the essay on *Greenland Ice Sheet Surface Velocity: New Data Sets* for further information on the velocity of these glaciers). Analysis of LANDSAT and ASTER imagery since 1999 of 45 of the widest and fastest-flowing marine-terminating glaciers reveals that they continue to retreat, although the rate of retreat has slowed since 2012 (**Fig. 3.5**). Between the end of the 2014 melt season and the end of the 2015 melt season, 22 of the 45 glaciers had retreated, but the advance of 9 relatively wide glaciers resulted in a low 1-year net area loss of 16.5 km^2. This is the lowest annual net area loss in the 16-year period of observations (1999-2015) and 7.7 times lower than the annual average area change trend of -127 km^2 (**Fig. 3.5**). The advance of Petermann Glacier (0.684 km advance across a width of 17.35 km gives an area increase of 11.87 km^2) and Kangerdlugssuaq Glacier (1.683 km advance across a width of 6.01 km gives an area increase of 10.12 km^2) contributed to the low net area loss of the 45 glaciers in 2014-2015.

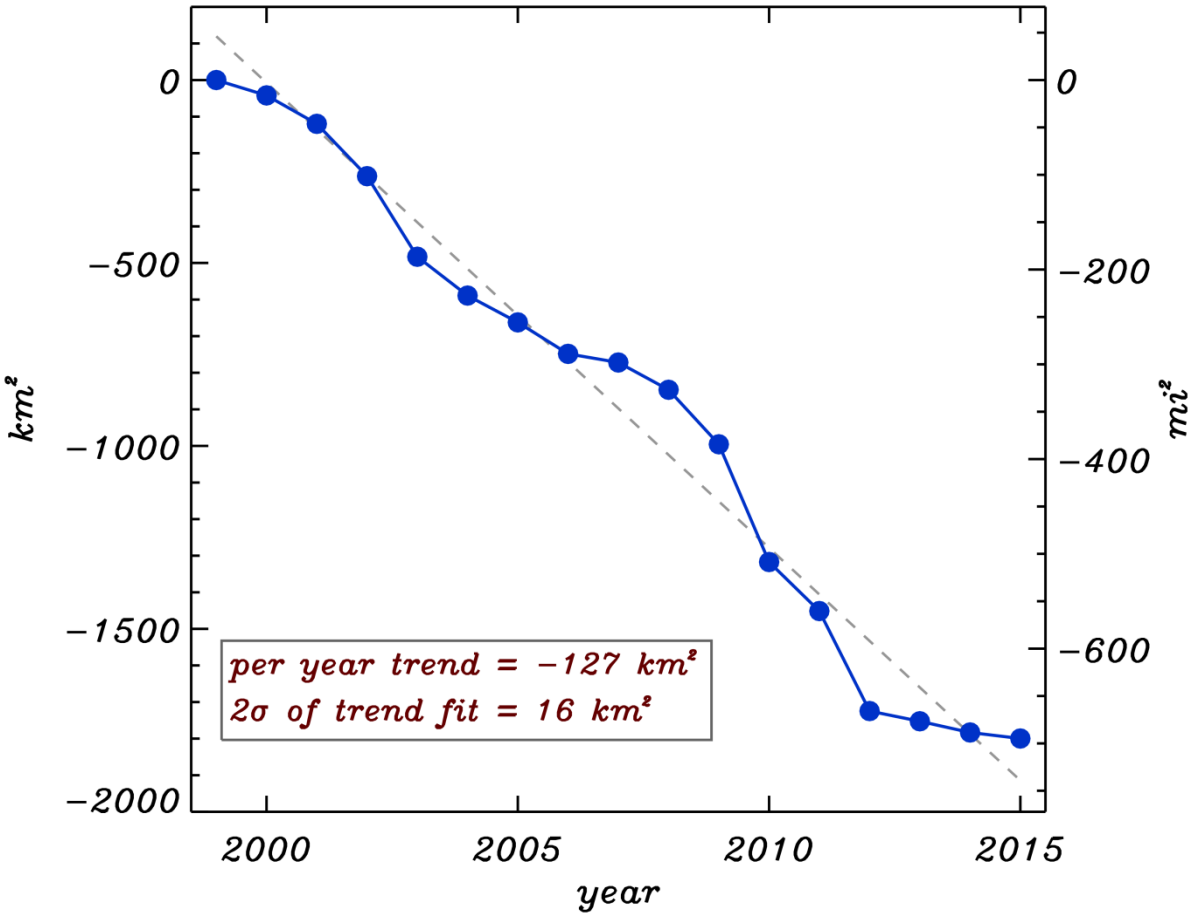

Fig. 3.5. Cumulative net area change (km^2 and square miles, left and right axes, respectively) at the 45 of the widest and fastest-flowing marine-terminating glaciers of the Greenland Ice Sheet (after Box and Decker 2011 and Jensen et al. unpublished). The linear regression is dashed.

Weather

Measurements at weather stations of the Danish Meteorological Institute (DMI, Cappelen 2015, **Table 3.1**) during spring 2015 indicate that temperatures at Nuuk (64.2°N,51.8°W), Paamiut (62.0°N, 49.7°W), Narsarsuaq (61.2°N,45.4°W), Qaqortoq (60.7°N, 46.0°W) and Prins Christian Sund (60.0°N,43.2°W) in south and southwest Greenland were 1.5 standard deviations below the 1981-2010 average, with temperature anomalies (relative to the 1981-2010 average) as much as -2.6°C at Narsarsuaq. The average May temperature at Danmarkshavn (76.8°N, 18.8°W) set a new record low, with a -4.6°C anomaly relative to the 1981-2010 average. These widespread low temperatures are consistent with the strong negative spring temperature anomaly centered over Greenland (see **Fig. 1.2c** in the essay on *Air Temperature*). Danmarkshavn also experienced the warmest January on record, with a +7.7 °C anomaly relative to the 1981-2010 average. Summer average temperature anomalies were positive at most stations around the Greenland coastline, with anomalies exceeding one standard deviation at Pituffik (76.5°N, 68.8°W, +1.2ºC), Upernavik (72.8°N, 56.2°W, +1.2°C), Nuuk (64.2°N, 51.8°W, +1.1°C) and Danmarkshavn (+0.9 °C). A new record August low temperature of -39.6 °C occurred on August 28 at Summit (3216 m a.s.l., 72.5796°N, 38.4592°W).

Table 3.1. Near-surface seasonal air temperature anomalies relative to the 1981-2010 average at thirteen stations distributed around Greenland. Standard deviation (SD) values, and the years when record maximum and minimum values occurred are also given. SON: September, October, November (fall); DJF: December, January, February (winter); MAM: March, April, May (spring); JJA: June, July, August (summer). Data are from Cappelen (2015) and from the Danish Meteorological Institute (DMI) for the period January-August 2015.

Location	First year of record	Statistics	SON	DJF	MAM	JJA
Pituffik/Thule AFB 76.5°N 68.8°W	1948	*Anomaly (°C)*	1.3	-1.4	0.7	1.2
		St. Deviation (SD)	0.9	-0.6	0.2	1.2
		Max. Year	2010	1986	1953	1957
		Min. Year	1964	1949	1992	1996
Upernavik 72.8°N 56.2°W	1873	*Anomaly (°C)*	1.2	-0.5	-0.8	1.2
		SD	1.0	0.0	-0.5	1.5
		Max. Year	2010	1947	1932	2012
		Min. Year	1917	1983	1896	1922
Kangerlussuaq 67.0°N 50.7°W	1949	*Anomaly (°C)*	-0.6	-2.9	-2.4	0.2
		SD	-0.3	-0.9	-0.9	0.1
		Max. Year	2010	1986	2005	2014
		Min. Year	1982	1983	1993	1983
Ilulissat 69.2°N 51.1°W	1873	*Anomaly (°C)*	0.5	-2.2	-1.2	-0.2
		SD	0.6	-0.4	-0.5	0.4
		Max. Year	2010	1929	1932	1960
		Min. Year	1884	1884	1887	1972
Aasiaat 68.7°N 52.8°W	1951	*Anomaly (°C)*	0.8	-1.6	-0.6	1.0
		SD	0.9	-0.6	-0.4	0.9
		Max. Year	2010	2010	2010	2012
		Min. Year	1986	1984	1993	1972
Nuuk 64.2°N 51.8°W	1873	*Anomaly (°C)*	0.4	-1.8	-2.1	1.1
		SD	0.6	-0.6	-1.5	1.1
		Max. Year	2010	2010	1932	2012
		Min. Year	1898	1984	1993	1914
Paamiut 62.0°N 49.7°W	1958	*Anomaly (°C)*	0.6	-0.7	-2.2	-0.1
		SD	0.5	-0.5	-1.3	0.0
		Max. Year	2010	2010	2005	2010
		Min. Year	1982	1984	1993	1969

Narsarsuaq 61.2°N 45.4°W	1961	*Anomaly (°C)*	0.1	-2.0	-2.6	0.5
		SD	0.2	-0.8	-1.3	0.7
		Max. Year	2010	2010	2010	2012
		Min. Year	1963	1984	1989	1983
Quaqortoq 60.7°N 46.0°W	1873	*Anomaly (°C)*	0.1	-1.8	-2.2	-0.6
		SD	0.5	-0.5	-1.5	-0.5
		Max. Year	2010	2010	1932	1928
		Min. Year	1874	1884	1989	1874
Danmarkshavn 76.8°N 18.8°W	1949	*Anomaly (°C)*	1.5	1.6	0.0	0.9
		SD	1.2	1.0	0.0	1.3
		Max. Year	2002	2005	1976	2008
		Min. Year	1971	1967	1966	1955
Ittoqqortoormiut 70.4°N 22.0°W	1948	*Anomaly (°C)*	2.2	1.1	0.9	-0.2
		SD	1.7	0.8	0.9	0.6
		Max. Year	2002	2014	1996	1949
		Min. Year	1951	1966	1956	1955
Tasiilaq 65.6°N 37.6°W	1895	*Anomaly (°C)*	1.1	0.3	1.1	0.2
		SD	1.2	0.4	0.6	0.0
		Max. Year	1941	1929	1929	2003
		Min. Year	1917	1918	1899	1983
Prins Christian Sund 60.0°N 43.2°W	1951	*Anomaly (°C)*	0.6	-0.7	-0.9	-0.3
		SD	0.7	-0.5	-1.0	-0.3
		Max. Year	2010	2010	2005	2010
		Min. Year	1982	1993	1989	1992

Summer 2015 was characterized by negative North Atlantic Oscillation (NAO) conditions, with a mean summer value of -1.3, similar to those of the summers (JJA) of 2007-2012 when enhanced surface melting occurred (Tedesco et al. 2013, 2014). NAO is defined as the difference in atmospheric pressure at sea level between the Icelandic Low and the Azores High and it has been shown to be connected to extreme melting events over Greenland (McLeod and Mote, 2015). However, a distinct difference in the atmospheric circulation associated with the NAO in summer 2015 and the summers of 2007-2012 affected melting on the ice sheet. During the summers of 2007-2012, the 500 mb geopotential height anomaly (typically used to describe NAO atmospheric circulation) with respect to the 1981-2012 average was persistently centered over the ice sheet and southerly air flow advected warm air across the ice sheet. In the summer of 2015 the anomaly was centered over the north-central ice sheet in July, which promoted warm, southerly airflow and enhanced melting. On the other hand, in June and August 2015 the anomaly was centered over the Labrador Sea southwest of Greenland, which promoted the advection of cold air from the Arctic Ocean and reduced melting (Tedesco et al., unpublished

manuscript). The spatial distribution of albedo and melting observed by remote sensing (**Fig. 3.1**) and with the in-situ surface mass balance measurements (e.g., **Fig. 3.2**) and summer air temperatures (**Table 3.1**) are consistent with these atmospheric circulation patterns.

References

Box, J. E., and D. T. Decker, 2011: Greenland marine-terminating glacier area changes: 2000-2010. *Ann. Glaciol.*, 52, 91-98, http://dx.doi.org/10.3189/172756411799096312.

Box, J. E., X. Fettweis, J. C. Stroeve, M. Tedesco, D. K. Hall, and K. Steffen, 2012. Greenland ice sheet albedo feedback: thermodynamics and atmospheric drivers. *The Cryosphere*, 6, 821-839, doi:10.5194/tc-6-821-2012.

Cappelen (ed), 2015. Greenland - DMI Historical Climate Data Collection 1784-2014. *Danish Meteorol. Inst. Tech. Rep.*, 15-04.

Fausto R. S., D. Van As and the PROMICE Project Team (2012) Ablation observations for 2008-2011 from the Programme for Monitoring of the Greenland Ice Sheet (PROMICE). *Geol. Surv. Denmark Greenland Bull.*, 26, 73-76.

Jensen, T., J. E. Box, and C. Hvidberg, unpublished: A sensitivity study of yearly Greenland ice sheet marine terminating outlet glacier changes: 1999-2013. Submitted to *J. Glaciol*.

McLeod, J. T., and T. L. Mote, 2015: Linking interannual variability in extreme Greenland blocking episodes to the recent increase in summer melting across the Greenland ice sheet. *Int. J. Climatol.*, DOI: 10.1002/joc.4440.

Mote, T. L., 2007: Greenland surface melt trends 1973-2007: Evidence of a large increase in 2007. *Geophys. Res. Lett.*, 34, L22507.

Nghiem, S. V., D. K. Hall, T. L. Mote, M. Tedesco, M. R. Albert, K. Keegan, C. A. Shuman, N. E. DiGirolamo, and G. Neumann, 2012: The extreme melt across the Greenland ice sheet in 2012. *Geophys. Res. Lett.*, 39, L20502, doi:10.1029/2012GL053611.

Tedesco, M., Snowmelt detection over the Greenland ice sheet from SSM/I brightness temperature daily variations. *Geophys. Res. Lett.*, 34, L02504,doi:10.1029/2006GL028466, January 2007.

Tedesco, M., X. Fettweis, T. Mote, J. Wahr, P. Alexander, J. Box, and B. Wouters, 2013: Evidence and analysis of 2012 Greenland records from spaceborne observations, a regional climate model and reanalysis data. *The Cryosphere*, 7, 615-630.

Tedesco, M., J. E. Box, J. Cappelen, X. Fettweis, T. Mote, A. K. Rennermalm, R. S. W. van de Wal, and J. Wahr, 2014: Greenland Ice Sheet. In *Arctic Report Card: Update for 2013*, http://www.arctic.noaa.gov/report13/greenland_ice_sheet.html.

Tedesco, M., T. Mote, J. Jeyaratnam, X. Fettweis, E. Hanna, and K. Briggs, Linkages between exceptional jet-stream conditions and atmospheric and surface records over the Greenland ice sheet during summer 2015. Manuscript in preparation for submission to *Nature Climate Change*.

Van As, D., R. S. Fausto, and PROMICE Project Team, 2011: Programme for Monitoring of the Greenland Ice Sheet (PROMICE): first temperature and ablation records. *Geol. Surv. Denmark Greenland Bull.*, 23, 73-76.

Van de Wal, R. S. W., W. Greuell, M. R. van den Broeke, C.H. Reijmer, and J. Oerlemans, 2005: Surface mass-balance observations and automatic weather station data along a transect near Kangerlussuaq, West Greenland. *Ann. Glaciol.*, 42, 311-316.

Van de Wal, R. S. W., W. Boot, C. J. P. P. Smeets, H. Snellen, M. R. van den Broeke, and J. Oerlemans, 2012: Twenty-one years of mass balance observations along the K-transect, West-Greenland. *Earth Syst. Sci. Data*, 4, 31-35, doi:10.5194/essd-4-31-2012.

Velicogna, I., and J. Wahr, 2013. Time-variable gravity observations of ice sheet mass balance: precision and limitations of the GRACE satellite data. *Geophys. Res. Lett.*, 40, 3055-3063, doi:10.1002/grl.50527.

Sea Ice

D. Perovich[1,2], W. Meier[3], M. Tschudi[4], S. Farrell[5], S. Gerland[6], S. Hendricks[7]

[1]ERDC - CRREL, 72 Lyme Road, Hanover USA
[2]Thayer School of Engineering, Dartmouth College, Hanover, NH, USA
[3]NASA Goddard Space Flight Center, Greenbelt, MD, USA
[4]Aerospace Engineering Sciences, University of Colorado, Boulder, CO, USA
[5]NOAA Earth System Science Interdisciplinary Center, University of Maryland, College Park, MD, USA
[6]Norwegian Polar Institute, Fram Centre, Tromsø, Norway
[7]Alfred Wegener Institute, Bremerhaven, Germany

December 15, 2015

Highlights

- The September 2015 Arctic sea ice minimum extent was 4.63 million km^2, 29% less than the 1981-2010 average minimum ice extent and the fourth lowest value in the satellite record (1979-2015).
- The lowest maximum ice extent in the satellite record (1979-2015) occurred on 25 February 2015, 15 days earlier than the 1981-2010 average (12 March); at 14.54 million km^2, it was 7% below the 1981-2010 average.
- In March 2015, multiyear ice (>1 years old) and first-year ice were 31% and 69% of the ice cover, respectively, differing little from the 2014 values.
- Multi-year sea ice continues to dominate the central Arctic Ocean, with a mean ice thickness that remains around 3.2 m.

Sea Ice Extent

Sea ice extent is the primary descriptor of the state of the Arctic sea ice cover. Satellite-based passive microwave instruments have been used to determine sea ice extent since 1979. There are two months each year that are of particular interest: September, at the end of summer, when the ice reaches its annual minimum extent, and March, at the end of winter, when the ice typically is at its maximum extent. Maps of monthly average ice extents in March 2015 and September 2015 are shown in **Fig. 4.1**.

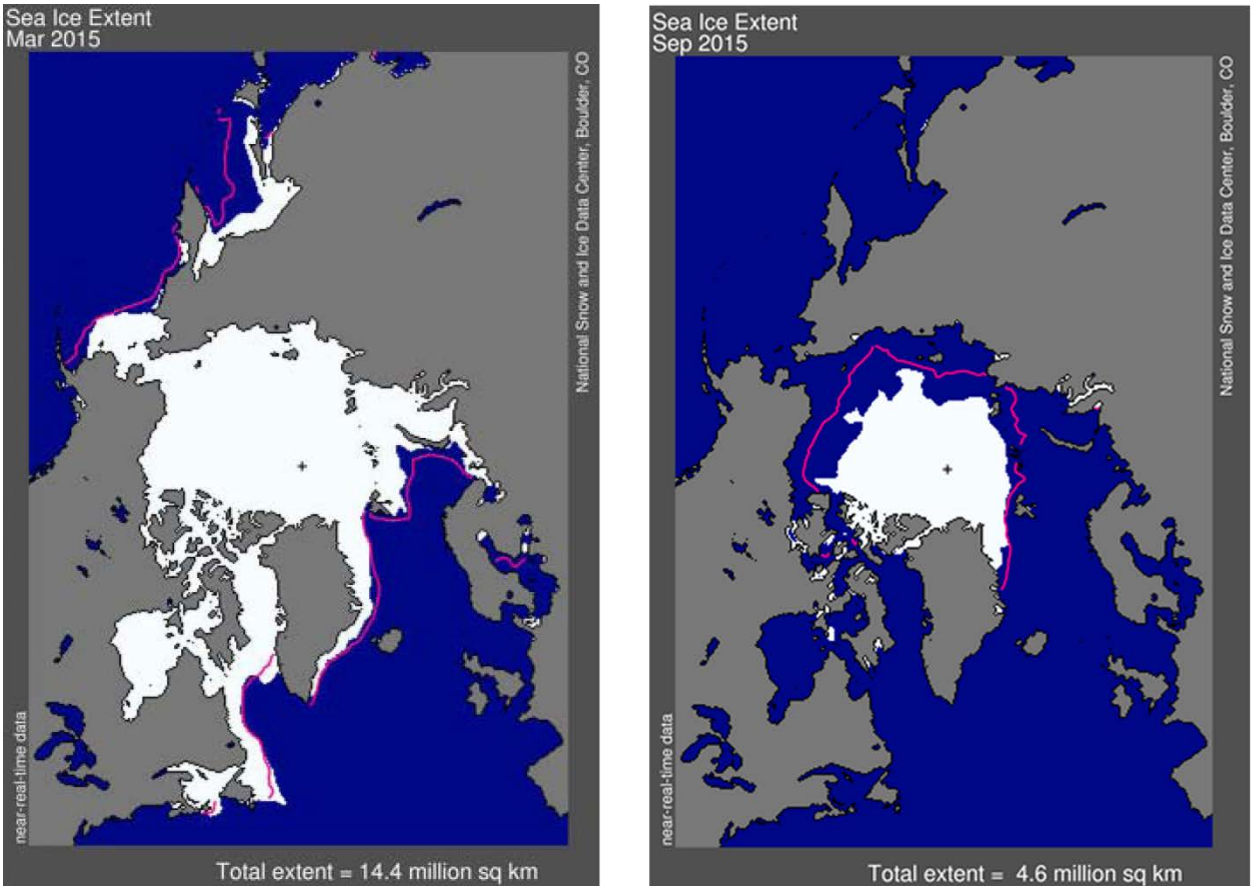

Fig. 4.1. Average sea ice extent in March 2015 (left) and September 2015 (right) illustrate the respective winter maximum and summer minimum extents. The magenta line indicates the median ice extents in March and September, respectively, during the period 1981-2010. Maps are from NSIDC at nsidc.org/data/seaice_index.

Based on estimates produced by the National Snow and Ice Data Center (NSIDC) the Arctic sea ice cover reached a minimum annual extent of 4.41 million km^2 on September 11, 2015. This was substantially higher (1.02 million km^2, 30%) than the record minimum of 3.39 million km^2 set in 2012. However, the 2015 summer minimum extent was still 1.81 million km^2 (29%) less than the 1981-2010 average minimum ice extent and was 0.62 million km^2 (12%) less than the 2014 minimum. On February 25, 2015 Northern Hemisphere ice extent reached a maximum value of 14.54 million km^2, 7% below the 1981-2010 average and the lowest maximum value in the satellite record. Also notable, the maximum extent occurred 15 days earlier than the 1981-2010 average (12 March) and was the second earliest of the satellite record.

Sea ice extent has decreasing trends in all months and virtually all regions (the exception being the Bering Sea during winter). The September monthly average trend for the entire Arctic Ocean is now -13.4% per decade relative to the 1981-2010 average (**Fig. 4.2**). Trends are smaller during March (-2.6% per decade), but are still decreasing at a statistically significant rate.

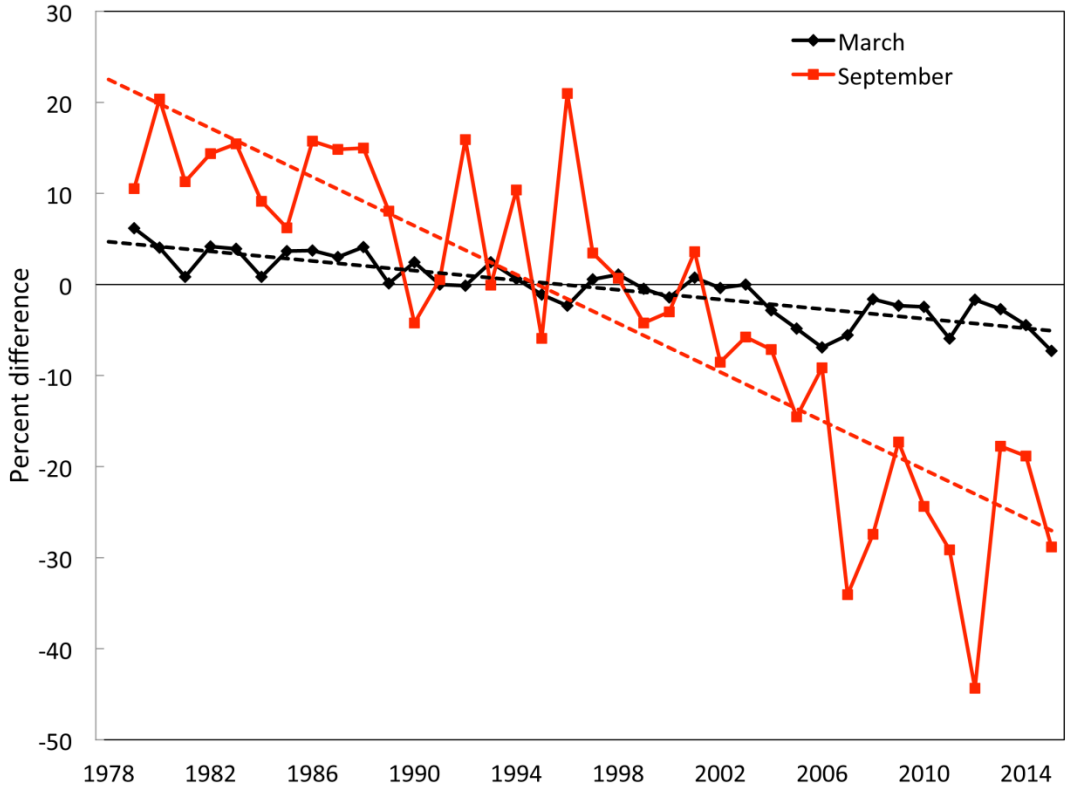

Fig. 4.2. Time series of Northern Hemisphere sea ice extent anomalies in March (the month of maximum ice extent) and September (the month of minimum ice extent). The anomaly value for each year is the difference (in %) in ice extent relative to the mean values for the period 1981-2010. The black and red dashed lines are least squares linear regression lines. The slopes of these lines indicate ice losses of -2.6% and -13.4% per decade in March and September, respectively. Both trends are significant at the 99% confidence level.

Before 2007, there had never been a March to September loss of more than 10 million km^2 of ice but now such large losses are not unusual. This year, 10.13 million km^2 of ice was lost between the March maximum and September minimum extent, typical of summer losses since 2007.

Age of the Ice

The age of sea ice is another descriptor of the state of the sea ice cover. It serves as an indicator for ice physical properties, including surface roughness, melt pond coverage and thickness. Older ice tends to be thicker and thus more resilient to changes in atmospheric and oceanic forcing compared to younger ice. The age of the ice is determined using satellite observations and drifting buoy records to track ice parcels over several years (Tschudi et al. 2010; Maslanik et al. 2011). This method has been used to provide a record of the age of the ice since the early 1980s (Tschudi et al. 2015).

The oldest ice (>4 years old) continues to make up a small fraction of the Arctic ice pack in March, when the sea ice extent has been at its maximum in most years of the satellite record (**Figs. 4.3a** and **4.3c**). In 1985, 20% of the ice pack was very old ice (**Fig. 3b**), but in March 2015 old ice only constituted 3% of the ice pack (**Fig. 3c**). Furthermore, we note that first-year ice now dominates the ice cover, comprising ~70% of the March 2015 ice pack, compared to

about half that in the 1980s. Note that the age distribution of the ice cover in March 2015 was the same as it was in February 2015, when maximum ice extent occurred. Given that older ice tends to be thicker, the sea ice cover has transformed from a strong, thick pack in the 1980s to a more fragile, thin and younger pack in recent years. The thinner, younger ice is more vulnerable to melting out in the summer, resulting in lower minimum ice extents. The distribution of ice age in March 2015 was similar to that in March 2014 (**Fig. 4.3a**).

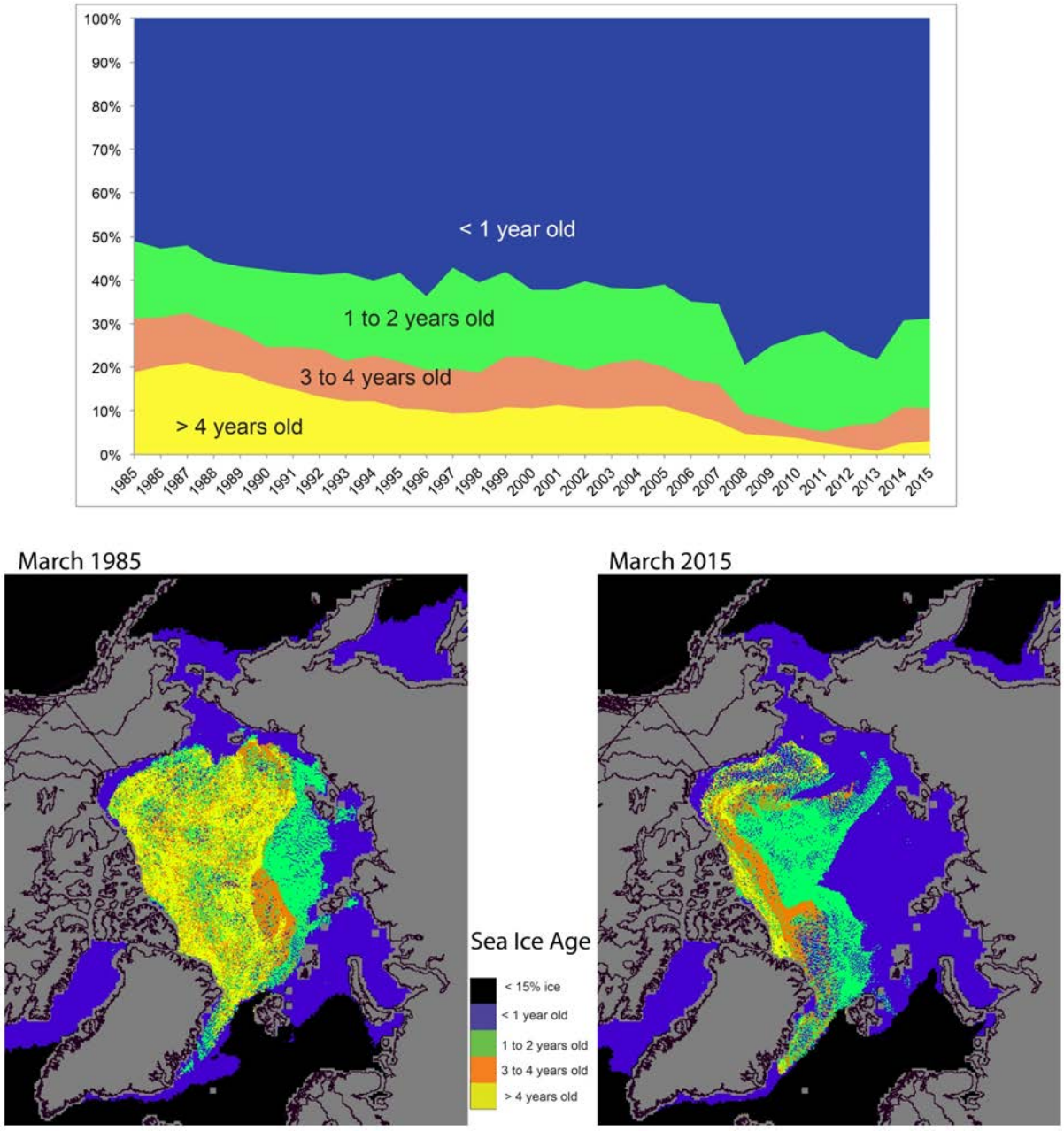

Fig. 4.3. A time series of sea ice age in March from 1985 to the present (a, top) and maps of sea ice age in March 1985 (b, lower left) and March 2015 (c, lower right).

Note that most of the oldest ice accumulates along the coast of North Greenland and the Queen Elizabeth Islands of the Canadian Arctic Archipelago, and much of this ice has resided in this

area for several years. In 2015, as in most years, ice transport patterns resulted in the movement of the old ice from this area into the Beaufort Sea. The lack of ice older than one year in the eastern Arctic (on the Eurasian side of the Arctic Basin) foreshadows its susceptibility to melt out in summer. The ice in the southern Beaufort and Chukchi seas has also melted completely in the past few summers, with even the oldest ice not surviving the season.

Sea Ice Thickness

Observations of sea ice thickness and volume from multiple sources have revealed the continued decline of the Arctic sea ice pack over the last decade (Kwok and Rothrock 2009; Laxon et al. 2013; Kwok and Cunningham 2015). These changes have impacts on the regional Arctic and sub-Arctic climate, environment and ecosystems. To understand these impacts, as the Arctic transitions from a predominantly multi-year ice pack to a seasonal ice cover (**Fig. 4.3**), continued monitoring of the state of the ice pack is required. Towards this end, multiple satellite, airborne and in-situ campaigns continue to obtain measurements of key sea ice properties, which are of particular interest for understanding the inter-annual variability of the ice pack. The NASA Operation IceBridge, a multi-instrumented aircraft mission, has been making annual surveys of sea ice since 2009 in the western Arctic (on the North American side of the Arctic Basin) at the end of the winter growth period. Meanwhile, the ESA CryoSat-2 satellite has been measuring sea ice freeboard (from which sea ice thickness and volume are derived) since 2010 (Tilling et al., 2015).

Figure 4.4a shows consistency between the independent CryoSat-2 and IceBridge estimates of Arctic sea ice thickness in March/April 2015, and with the map of ice age (**Fig. 3c**). The oldest ice north of Greenland and the Canadian Arctic Archipelago remains thicker than 3 m. Also, there is a strong gradient to thinner, seasonal ice in the Canada Basin and the eastern Arctic Ocean, where ice is between 1 m and 2 m thick. Operation IceBridge also provides details of the inter-annual variability in the sea ice thickness distribution over a seven-year period from March/April 2009 to March/April 2015 (**Figs. 4.4b** and **4.4c**). Sea ice in the central Arctic is predominantly multi-year in nature, with mean and modal ice thickness remaining stable at around 3.2 m and 2.5 m, respectively (**Fig. 4.4b**). Richter-Menge and Farrell (2013) showed that sea ice in the Beaufort and Chukchi seas region is more seasonal in nature and is a mix of multiyear (~25%) and first-year ice (~75%). Here, the inter-annual variability of the ice thickness distribution over the last seven years has been more variable (**Fig. 4.4c**), with mean and modal ice thickness around 2.1 m and 1.8 m, respectively. Year-to-year variability is primarily related to the presence and location of a band of multi-year sea ice in the southern Beaufort Sea (Richter-Menge and Farrell 2013).

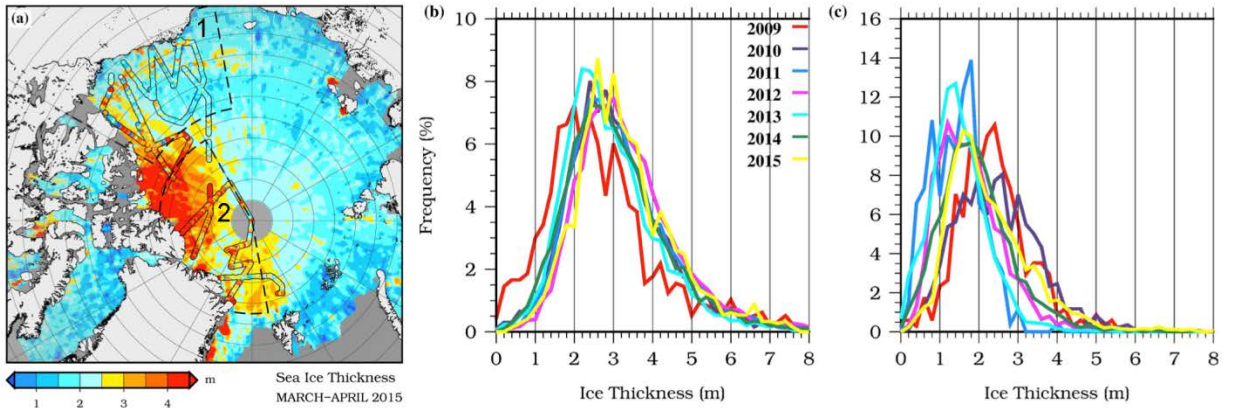

Fig. 4.4. Observations of sea ice thickness. (a) Sea ice thickness derived from ESA CryoSat-2 (background map) and NASA Operation IceBridge measurements (color coded lines) for March/April 2015. Ice thickness distributions obtained by Operation IceBridge in spring for 2009 - 2015 in (b) the Central Arctic and (c) the Beaufort and Chukchi seas (denoted by the dashed black lines). Note the different frequency (vertical) scales in (b) and (c).

Summer Melt

The impact of seasonal melting on ice conditions is illustrated further in **Fig. 4.5**, which compares observations of total summer surface and bottom melt in the Beaufort Sea and in the vicinity of the North Pole between 1959 and 2015. These observations were made either by personnel at drifting ice stations or by autonomous buoys (Perovich and Richter-Menge 2015). Data from 1959 in the Beaufort Sea show less melting overall than in the past decade. Between the end of May and mid-August 2015 at the Beaufort Sea site there was 2.05 m of total melt (0.55 m at the surface, 1.50 m at the bottom), enough to completely melt the multiyear floe where the measurements were made. In contrast, in 2015 at the North Pole site, there was 1.06 m of melt (0.56 m at the surface, 0.50 m at the bottom) between the beginning of melt at this location in early June and the end of the melt season in late-September.

The time series of summer melting indicates that, over the past decade, there has been a significant increase in the amount of bottom melting in the Beaufort Sea. In 2007, 2008, 2014 and 2015, at least 1.5 m of bottom melting occurred, more than twice as much as surface melting and enough to remove much of the multiyear ice in the region. This is in contrast to years prior to 2007, when surface melting was typically greater than bottom melting. Near the North Pole, overall melting was consistently less than in the Beaufort Sea and the multiyear ice never completely melted. On average, there is significantly more surface melt and bottom melt at the Beaufort Sea sites than at the North Pole. The greater amount of bottom melting in the Beaufort Sea, on both an inter-annual and regional basis, is a direct consequence of solar heating of the upper ocean (Perovich and Richter-Menge 2015; see also the essay on *Sea Surface Temperature*). Considerable inter-annual variability is evident in both surface and bottom melting for the Beaufort Sea and North Pole sites.

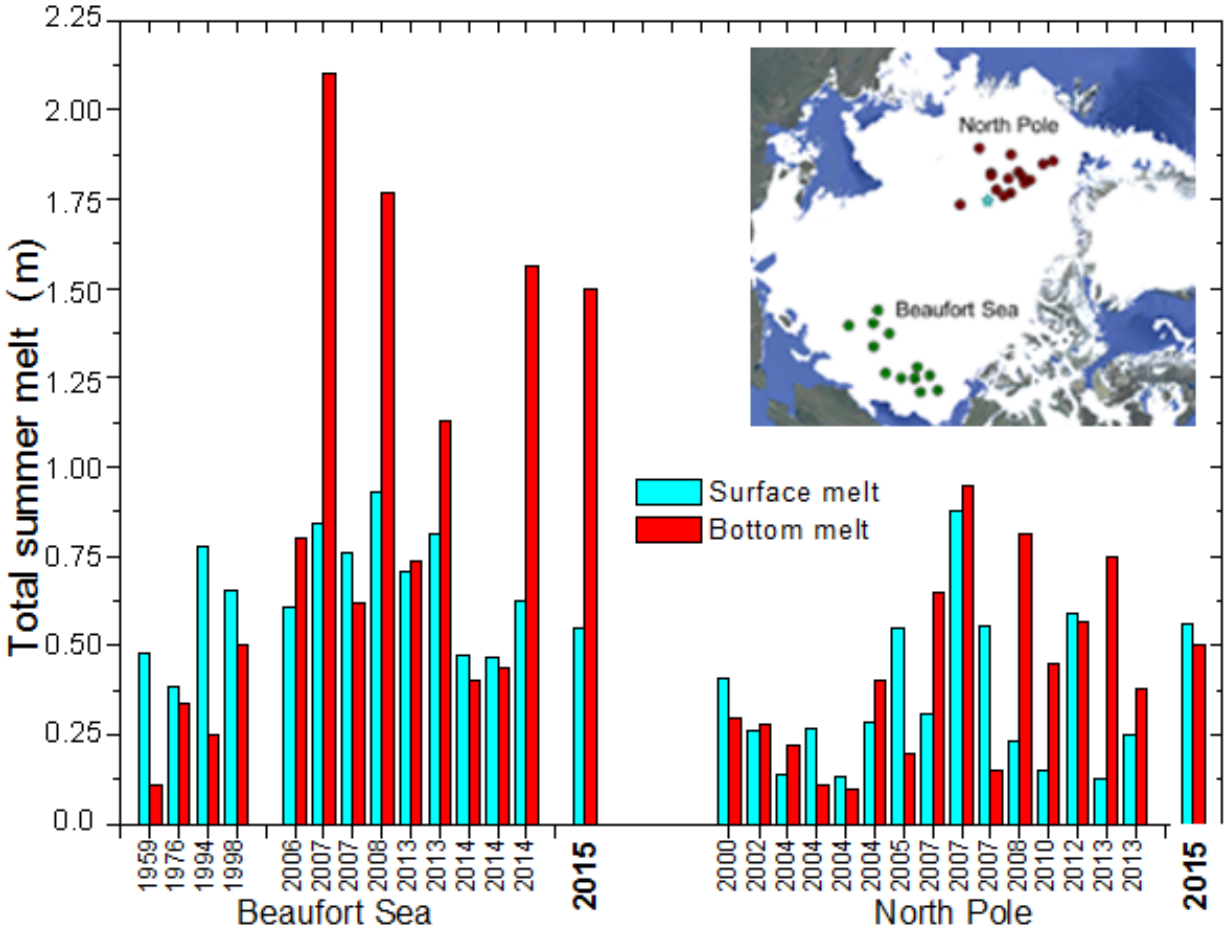

Fig. 4.5. Total amount of summer melt at the ice surface and at the bottom of the ice for various years in the Beaufort Sea and in the vicinity of the North Pole. The insert shows the location of the Beaufort Sea and North Pole measurement sites.

References

Kwok, R., and G. F. Cunningham, 2015: Variability of Arctic sea ice thickness and volume from CryoSat-2, *Phil. Trans. Royal Soc. London A: Math., Phys. Eng. Sci.*, 373, 2045, doi.org/10.1098/rsta.2014.0157.

Kwok, R., and D. A. Rothrock, 2009: Decline in Arctic sea ice thickness from submarine and ICESat records: 1958-2008, *Geophys. Res. Lett.*, 36, doi:10.1029/2009GL039035.

Laxon, S. W., K. A. Giles, A. L. Ridout, D. J. Wingham, R. Willatt, R. Cullen, R. Kwok, A. Schweiger, J. Zhang, C. Haas, S. Hendricks, R. Krishfield, N. Kurtz, S. L. Farrell, M. Davidson, 2013: CryoSat estimates of Arctic sea ice Volume, *Geophys. Res. Lett.*, 40, doi:10.1002/grl.50193.

Maslanik, J., J. Stroeve, C. Fowler, and W. Emery, 2011: Distribution and trends in Arctic sea ice age through spring 2011. *Geophys. Res. Lett.*, 38, doi:10.1029/2011GL047735.

NSIDC at nsidc.org/data/seaice_index.

Perovich, D. K. and J. A. Richter-Menge, Regional variability in sea ice melt in a changing Arctic, 2015: *Proc. Royal Soc.*, 373, doi.org/10.1098/rsta.2014.0165.

Richter-Menge, J., and S. L. Farrell, 2013: Arctic sea ice conditions in spring 2009 - 2013 prior to melt, *Geophys. Res. Lett.*, 40, 5888-5893, doi: 10.1002/2013GL058011.

Tilling, R. L., A. Ridout, A. Shepherd, and D. J. Wingham, 2015; Increased Arctic sea ice volume after anomalously low melting in 2013. *Nat. Geosci.*, 8, 643-646. doi:10.1038/ngeo2489.

Tschudi, M. A., C. Fowler, J. A. Maslanik, and J. A. Stroeve, 2010: Tracking the movement and changing surface characteristics of Arctic sea ice. *IEEE J. Sel. Topics Earth Obs. and Rem. Sens.*, 3, doi: 10.1109/JSTARS.2010.2048305.

Tschudi, M., C. Fowler, and J. Maslanik, 2015: EASE-Grid Sea Ice Age, Version 2. Boulder, Colorado USA. NASA National Snow and Ice Data Center Distributed Active Archive Center, doi.org/10.5067/1UQJWCYPVX61.

Sea Surface Temperature

M. -L. Timmermans[1], A. Proshutinsky[2]

[1]Yale University, New Haven, CT, USA
[2]Woods Hole Oceanographic Institution, Woods Hole, MA, USA

November 25, 2015

Highlights

- Sea surface temperatures (SSTs) in August 2015 off the west coast of Greenland (eastern Baffin Bay) and in the Kara Sea were up to +4°C warmer than the 1982-2010 August mean in these regions.
- The Chukchi Sea and eastern Baffin Bay show the largest ocean surface warming trends; August SSTs are increasing at ~0.5°C/decade in these regions.
- In the Arctic Basin, spatial patterns of August 2015 SST anomalies relative to the 1982-2010 August mean are linked to regional variability in sea-ice retreat.

Summer sea surface temperatures (SSTs) in the Arctic Ocean are set by absorption of solar radiation into the surface layer. In the Barents and Chukchi seas, there is an additional contribution from advection of warm water from the North Atlantic and Pacific oceans, respectively. Solar warming of the ocean surface layer is influenced by the distribution of sea ice (with more solar warming in ice-free regions), and by cloud cover, water color and upper-ocean stratification. August SSTs are an appropriate representation of Arctic Ocean summer SSTs and are not affected by the cooling and subsequent sea-ice growth that takes place in the latter half of September. Here we use SST data from the NOAA Optimum Interpolation (OI) SST Version 2 monthly product, which is a blend of in situ and satellite measurements available at the NOAA/OAR/ESRL PSD, Boulder, Colorado (Reynolds et al. (2002, 2007; http://www.esrl.noaa.gov/psd/data/gridded/data.noaa.oisst.v2.html).

Mean SSTs in August 2015 in ice-free regions ranged from ~0°C in some places to around +7 to +8°C in the Chukchi, Barents, and Kara seas and eastern Baffin Bay off the west coast of Greenland (**Fig. 5.1a**). August 2015 SSTs show the same general spatial distribution as the August mean for the period 1982-2010 (shown in Arctic Report Card 2014, Fig. 5.1a). The August 2015 SST pattern is also similar to that of recent years, e.g., 2012 (**Fig. 5.1b**), which was the summer of lowest minimum sea-ice extent in the satellite record (1979-present).

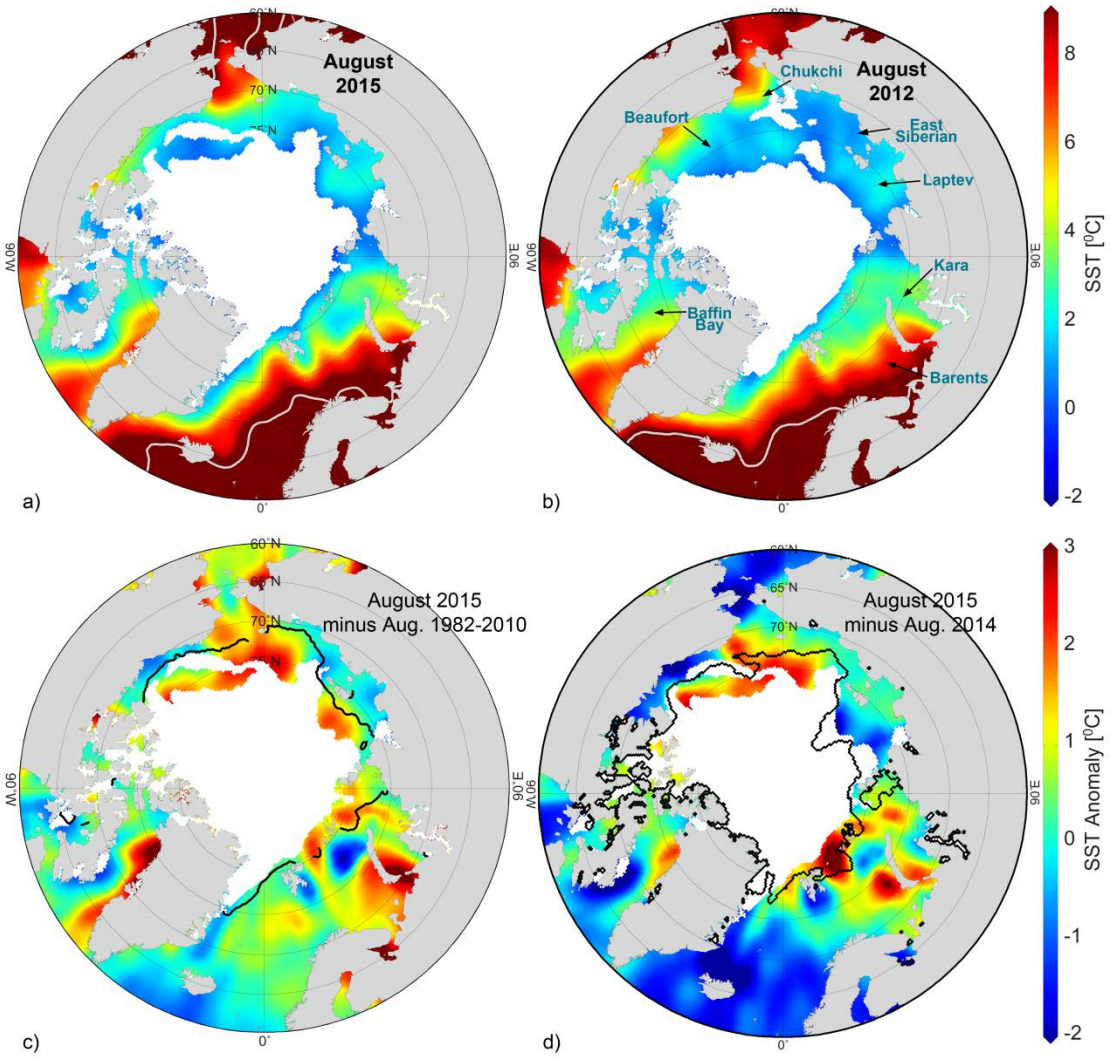

Fig. 5.1. (a) Mean sea surface temperature [SST in °C] in August 2015. White shading is the August 2015 mean sea-ice extent. (b) Mean SST in August 2012; white shading is the August 2012 sea-ice extent. Grey contours in (a) and (b) indicate the 10°C SST isotherm. (c) SST anomalies [°C] in August 2015 relative to the August mean for the period 1982-2010; white shading is the August 2015 mean ice extent and the black line indicates the median ice edge in August for the period 1982-2010. (d) SST anomalies [°C] in August 2015 relative to August 2014; white shading is the August 2015 mean ice extent and the black line indicates the median ice edge for August 2014. Sea-ice extent and ice edge data are from the National Snow and Ice Data Center (NSIDC).

Most boundary regions and marginal seas of the Arctic had anomalously warm SSTs in August 2015 compared to the 1982-2010 August mean (**Fig. 5.1c**). SSTs in these seas, which are mostly ice-free in August, are linked to the timing of local sea-ice retreat; anomalously warm SSTs (up to +3°C relative to 1982-2010) in August 2015 in the Beaufort and Chukchi seas were associated with low sea-ice extents and exposure of surface waters to direct solar heating (**Fig. 5.1c**; see also the essay on *Sea Ice*). The relationship between warm SSTs and reduced sea-ice is further apparent in a comparison between August 2015 and August 2014 SSTs: anomalously warm regions (including to the east of Svalbard, where SSTs were up to +3°C warmer than 1982-2010) are associated with relatively lower sea-ice extents in 2015 compared to 2014 (**Fig. 5.1d**). Although SSTs were warmer in general, August 2015 SSTs were cooler relative to the 1982-2010 average in some regions, e.g., along the southern boundaries of the

Beaufort and East Siberian seas (**Fig. 5.1c**), where summer air temperatures were also below average (see **Fig. 1.2d** in the essay on *Air Temperature*).

Anomalously warm August 2015 SSTs in eastern Baffin Bay are notable this year, with values as much as +4°C warmer than the 1982-2010 August mean; SSTs over the region indicate a general warming trend of about 0.5°C/decade since 1982 (**Fig. 5.2**). If only the past two decades are considered, the linear warming trend in the surface waters of eastern Baffin Bay is about 1°C/decade (+0.10 ± 0.05°C/year). Along the boundaries of the Arctic Basin, the only marginal seas to exhibit statistically significant warming trends are the Chukchi and the Kara seas. Chukchi Sea August SSTs are warming at a rate of about +0.5°C/decade, commensurate with declining trends in summer sea-ice extent in the region. In the Kara Sea, August 2015 SSTs were also around +4°C warmer than the 1982-2010 August mean; SSTs in this sea have warmed by about +0.3°C/decade since 1982. In other marginal seas, warm August SST anomalies observed in 2015 are of similar magnitude to warm anomalies observed in past decades (shown in Arctic Report Card 2014, Fig. 5.3).

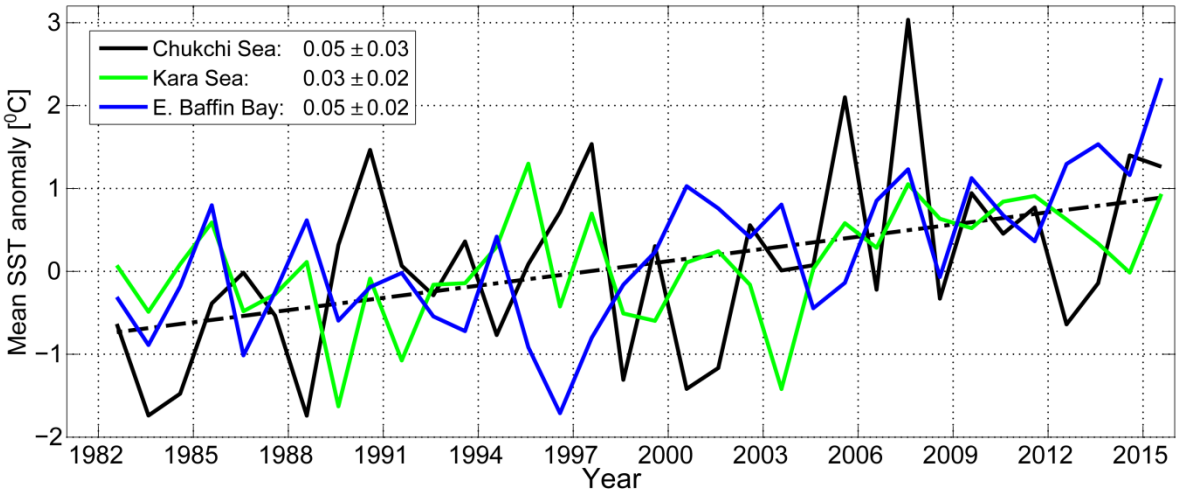

Fig. 5.2. Time series of area-averaged SST anomalies [°C] for August of each year relative to the August mean for the period 1982-2010 for the Chukchi and Kara seas and eastern Baffin Bay (see **Fig. 5.1b**). The dash-dotted black line shows the linear SST trend for the Chukchi Sea (the same warming trend as eastern Baffin Bay). Numbers in the legend correspond to linear trends (with 95% confidence intervals) in °C/year.

References

Reynolds, R. W., N. A. Rayner, T. M. Smith, D. C. Stokes, and W. Wang, 2002: An improved in situ and satellite SST analysis for climate. *J. Climate*, 15, 1609-1625.

Reynolds, R. W., T. M. Smith, C. Liu, D. B. Chelton, K. S. Casey, and M. G. Schlax, 2007: Daily high-resolution-blended analyses for sea surface temperature. *J. Climate*, 20, 5473-5496.

Simmonds, I., 2013: [The Arctic] Sidebar 5.1: The extreme storm in the Arctic Basin in August 2012 [in "State of the Climate in 2012"]. *Bull. American Met. Soc.*, 94(8), S114-S115.

Arctic Ocean Primary Productivity

K. E. Frey[1], J. C. Comiso[2], L. W. Cooper[3], R. R. Gradinger[4], J. M. Grebmeier[3], J. -É. Tremblay[5]

[1]Graduate School of Geography, Clark University, Worcester, Massachusetts, USA
[2]Cryospheric Sciences Laboratory, NASA Goddard Space Flight Center, Greenbelt, MD, USA
[3]Chesapeake Biological Laboratory, University of Maryland Center for Environmental Science, Solomons, MD, USA
[4]Institute of Marine Research, Tromsø, Norway
[5]Québec-Océan and Takuvik, Biology Department, Université Laval, Québec City, QC, Canada

November 25, 2015

Highlights

- Anomalously high chlorophyll-*a* concentrations were observed in 2015 in a number of locations. The most notable 2015 positive anomalies occurred in regions along the shelfbreak in the Bering Sea, southwest of Greenland in the Labrador Sea, and west of Novaya Zemlya in the Barents Sea during May; regions to the east of Greenland south of Fram Strait during June; and localized regions in the Siberian Kara and Laptev seas during July and August.
- The steepest increasing trends in chlorophyll-*a* concentrations during the period 2003-2015 occurred to the southwest of Greenland in the Labrador Sea and the eastern Barents Sea in May, and in the eastern Laptev Sea in July and August.
- Estimates of ocean primary productivity showed widespread positive anomalies for 2015. The highest anomalies for 2015 occurred in the Barents Sea (+16.98 g C/m^2/yr, or 21.0%), the Sea of Okhotsk (+13.26 g C/m^2/yr, or 18.3%), and Baffin Bay/Labrador Sea (+11.20 g C/m^2/yr, or 20.2%). The lowest anomalies occurred in Hudson Bay (+0.31 g C/m^2/yr, or 0.7%) and the western (North American) Arctic (+3.69 g C/m^2/yr, or 10.2%).
- Statistically significant increasing primary productivity trends during the period 2003-2015 occurred in the eastern (Eurasian) Arctic, Barents Sea, Greenland Sea, and North Atlantic; the steepest trends were in the eastern Arctic (19.26 g C/m^2/yr/dec, a 41.9% increase) and the Barents Sea (17.98 g C/m^2/yr/dec, a 30.2% increase).

Introduction

Primary productivity is the rate at which atmospheric or aqueous carbon dioxide is converted by autotrophs (primary producers) to organic material. It occurs most commonly by photosynthesis (i.e., with light as an energy source) but it is also facilitated by chemosynthesis (i.e., using oxidation of methane or other reduced inorganic molecules as an energy source instead of light). Primary production via photosynthesis is a key process, as the producers form the base of the entire food web, both on land and in the oceans. Algae are responsible for nearly all photosynthesis occurring in the oceans, and measurements of the algal pigment chlorophyll (e.g. chlorophyll-*a*) serve as a proxy for the amount of algal biomass present as well as overall plant health. The oceans play a significant role in global carbon budgets via photosynthesis, as approximately half of all global net annual photosynthesis occurs in the oceans, with ~10-15%

of production occurring on the continental shelves alone (Müller-Karger et al. 2005). In the Arctic, inflow shelves alone account for 75% of annual vertically integrated primary production yet only represent 50% of total Arctic Ocean open water (Hill et al. 2013). Furthermore, primary production is strongly dependent upon light availability and the presence of nutrients, and is thus highly seasonal in the Arctic region. In particular, the melting and retreat of sea ice during spring are strong drivers of primary production in the Arctic Ocean and its adjacent shelf seas by enhancing light availability (Barber et al. 2015, Leu et al. 2015).

Recent declines in Arctic sea ice extent (see the essay on *Sea Ice*) have contributed substantially to shifts in primary productivity throughout the Arctic Ocean. One of the most recently published studies investigating trends in Arctic Ocean primary productivity showed that annual net primary productivity across the Arctic Ocean increased ~30% during the period 1998-2012, particularly on interior shelves near the shelfbreak (and to a lesser extent on inflow shelves), where sea ice declines are also accompanied by the presence of upwelled nutrients that are sufficient to support production (Arrigo and van Dijken 2015; Falk-Petersen et al. 2015). In contrast, outflow shelves showed either no change or a significant decline in primary production over the same time period, possibly because nutrients had already been consumed upstream of these regions (Arrigo and van Dijken 2015). However, a recent review indicates that the response of outflow shelves to a changing climate is likely more complex than previously thought, with notable spatial heterogeneity (Michel et al. 2015). Declines in sea ice can also have localized negative effects on primary production through freshening and stratification. This occurrence has been particularly strong in the Canada Basin, where sea ice melt since the 1990s has caused a deepening of the nitracline and establishment of a subsurface chlorophyll maximum where light conditions are not ideal for production (Coupel et al. 2015). In the central Arctic Ocean, where primary productivity is relatively low, sea ice algae can contribute up to 60% of total primary production (owing primarily to low pelagic primary productivity) and have recently been found to be principally limited by nitrate off the slope from the Laptev Sea and silicate at the ice margin near the Atlantic inflow (Fernández-Méndez et al. 2015). Important remaining questions include whether the production of sea ice algae in the central Arctic Ocean has increased over recent years owing to thinning ice and/or if nutrients are sufficient to sustain an increase in phytoplankton concentration with overall sea ice retreat (e.g., Fernández-Méndez et al. 2015). However, it is clear that the response of primary production to sea ice loss is likely both seasonally and spatially dependent (e.g., Tremblay et al. 2015).

Chlorophyll-*a*

Here we present the complete, updated MODIS-Aqua satellite chlorophyll-*a* record for 2003-2015. The 2015 data show anomalously high chlorophyll-*a* concentrations in a number of locations across the Arctic Ocean region, where patterns are spatially and temporally heterogeneous (**Fig. 6.1**). A base period of 2003-2014 was chosen when calculating the 2015 anomalies to maximize the length of the short satellite-based time series. During May 2015, anomalously high concentrations of chlorophyll-*a* occurred along the shelf-break in the Bering Sea (**Figs. 6.1a** and **6.11e**), which is associated with earlier breakup of sea ice in that region (**Fig. 6.1i**). This earlier spring phytoplankton bloom in the Bering Sea and earlier breakup of sea ice are a shift away from recent trends of increasing sea ice cover starting in the early 2000s, primarily during winter (January, February, and March) and spring (April and May) (Frey et al. 2015). The high chlorophyll-*a* anomalies in southeast Greenland in June (**Fig. 6.1f**) are likely associated with sea ice cover as well. Although a significant retreat of sea ice is not apparent in the Greenland Sea during this period (**Fig. 6.1j**), a large fraction of the ice cover that is transported out of the Arctic through Fram Strait ends up in the Greenland Sea where it

ultimately melts. Anomalously high concentrations of chlorophyll-*a* during May 2015 are also found along the southwest coast of Greenland in the northeastern Labrador Sea, where concentrations across a broad area (~600 x 700 km) average over ~16 mg m^{-3} higher than the 2003-2014 mean (**Fig. 6.1e**). Later in the season, anomalously high concentrations emerge mainly in the Kara and Laptev seas during July and August (**Figs 6.1g** and **6.1h**), particularly northeast of Novaya Zemlya and west of the New Siberian Islands.

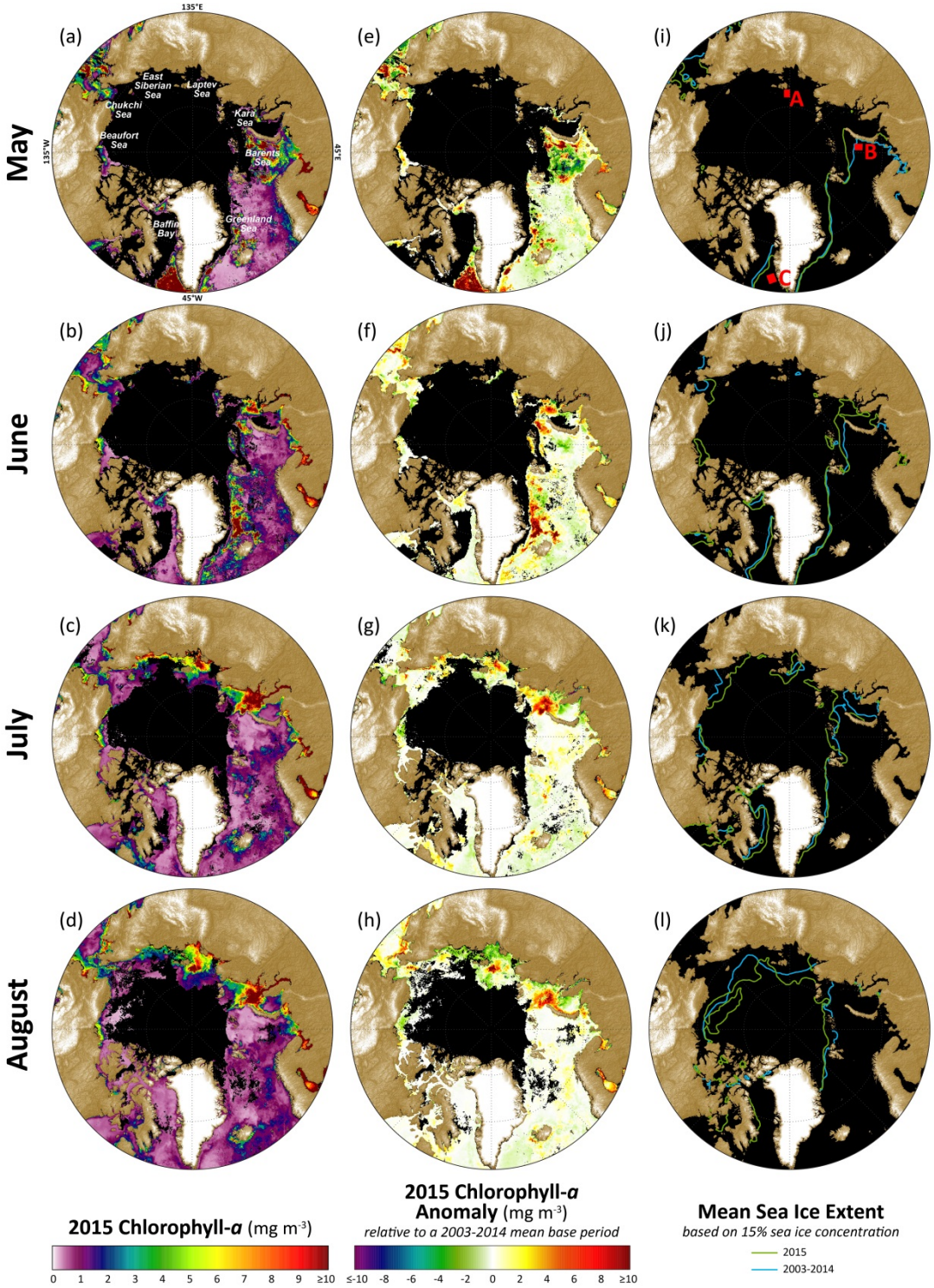

Fig. 6.1. Satellite-based chlorophyll-*a* data across the pan-Arctic region derived using the MODIS-Aqua Reprocessing 2014.0, OC3 algorithm: http://oceancolor.gsfc.nasa.gov/. Chlorophyll-*a* concentrations are shown here (rather than rates of primary production) to foster direct measurements of ocean color and minimize the use of model output. Mean monthly chlorophyll-*a* concentrations during 2015 are shown for (a) May, (b) June, (c) July and (d) August. Monthly anomalies of chlorophyll-*a* concentrations for 2015 (relative to a 2003-2014 mean base period) are also shown (e-h). A base period of 2003-2014 was chosen to maximize the length of the short satellite-based time series. Black areas (a-h) denote a lack of data owing to either clouds or sea ice. Sea ice extent (designated by a 15% sea ice concentration threshold) based on SSM/I data (Cavalieri et al. 1996; Maslanik and Stroeve 1999) for 2003-2014 and 2015 is shown for each of the four months (i-l). The locations A, B and C in (i) indicate the locations for the time series shown in **Fig. 6.3**.

Non-parametric Thiel-Sen median trends indicate the most significant rates of change in the 2003-2015 MODIS-Aqua satellite record in May occur to the southwest of Greenland in the Labrador Sea and to the west of Novaya Zemlya in the Barents Sea (**Fig. 6.2a**), where the latter is associated with declines in sea ice (**Fig. 6.1i**) linked to the Atlantic Water inflow (e.g., Alexeev et al. 2013). During July and August 2015, significant increases in chlorophyll-*a* concentrations are found primarily in the Laptev Sea to the west of the New Siberian Islands (**Figs. 6.2c** and **6.2d**), consistent with the steepest trends identified by Petrenko et al. (2013) utilizing the MODIS-Aqua and SeaWiFS satellite platforms and also linked to declining sea ice cover (**Figs. 6.1k** and **6.1l**). To illustrate the quantitative nature of these trends, three example "hotspot" regions with notably steep trends in chlorophyll-*a* for May, June, July and August 2003-2015 are shown in **Fig. 6.3** (the locations are shown in **Fig. 6.1i**), which include regions in the (A) Laptev Sea northwest of the New Siberian Islands; (B) Barents Sea west of Novaya Zemlya; and (C) Labrador Sea southwest of Greenland. Location A shows significant ($p < 0.1$) trends during July and August, while locations B and C show significant ($p < 0.1$) trends during May. Whereas most non-semi-analytical satellite algorithms (as used here) are affected by large concentrations of CDOM (and may result in erroneously high chlorophyll-*a* concentrations, e.g., Chaves et al. 2015), the sites described above are far enough north that they should not be heavily influenced by Siberian river plumes.

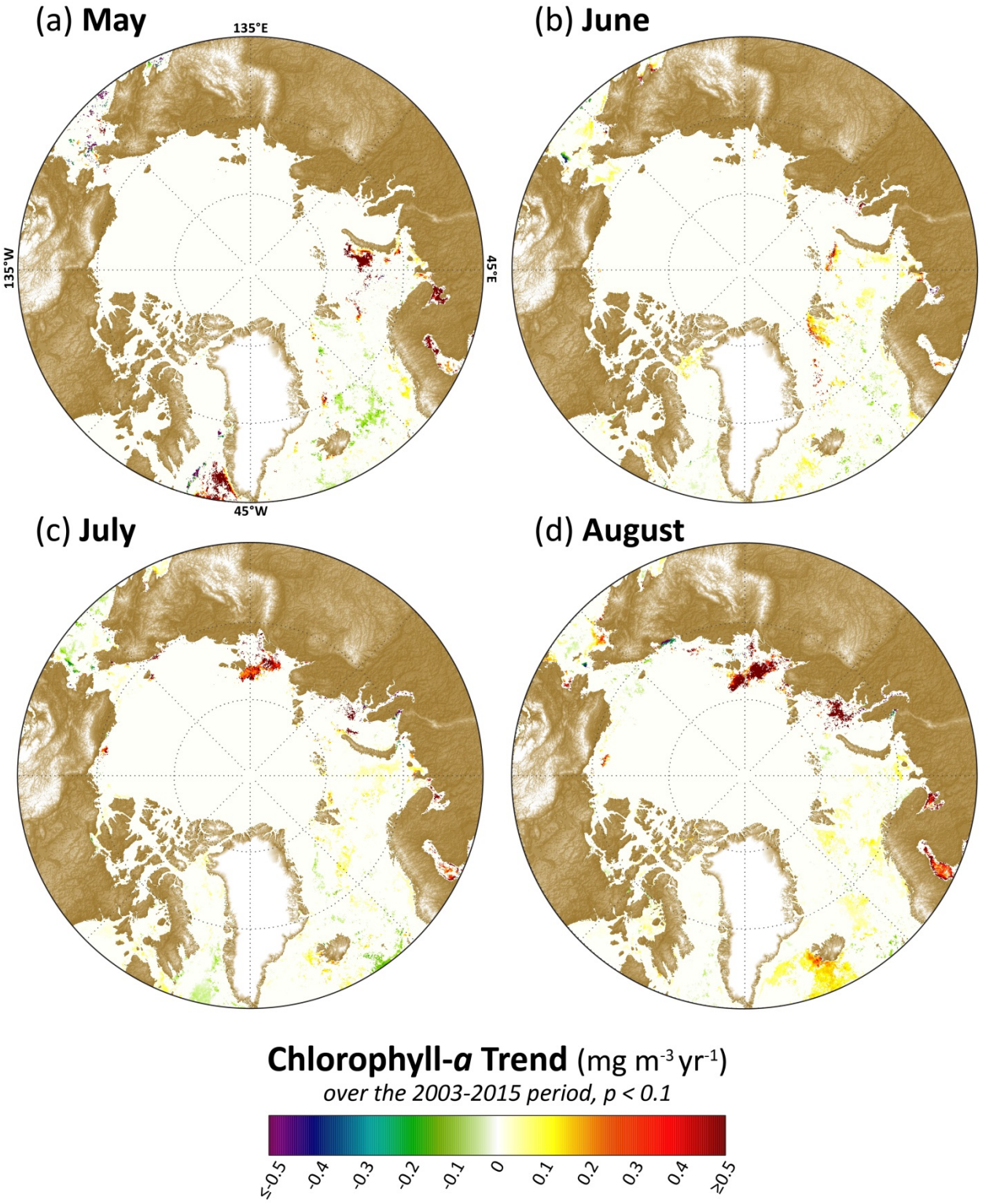

Fig. 6.2. Linear trends in satellite-based chlorophyll-*a* data across the pan-Arctic region derived using the MODIS-Aqua Reprocessing 2014.0, OC3 algorithm: http://oceancolor.gsfc.nasa.gov/. Theil-Sen median trends (2003-2015) in chlorophyll-*a* concentrations for each of the four months are shown (a-d), highlighting only statistically significant trends ($p < 0.1$, using the Mann-Kendall test for trend).

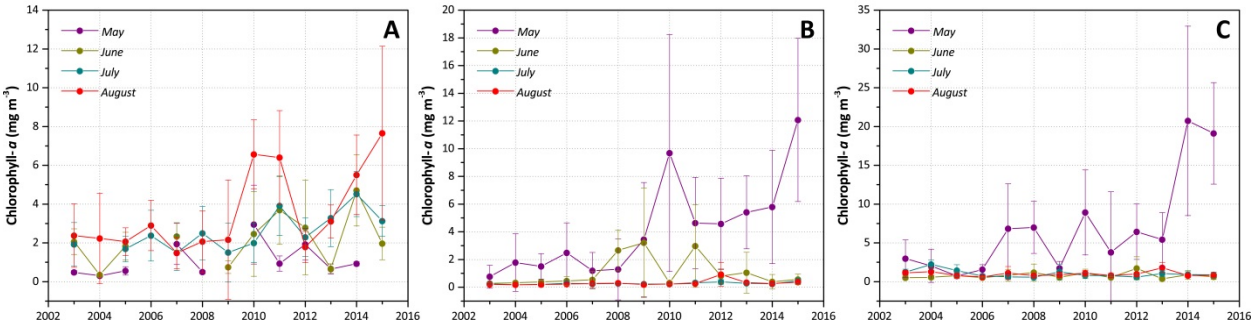

Fig. 6.3. Mean (±1 standard deviation) monthly chlorophyll-*a* concentrations (based on MODIS-Aqua satellite data) for May, June, July and August 2003-2015 for three example "hotspot" locations with notably steep trends in chlorophyll-*a*. The locations (shown in **Fig. 6.1i**) include (A) a ~22,500 km^2 region in the Laptev Sea northwest of the New Siberian Islands; (B) a ~25,400 km^2 region in the Barents Sea west of Novaya Zemlya; and (C) a 32,600 km^2 region in the Labrador Sea southwest of Greenland.

Primary Productivity

Estimates of ocean primary productivity for nine regions (and the average of these nine regions) across the Arctic show increasing trends during the period 2003-2015 in all regions, as well as positive anomalies for 2015 (**Fig. 6.4**, **Table 4.1**). The highest anomalies for 2015 include the Barents Sea (+16.98 g C/m^2/yr, or +21.0%), the Sea of Okhotsk (+13.26 g C/m^2/yr, or +18.3%), and Baffin Bay/Labrador Sea (+11.20 g C/m^2/yr, or +20.2%), while the lowest anomalies include Hudson Bay (+0.31 g C/m^2/yr, or +0.7%) and the western (North American) Arctic (+3.69 g C/m^2/yr, or +10.2%) (**Table 6.1**). Statistically significant trends between 2003 and 2015 occur in the eastern (Eurasian) Arctic, Barents Sea, Greenland Sea, Hudson Bay and North Atlantic, with the steepest trends in the eastern Arctic (19.26 g C/m^2/yr/dec, or a 41.9% increase) and the Barents Sea (17.98 g C/m^2/yr/dec, or a 30.2% increase). There are no statistically significant trends for the western Arctic, Sea of Okhotsk, Bering Sea, Hudson Bay or Baffin Bay/Labrador Sea. Similar trends (except for the North Atlantic) have been reported previously for these regions using both SeaWiFS and MODIS data (Comiso 2015). However, satellite evidence suggests that recent increases in cloudiness have dampened the increases in productivity that would have otherwise occurred as a function of sea ice decline alone (Bélanger et al. 2013). Further challenges remain with linking primary productivity rates as well as depth-integrated chlorophyll biomass throughout the water column to satellite-based surface chlorophyll-*a* values (Tremblay et al. 2015). Satellite-based chlorophyll-*a* and primary productivity estimates are additionally confounded by issues such as river turbidity in coastal regions (e.g., Demidov et al. 2014, Chaves et al. 2015). Efforts to improve satellite retrieval algorithms based on *in situ* observations are thus critical to continue in all regions of the Arctic.

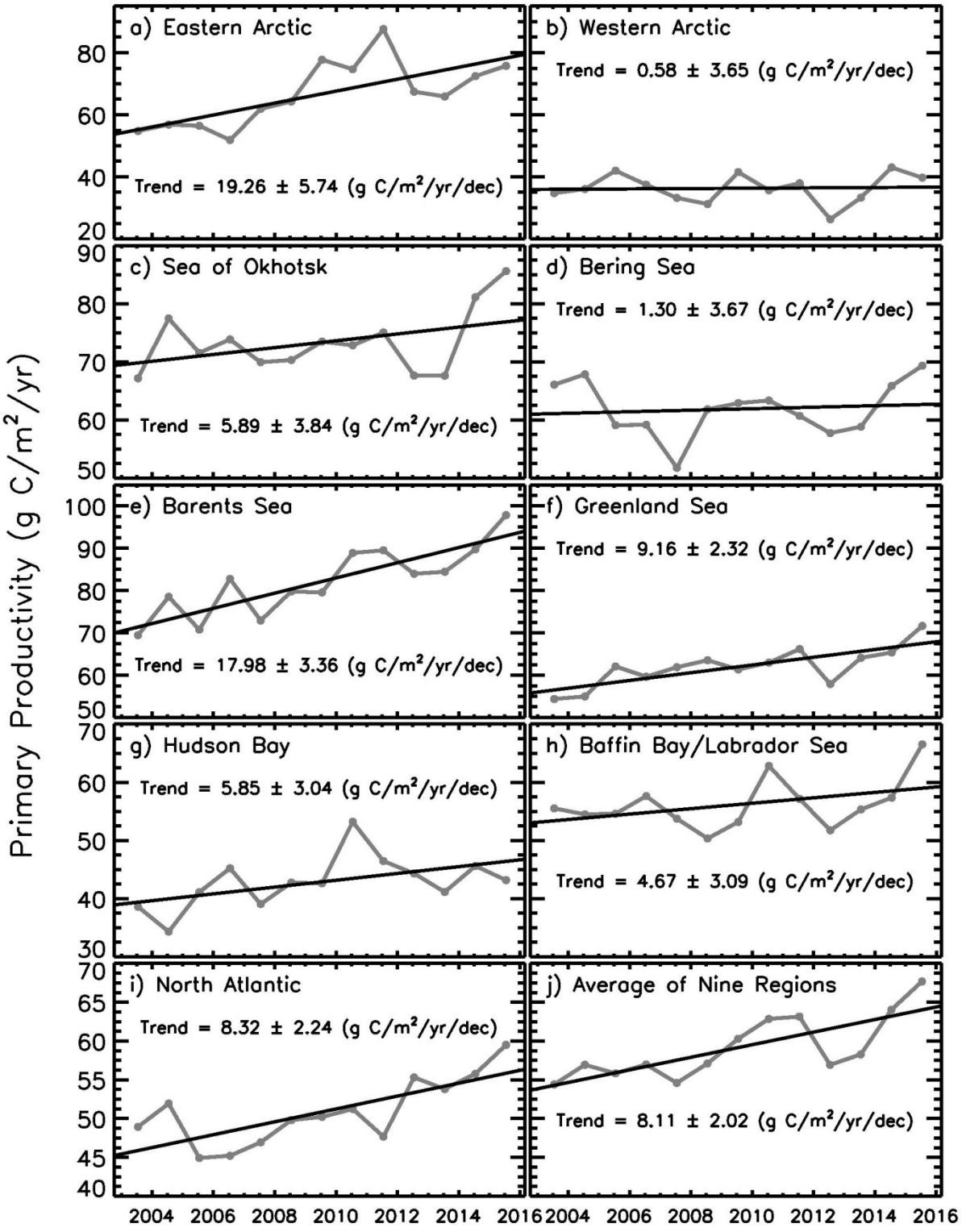

Fig. 6.4. Primary productivity (March-September only) in nine different regions of the Northern Hemisphere, as well as the average of these nine regions, derived using chlorophyll-*a* concentrations from MODIS-Aqua data, AVHRR sea surface temperature data, and additional parameters. Values are calculated according to techniques described by Behrensfield and Falkowski (1997) and represent net primary productivity (NPP). Additional information regarding these data can be found in **Table 6.1**.

Table. 6.1. Linear trends, statistical significance, percent change and primary productivity anomalies in 2015 (March-September) in the nine regions, and overall average, shown in **Fig. 6.4**. Utilizing the Mann-Kendall test for trend, values in **bold** are significant at the 99% confidence level. The percent change is estimated from the linear regression of the 13-year time series. All trends, percent changes, and anomalies are positive.

Region	Trend, 2003-2015 (g C/m^2/yr/dec)	Mann-Kendall *p*-value	% Change	2015 Anomaly (g C/m^2/yr) *from a 2003-2014 base period*	2015 Anomaly (%) *from a 2003-2014 base period*
Eastern Arctic	**19.26**	0.007	41.9	9.78	14.8
Western Arctic	0.58	0.765	1.9	3.69	10.2
Sea of Okhotsk	5.89	0.367	10.1	13.26	18.3
Bering Sea	1.30	0.858	2.6	8.06	13.2
Barents Sea	**17.98**	0.000	30.2	16.98	21.0
Greenland Sea	**9.16**	0.003	19.5	10.45	17.1
Hudson Bay	5.85	0.057	17.8	0.31	0.7
Baffin Bay/Labrador Sea	4.67	0.435	10.5	11.20	20.2
North Atlantic	**8.32**	0.003	21.7	9.35	18.6
Average of Nine Regions	**8.11**	0.001	17.9	9.23	15.8

References

Alexeev, V. A., V. V. Ivanov, R. Kwok, and L. H. Smedsrud, 2013: North Atlantic warming and declining volume of arctic sea ice. *The Cryosphere Discuss.*, 7, 245-265, doi:10.5194/tcd-7-245-2013.

Arrigo, K. R., and G. L. van Dijken, 2015: Continued increases in Arctic Ocean primary production. *Progress in Oceanography*, 136, 60-70.

Barber, D. G., H. Hop, C. J. Mundy, B. Else, I. A. Dmitrenko, J.-É. Tremblay, J. K. Ehn, P. Assmy, M. Daase, L. M. Candlish, and S. Rysgaard. 2015: Selected physical, biological and biogeochemical implications of a rapidly changing Arctic Marginal Ice Zone. *Progress in Oceanography*, doi:10.1016/j.pocean.2015.09.003.

Behrenfeld, M. J., and P. G. Falkowski, 1997: Photosynthetic rates derived from satellite-based chlorophyll concentration. *Limnology and Oceanography*, 42(1), 1-20.

Bélanger, S., M. Babin, and J. É. Tremblay, 2013: Increasing cloudiness in Arctic damps the increase in phytoplankton primary production due to sea ice receding. *Biogeosci.*, 10, 4087-4101, doi:10.5194/bg-10-4087-2013.

Cavalieri, D. J., C. L. Parkinson, P. Gloersen, and H. Zwally, 1996, updated yearly: *Sea Ice Concentrations from Nimbus-7 SMMR and DMSP SSM/I-SSMIS Passive Microwave Data*. [2003-2014]. Boulder, Colorado USA: NASA DAAC at the National Snow and Ice Data Center.

Chaves, J., P. J. Werdell, C. W. Proctor, A. R. Neeley, S. A. Freeman, C. S. Thomas, and S. B. Hooker, 2015: Assessment of ocean color data records from MODIS-Aqua in the western Arctic Ocean. *Deep-Sea Research II*, 118, Part A, 32-43, doi:10.1016/j.dsr2.2015.02.011.

Comiso, J. C., 2015: Variability and trends of the Global Sea Ice Covers and Sea Levels: Effects on Physicochemical Parameters. *Climate and Fresh Water Toxins*, Luis M. Botana, M. Carmen Lauzao and Natalia Vilarino, Eds., De Gruyter, Berlin, Germany.

Coupel, P., D. Ruiz-Pino, M. A. Sicre, J. F. Chen, S. H. Lee, N. Schiffrine, H. L. Li, and J. C. Gascard, 2015: The impact of freshening on phytoplankton production in the Pacific Arctic Ocean. *Progress in Oceanography*, 131, 113-125.

Demidov, A. B., S. A. Mosharov, and P. N. Makkaveev, 2014: Patterns of the Kara Sea primary production in autumn: Biotic and abiotic forcing of subsurface layer. *J. Marine Systems*, 132, 130-149, doi:10.1016/j.jmarsys.2014.01.014.

Falk-Petersen, S., V. Pavlov, J. Berge, F. Cottier, K. M. Kovacs, and C. Lydersen, 2015: At the rainbow's end: high productivity fueled by upwelling along an Arctic shelf. *Polar Biol.*, 38, 5-11, doi:10.1007/s00300-014-1482-1.

Fernandez-Mendez, M., C. Katlein, B. Rabe, M. Nicolaus, I. Peeken, K. Bakker, H. Flores, and A. Boetius, 2015: Photosynthetic production in the central Arctic Ocean during the record sea-ice minimum in 2012. *Biogeosci.*, 12, 3525-3549.

Frey, K. E., G. W. K. Moore, J. M. Grebmeier, and L. W. Cooper, 2015: Divergent Patterns of Recent Sea Ice Cover across the Bering, Chukchi, and Beaufort Seas of the Pacific Arctic Region. *Progress in Oceanography*, 136, 32-49, http://dx.doi.org/10.1016/j.pocean.2015.05.009.

Hill, V. J., P. A. Matrai, E. Olson, S. Suttles, M. Steele, L. A. Codispoti, and R. C. Zimmerman, 2013: Synthesis of integrated primary production in the Arctic Ocean: II. In situ and remotely sensed estimates. *Progress in Oceanography*, 110, 107-125, doi:10.1016/j.pocean.2012.11.005.

Leu, E., C. J. Mundy, P. Assmy, K. Campbell, T. M. Gabrielsen, M. Gosselin, T. Juul-Pedersen, and R. Gradinger, 2015: Arctic spring awakening - Steering principles behind the phenology of vernal ice algal blooms. *Progress in Oceanography,* http://dx.doi.org/10.1016/j.pocean.2015.07.012.

Maslanik, J., and J. Stroeve, 1999, updated daily: *Near-Real-Time DMSP SSM/I-SSMIS Daily Polar Gridded Sea Ice Concentrations*. [2015]. Boulder, Colorado USA: NASA DAAC at the National Snow and Ice Data Center.

Michel, C., J. Hamilton, E. Hansen, D. Barber, M. Reigstad, J. Iacozza, L. Seuthe, and A. Niemi, 2015: Arctic Ocean outflow shelves in the changing Arctic: A review and perspectives. *Progress in Oceanography*, doi:10.1016/j.pocean.2015.08.007.

Müller-Karger, F. E., R. Varela, R. Thunell, R. Luerssen, C. Hu, and J. J. Walsh, 2005: The importance of continental margins in the global carbon cycle. *Geophys. Res. Lett.*, 32, L01602, doi:10.1029/2004GL021346.

Petrenko, D., D. Pozdnyakov, J. Johannessen, F. Counillon, and V. Sychov, 2013: Satellite-derived multi-year trend in primary production in the Arctic Ocean. *Int. J. Remote Sens.*, 34, 3903-3937, http://dx.doi.org/10.1080/01431161.2012.762698.

Tremblay J.-É., L. G. Anderson, P. Matrai, S. Bélanger, C. Michel, P. Coupel, and M. Reigstad, 2015: Global and regional drivers of nutrient supply, primary production and CO_2 drawdown in the changing Arctic Ocean. *Progress in Oceanography*, doi:10.1016/j.pocean.2015.08.009.

Tundra Greenness

H. E. Epstein[1], U. S. Bhatt[2], M. K. Raynolds[3], D. A. Walker[3], P. A. Bieniek[2], C. J. Tucker[4], J. Pinzon[4], I. H. Myers-Smith[5], B. C. Forbes[6], M. Macias-Fauria[7], N. T. Boelman[8], S. K. Sweet[8]

[1]Department of Environmental Sciences, University of Virginia, Charlottesville, VA, USA
[2]Geophysical Institute, University of Alaska Fairbanks, Fairbanks, AK, USA
[3]Institute of Arctic Biology, University of Alaska Fairbanks, Fairbanks, AK, USA
[4]Biospheric Science Branch, NASA Goddard Space Flight Center, Greenbelt, MD, USA
[5]School of GeoSciences, University of Edinburgh, Edinburgh, UK
[6]Arctic Centre, University of Lapland, Rovaniemi, Finland
[7]School of Geography and the Environment, University Oxford, Oxford, UK
[8]Lamont-Doherty Earth Observatory, Columbia University, Palisades, NY, USA

November 17, 2015

Highlights

- Following a general increase over nearly three decades, tundra greenness, derived from remote sensing data, has been declining consistently for the past 2-4 years throughout the Arctic.
- MaxNDVI in 2014 in the Eurasian Arctic and the Arctic as a whole was below the 33-year (1982-2014) average. Temporally-integrated greenness (TI-NDVI) in 2014 had the lowest value on record for Eurasia and the second lowest value for the Arctic as a whole.
- Long-term MaxNDVI and TI-NDVI trends (1992-2014) show tundra "browning" extending over larger areas.
- In contrast to remote sensing observations, field monitoring and experimental studies continue to report increased tundra shrub growth in response to rising air temperatures.

Until recently, the above-ground biomass of Arctic tundra vegetation had been increasing, i.e., vegetation has been "greening", for at least the past three decades (Bhatt et al. 2013, Frost and Epstein 2014). These vegetation changes have not been spatially homogenous throughout the Arctic (e.g., Bhatt et al. 2013), and they now also appear to be changing direction. In fact, the greenness of above-ground tundra vegetation has been declining for the past 2-4 years (Bhatt et al. 2013; Bieniek et al. 2015). These tundra vegetation changes have implications for numerous aspects of arctic ecosystems, including uptake of atmospheric carbon dioxide through photosynthesis, surface energy and water exchanges, plant-herbivore interactions, the state of the active layer and permafrost, and feedbacks to regional and global climate.

Satellite remote sensing has provided the tool for examining the spatio-temporal patterns of Arctic tundra vegetation change with images dating back to the Cold-War era satellites of the 1960s (Frost and Epstein 2014; Epstein et al. 2015). Providing circumpolar coverage of Arctic vegetation greenness since 1982, the Global Inventory Modeling and Mapping Studies (GIMMS-3g) dataset (GIMMS 2013) is a biweekly, Normalized Difference Vegetation Index (NDVI, an index of photosynthetic activity) time series derived largely from Advanced Very High Resolution Radiometer (AVHRR) sensors aboard NOAA satellites. Two vegetation greenness indices are

calculated from the GIMMS-3g: MaxNDVI (maximum annual value) and Time Integrated NDVI (TI-NDVI, sum of the biweekly growing season values of NDVI) (Raynolds et al. 2012; Bhatt et al. 2013). Here we report MaxNDVI and TI-NDVI through 2014, the most recent year for which data are available.

Peak tundra greenness (MaxNDVI) for North America in 2014 ranked 12th and was slightly higher than the mean and mode values for the 33-year record (**Fig. 7.1a**). However, MaxNDVI for the Arctic as a whole and Eurasia were both below the mean values for the record, ranking 19th and 26th, respectively. MaxNDVI has declined 8.4% since 2011 throughout the Arctic. TI-NDVI for 2014 was extremely low; in fact, it was the lowest year on record for Eurasia, and the second lowest year on record for the Arctic as a whole. TI-NDVI for North America ranked 24th and was slightly below the mean value (**Fig. 7.1b**). Since 2011, TI-NDVI has decreased 8.7% for the Arctic as a whole and 12% for Eurasia. Other studies corroborate these recent findings. Bhatt et al. (2013) found a significant breakpoint in the TI-NDVI record for Eurasia in 2005, after which the trend became negative. In addition, Piao et al. (2014) found that the strength of the relationship between growing season NDVI and growing season temperature of Arctic ecosystems declined between 1982 and 2011. Finally, from a field perspective, a long-term experimental warming study conducted in Barrow and Atqasuk, Alaska, demonstrated that plant responses to warming surface air temperatures declined between 1994 and 2012 (Kremers et al. 2015).

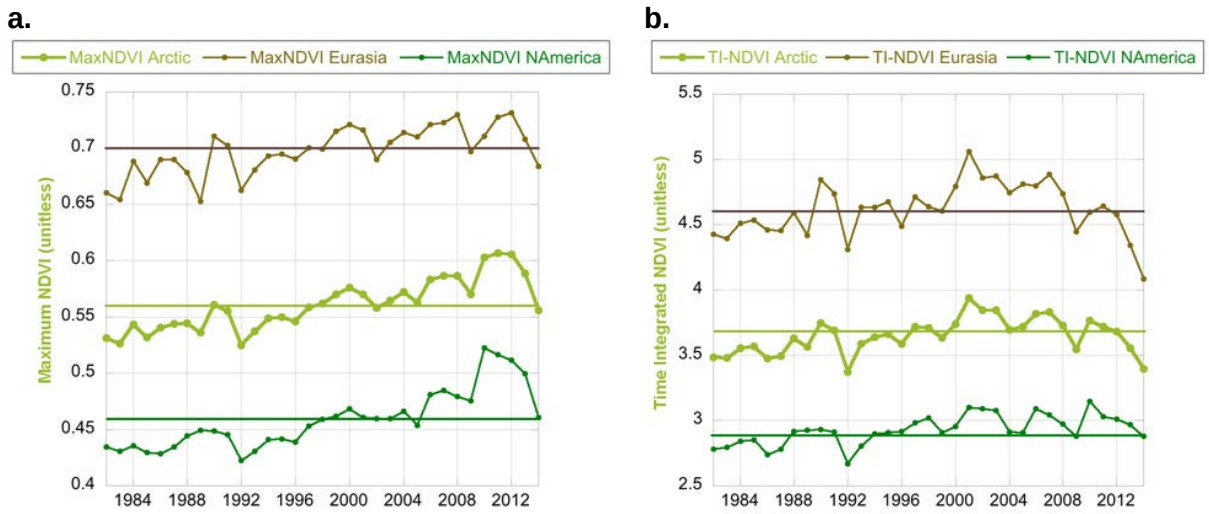

Fig. 7.1. (a, left) MaxNDVI and (b, right) TI-NDVI for North America, Eurasia and the Arctic as a whole over the 33-year satellite remote sensing record (1982-2014). The horizontal lines are the mean values for each data set: MaxNDVI: Arctic 0.56; Eurasia 0.70; North America 0.46; TI-NDVI: Arctic 3.7; Eurasia 4.6; North America 2.9.

In a more detailed remote sensing analysis, Bieniek et al. (2015) evaluated the long-term trends in bi-weekly NDVI values for the period 1982-2013 in three regions in Alaska, defined according to their adjacent seas (Beaufort, East Chukchi and East Bering). They found that trends in bi-weekly NDVI values were greatest (positive) for the Beaufort Sea region during the peak of the growing season (July and August). For the East Chukchi region, trends in NDVI were positive for most of the growing season (with lower magnitudes than the Beaufort region), with the exception of early in the growing season (May), when trends were negative. For the East Bering region, NDVI trends were only positive late in the growing season (September) and the greatest negative trends were early in the growing season (May and June). The negative NDVI trends during the early part of the growing season were correlated with increasing snow water

equivalent values also during May and early June, indicating greater amounts and a longer duration of snow cover. Changes in snow cover (see the essay on *Terrestrial Snow Cover*) and freeze-thaw events are likely to influence tundra vegetation, particularly shrubs (Bienau et al. 2014; Bjorkman et al. 2015; Boulanger-Lapointe et al. 2014; Hollesen et al. 2015; Preece and Phoenix 2015; Ropars et al. 2015), but the patterns of such climatic changes and the mechanisms by which they affect plants remain unclear.

For the entire period of record (1982-2014), linear trends in MaxNDVI continue to show general circumpolar increases in tundra greenness (**Fig. 7.2a**). However, since 1992, there are regions of long-term "browning" (decreasing MaxNDVI values) in northwestern Russia, the Yukon Delta region of western Alaska, and the far northern Canadian Arctic Archipelago. Linear trends in TI-NDVI from 1982-2014 also show browning (decreasing TI-NDVI values) in these regions (**Fig. 7.2b**); however, the vegetation declines extend to Chukotka in northeastern Russia, and to a greater spatial extent in northeastern Siberia, including the Yamal and Taimyr Peninsulas.

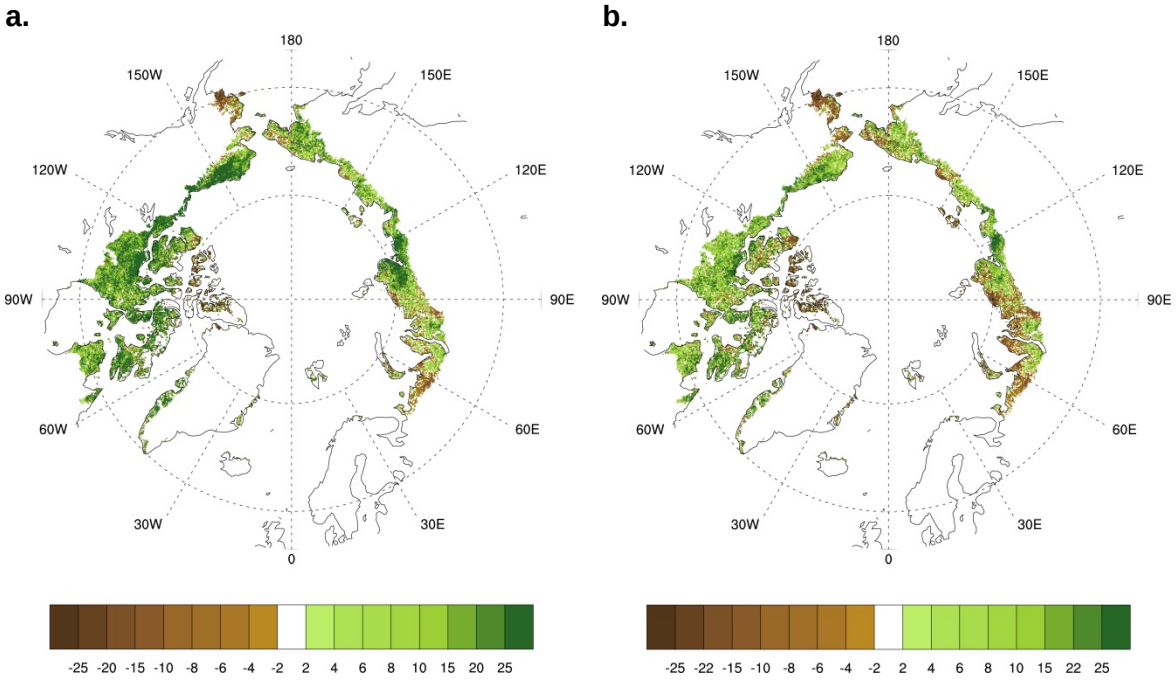

Fig. 7.2. Circumarctic trends (% change, 1982-2014) in the magnitude of (a, left) MaxNDVI for 1982-2014 and (b, right) TI-NDVI.

While there are clear indications from remote sensing and some field observations of recent decreases in tundra vegetation greenness, and browning trends occurring over larger areas, a number of field-based studies are still widely reporting increases in the growth of tundra shrubs (with some exceptions, e.g., Bjerke et al. 2014; Ropars et al. 2015). For instance, increased growth of tundra shrubs throughout the Arctic continues to be reported, but, in a new synthesis of tundra shrub dynamics (Myers-Smith et al. 2015), climate variables explained slightly less than 50% of the variation in shrub growth. This synthesis of shrub growth from 37 tundra sites across nine countries, and utilizing ~42,000 annual growth records of 25 species over the past 60 years, demonstrated that the climate sensitivity of shrub growth varied across the tundra biome, with European sites showing greater sensitivity to summer air temperature than North American sites. Sensitivity to air temperature was greater at sites with higher soil moisture content and for taller shrubs (e.g., alders, willows) growing at the edges of their northern or

upper elevation ranges. Overall, the climate sensitivity of shrub growth was found to be greatest near the center of the north-south extent of the arctic tundra, where a significant amount of carbon is stored in the permafrost as frozen dead organic matter (Hugelius et al. 2013). Thus, shrub growth is most sensitive to climate in the parts of the tundra biome where the greatest impacts of climate change may occur.

In addition to the Myers-Smith et al. (2015) synthesis, other recently published observational studies (in western Greenland, the western Canadian Arctic and Svalbard) have shown increases in growth by a range of morphological shrub types (prostrate dwarf, erect dwarf and tall) due to both summer warming (van der Wal and Stien 2014; Jørgensen et al. 2015) and winter warming (Fraser et al. 2014; Hollesen et al. 2015), as well as by disturbances caused by wildfires, drained lakes and industrial infrastructure (Fraser et al. 2014). These observational studies show positive responses in both evergreen and deciduous shrubs. Newly published experimental warming studies found greater responses in evergreen shrubs compared to deciduous shrubs; experimentally increased summer air temperatures yielded substantial increases in evergreen shrub cover in Barrow and Atqasuk, Alaska (Hollister et al. 2015) and evergreen shrub above-ground biomass in the central Canadian Low Arctic (Zamin et al. 2014). Based on field data collected from two sites on the North Slope of Alaska (in the vicinity of the Toolik Lake Field Station), Sweet et al. (2015) found that greater deciduous shrub abundance almost tripled the ecosystem net carbon uptake compared to evergreen shrub-graminoid communities due to greater leaf area and a 10-day extension of the period of peak greenness.

References

Bhatt, U. S., D. A. Walker, M. K. Raynolds, P. A. Bieniek, H. E. Epstein, J. C. Comiso, J. E. Pinzon, C. J. Tucker, and I. V. Polyakov, 2013: *Recent declines in warming and arctic vegetation greening trends over pan-Arctic tundra, Remote Sensing* (Special NDVI3g Issue), 5, 4229-4254; doi:10.3390/rs5094229.

Bienau, M. J., D. Hattermann, M. Kröncke, L. Kretz, A. Otte, W. L. Eiserhardt, A. Milbau, B. J. Graae, W. Durka, and R. Lutz Eckstein, 2014: Snow cover consistently affects growth and reproduction of *Empetrum hermaphroditum* across latitudinal and local climate gradients. *Alpine Botany*, 124, 115-129.

Bieniek, P. A., U. S. Bhatt, D. A. Walker, M. K. Raynolds, J. C. Comiso, H. E. Epstein, J. E. Pinzon, C. J. Tucker, R. L. Thoman, H. Tran, N. Mölders, M. Steele, J. Zhang, and W. Ermold, 2015: Climate drivers linked to changing seasonality of Alaska coastal tundra vegetation productivity. *Earth Interactions*, in press.

Bjerke, J. W., S. R. Karlsen, Høgda, E. Malnes, J. U. Jepsen, S. Lovibond, D. Vikhamar-Schuler, and H. Tømmervik, 2014: Record-low primary productivity and high plant damage in the Nordic Arctic Region in 2012 caused by multiple weather events and pest outbreaks, *Environ. Res. Lett.*, 9, 084006.

Bjorkman, A. D., S. C. Elmendorf, A. L. Beamish, M. Velland, and G. H. R. Henry, 2015: Contrasting effects of warming and increased snowfall on Arctic tundra plant phenology over the past two decades, *Global Change Biol.*, doi:10.1111/gcb.13051.

Boulanger-Lapointe, N., E. Lévesque, S. Boudreau, G.H.R. Henry, and N. Martin Schmidt, 2014: Population structure and dynamics of willow (*Salix arctica*) in the High Arctic. *J. Biogeogr.*, 41, 1967-1978.

Elmendorf, S. C., G. H. R. Henry, R. D. Hollister, A. M. Fosaa, W. A. Gould, L. Hermanutz, A. Hofgaard, I. S. Jónsdóttir, J. C. Jorgenson, E. Lévesque, B. Magnusson, U. Molau, I. H. Myers-Smith, S. F. Oberbauer, C. Rixen, C. E. Tweedie, and M. D. Walker, 2015: Experiment, monitoring, and gradient methods used to infer climate change effects on plant communities yield consistent patterns. *Proc. Nat. Acad. Sci.*, 112, 448-452.

Epstein, H. E., G. V. Frost, D. A. Walker, and R. Kwok, 2015: The Arctic - Declassified high-resolution visible imagery for observing the Arctic. In, State of the Climate in 2014. *Bull. Amer. Meteorol. Soc.*, 96, S142-S143.

Fraser, R. H., T. C. Lantz, I. Olthof, S. V. Kokelj, and R.A. Sims, 2014: Warming-induced shrubs expansion and lichen decline in the western Canadian Arctic. *Ecosystems*, 17, 1151-1168.

Frost, G. V. and H. E. Epstein, 2014: Tall shrub and tree expansion in Siberian tundra ecotones since the 1960s. *Global Change Biol.*, 20, 1264-1277.

Global Inventory Modeling and Mapping Studies (GIMMS), 2013: Available online: http://gcmd.nasa.gov/records/GCMD_GLCF_GIMMS.html.

Hollesen, J., A. Buchwal, G. Rachlewicz, B. U. Hansen, M. O. Hansen, O. Stecher, and B. Elberling, 2015: Winter warming as an important co-driver for *Betula nana* growth in western Greenland during the past century. *Global Change Biology*, 21, 2410-2423.

Hollister, R. D., J. L. May, K. S. Kremers, C. E. Tweedie, S. F. Oberbauer, J. A. Liebig, T. F. Botting, R. T. Barrett, and J. L. Gregory, 2015: Warming experiments elucidate the drivers of observed directional changes in tundra vegetation. *Ecology and Evolution*, 5, 1881-1895.

Hugelius, G., J. G. Bockheim, P. Camill, B. Elberling, G. Grosse, J. W. Harden, K. Johnson, T. Jorgenson, C. D. Koven, P. Kuhry, G. Michaelson, U. Mishra, J. Palmtag, C. L. Ping, J. O'Donnell, L. Chirmeister, E. A. G. Schuur, Y. Sheng, L. C. Smith, J. Strauss, and Z. Yu, 2013: A new data set for estimating organic carbon storage to 3m depth in soils of the northern circumpolar permafrost region. *Earth System Sci. Data*, 5, 393-402.

Jørgensen, R. H., M. Hallinger, S. Ahlgrimm, J. Friemel, J. Kollmann, and H. Meilby, 2015: Growth response to climatic change over 120 years for Alnus viridis and Salix glauca in West Greenland. *J. Vegetation Sci.*, 26, 155-165.

Kremers, K. S., R. D. Hollister, and S. F. Oberbauer, 2015: Diminished response of arctic plants to warming over time. *PLOS One*, 10, e0116586.

Myers-Smith, I. H., S. C. Elmendorf, P. S. A. Beck, M. Wilmking, M. Hallinger, D. Blok, K. D. Tape, S. A. Rayback, M. Macias-Fauria, B. C. Forbes, J. D. M. Speed, N. Boulanger-Lapointe, C. Rixen, E. Lévesque, N. Martin Schmidt, C. Baittinger, A. J. Trant, L. Hermanutz, L. Sieqwart Collier, M. A. Dawes, T. C. Lantz, S. Weijers, R. Halfdan Jørgensen, A. Buchwal, A. Buras, A. T. Naito, V. Ravolainen, G. Schaepman-Strub, J. A. Wheeler, S. Wipf, K. C. Guay, D. S. Hik, and M. Vellend, 2015: Climate sensitivity of shrub growth across the tundra biome. *Nature Climate Change*, doi:10.1038/nclimate2697.

Piao, S., H. Nan, C. Huntingford, P. Ciais, P. Friedlingstein, S. Sitch, S. Peng, A Ahlström, J. G. Canadell, N. Cong, S. Levis, P. E. Levy, L. Liu, M. R. Lomas, J. Mao, R. B. Myneni, P. Peylin, B. Poulter, S. Shi, G. Yin, N. Viovy, T. Wang, X. H. Wang, S. Zaehle, N. Zeng, Z. Z. Zeng, and A.

P. Chen, 2014: Evidence for a weakening relationship between interannual temperature variability and northern vegetation activity. *Nature Communications* 5, 5018.

Preece, C., and G. K. Pheonix, 2014: Impact of early and late winter icing events on sub-arctic dwarf shrubs. *Plant Biol.*, 15, 125-132.

Raynolds M. K., D. A. Walker, H. E. Epstein, J. E. Pinzon, and C. J. Tucker, 2012: A new estimate of tundra-biome phytomass from trans-Arctic field data and AVHRR NDVI. *Remote Sens. Lett.*, 3, 403-411.

Ropars, P., E. Lévesque, and S. Boudreau, 2015: How do climate and topography influence greening of the forest-tundra ecotone in northern Québec? A dendrochronological analysis of *Betula glandulosa*. *J. Ecology*, 103, 679-690.

Sweet, S. K., K. L. Griffin, H. Steltzer, L. Gough, and N. T. Boelmann, 2015: Greater deciduous shrub abundance extends tundra peak season and increases modeled net CO2 uptake. *Global Change Biol.*, doi:10.1111/gcb.12852.

van der Wal, R., and A. Stien, 2014: High-arctic plants like it hot: a long-term investigation of between-year variability in plant biomass. *Ecology*, 95, 3414-3427.

Zamin, T. J., M. S. Bret-Harte, and P. Grogan, 2014: Evergreen shrubs dominate responses to experimental summer warming and fertilization in Canadian mesic low arctic tundra. *J. Ecology*, 102, 749-766.

River Discharge

R. M. Holmes[1], A. I. Shiklomanov[2,3], S. E. Tank[4], J. W. McClelland[5], M. Tretiakov[6]

[1]Woods Hole Research Center, Falmouth, MA, USA
[2]University of New Hampshire, Durham, NH, USA
[3]Shirshov Institute of Oceanology, Moscow, Russia
[4]University of Alberta, Edmonton, AB, Canada
[5]University of Texas at Austin, Marine Science Institute, Port Aransas, TX, USA
[6]Arctic and Antarctic Research Institute, St. Petersburg, Russia

November 17, 2015

Highlights

- In 2014, combined discharge from the eight largest Arctic rivers (2,487 km^3) was 10% greater than average discharge for the period 1980-1989. Values for 2013 (2,282 km^3) and 2012 (2,240 km^3) were 1% greater than and 1% less than the 1980-1989 average, respectively.
- For the first seven months of 2015, the combined discharge for the six largest Eurasian Arctic rivers shows that peak discharge was 10% greater and five days earlier than the 1980-1989 average for those months.

River discharge integrates hydrologic processes occurring throughout the surrounding landscape; consequently, changes in the discharge of large rivers can be a sensitive indicator of widespread changes in watersheds (Rawlins et al. 2010, Holmes et al. 2012). Changes in river discharge also impact coastal and ocean chemistry, biology and circulation. This interaction is particularly strong in the Arctic because rivers in this region transport >10% of global river discharge but the Arctic Ocean contains only ~1% of the global ocean volume (Aagaard and Carmack 1989, McClelland et al. 2012).

Here we report annual river discharge values for the eight largest Arctic rivers since 2011, when river discharge was last featured in the Arctic Report Card (Shiklomanov and Lammers 2011), and compare these recent observations to a 1980-1989 reference period (the first decade with data from all eight rivers). Six of the eight rivers lie in Eurasia, and the other two are in North America. Together, the watersheds of these eight rivers cover 70% of the pan-Arctic drainage area, so the rivers featured here account for the majority of riverine freshwater inputs to the Arctic Ocean (**Fig. 8.1**).

Fig. 8.1. Map showing the watersheds of the eight rivers featured in this report. Together they cover 70% of the 16.8 x 10^6 km^2 pan-Arctic watershed. The red dots show the location of the discharge monitoring stations and the red line shows the boundary of the pan-Arctic watershed.

A long-term increase in Arctic river discharge has been well documented and is primarily a function of increasing precipitation linked to global warming (Peterson et al. 2002, McClelland et al. 2006, Shiklomanov and Lammers 2009, Overeem and Syvitski 2010, Rawlins et al. 2010). The long-term discharge trend is greatest for rivers of the Eurasian Arctic and constitutes the strongest evidence of intensification of the Arctic freshwater cycle (Rawlins et al. 2010).

The results presented here demonstrate that Eurasian Arctic river discharge generally declined between 2007 and 2012 and then began to increase again in 2013 and 2014 (**Fig. 8.2**, **Table 8.1**). The discharge increase seems to be continuing in 2015, as over the first seven months of 2015 the combined discharge of these rivers was 10% greater than the 1980-1989 average for those same months (**Table 8.2**). The short-term variability in Eurasian Arctic river discharge is consistent with previous increases and decreases over 4-6 year intervals in the past (**Fig. 8.2**). Overall, the most recent data indicate a continuing long-term increase in Eurasian Arctic river discharge.

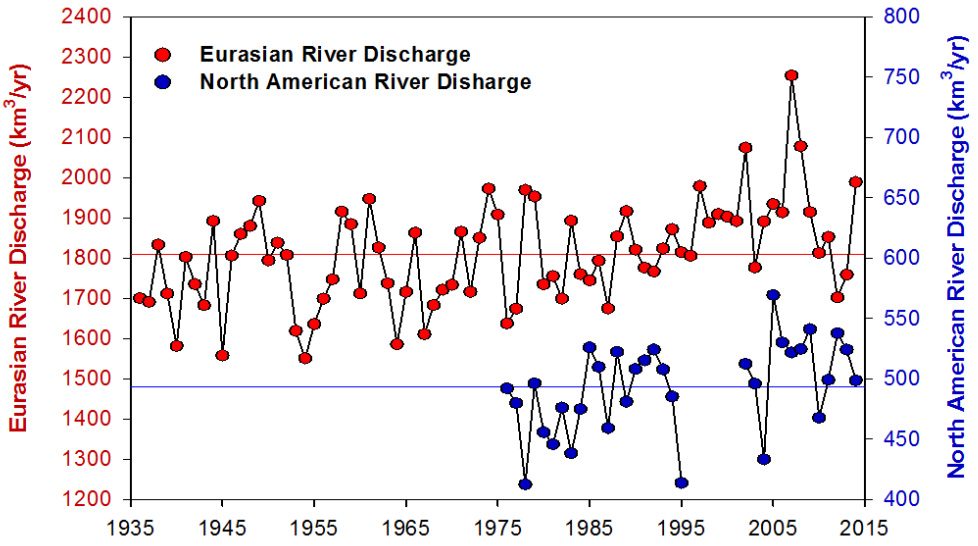

Fig. 8.2. Long-term records of annual discharge for Eurasian and North American Arctic rivers. The Eurasian rivers are the Severnaya Dvina, Pechora, Ob', Yenisey, Lena, and Kolyma. The North American rivers are the Yukon and Mackenzie. Note the different scales for the Eurasian and North American river discharge; discharge from the former is 3-4 times greater than it is from the latter. The horizontal lines show long-term mean discharge values for the Eurasian (1,809 km^3 y^{-1}) and North American (493 km^3 y^{-1}) rivers.

Table 8.1. Annual discharge for 2012, 2013 and 2014 for the eight largest Arctic rivers compared to long-term and decadal averages back to the start of observations. Red values indicate provisional data, which are subject to modification before official data are published. In practice, the modifications usually do not substantially impact annual discharge estimates.

Discharge (km^3/y)									
	Yukon	**Mackenzie**	**Pechora**	**S. Dvina**	**Ob'**	**Yenisey**	**Lena**	**Kolyma**	**Sum**
2014	*227*	272	116	91	448	640	607	86	2487
2013	213	311	82	97	372	527	600	80	2282
2012	232	306	103	117	300	458	665	59	2240
Average 2010-2014	212	293	106	95	385	582	582	74	2329
Average 2000-2009	207	305	124	103	415	640	603	78	2475
Average 1990-1999	217	275	117	111	405	613	532	68	2338
Average 1980-1989	206	273	108	100	376	582	549	68	2262
Average 1970-1979	184	292	108	94	441	591	529	65	2304
Average 1960-1969			112	98	376	546	535	73	
Average 1950-1959			110	108	380	566	511	74	
Average 1940-1949			102	100	424	578	498	72	
Average for Period of Record	206	286	110	100	400	588	539	71	2300

For the North American Arctic rivers considered here (Yukon and Mackenzie), the combined discharge declined each year from 2012 to 2014, yet in each of those years the combined discharge was greater than the long-term average (**Fig. 8.2**, **Table 8.1**). Thus, as discussed for Eurasian rivers, these most recent data indicate a longer-term pattern of increasing river discharge (**Fig. 8.2**). Indeed the overall trends of increasing discharge since 1976 are remarkably similar for the North American and Eurasian rivers. Increases per decade since 1976 were 3.1±2.0% for the Eurasian rivers and 2.6±1.7% for the North American rivers. Increases per decade follow a Mann-Kendall trend analysis; error bounds are 95% confidence intervals for the trend.

Considering the eight Eurasian and North American Arctic rivers together, their combined discharge in 2014 (2487 km^3) was 10% greater than average discharge from 1980-1989. Comparing 2014 to 2012, the combined discharge of these eight rivers was almost 250 km^3 greater in 2014. For perspective, 250 km^3 is approximately 14 times the annual discharge of the Hudson River, the largest river on the East Coast of the United States.

An assessment of the combined daily discharge of Eurasian Arctic rivers for the period January 1 through July 31 2015 reveals an earlier and higher peak discharge compared to the 1980-1989 average (**Fig. 8.3**, **Table 8.2**). The 2015 peak discharge for these six rivers was 10% higher and five days earlier than the 1980-1989 average. The higher and earlier discharge peak is consistent with the early spring melt of deeper snow in Eurasia (see the essay on *Terrestrial Snow Cover*).

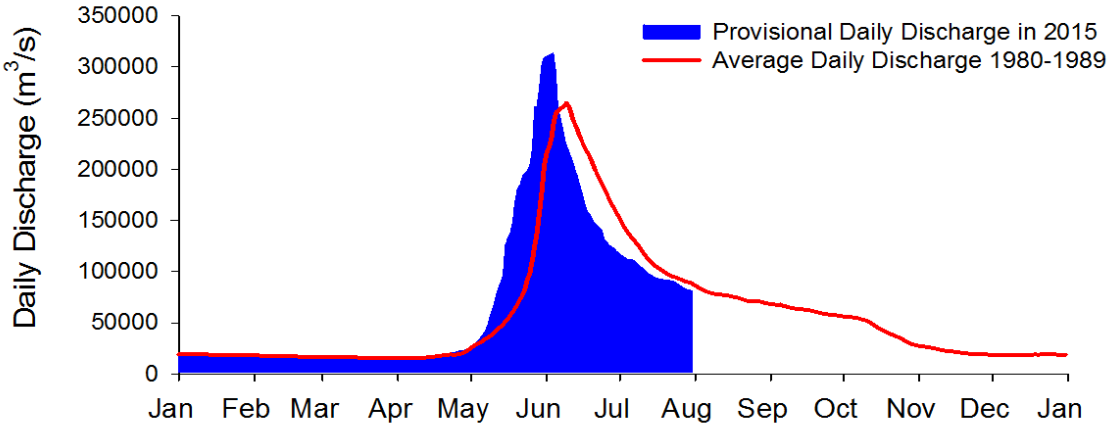

Fig. 8.3. Average combined daily discharge for the six Eurasian Arctic rivers for the period 1 January through 31 July 2015 compared to the 1980-1989 average for those months.

Table 8.2. Cumulative Eurasian river discharge for the first seven months of 2015 compared to the January-July average for 1980-1989. All 2015 data are provisional.

1 January – 31 July Discharge (km^3)							
	Pechora	**S. Dvina**	**Ob'**	**Yenisey**	**Lena**	**Kolyma**	**Sum**
2015	95	51	290	447	421	51	1355
1980-1989 Ave.	82	73	244	426	361	44	1229

References

Aagaard, K., and E. C. Carmack, 1989: The role of sea ice and other fresh water in the Arctic circulation. *J. Geophys. Res.* 94(C10): 14485-14498.

Holmes, R. M., M. T. Coe, G. J. Fiske, T. Gurtovaya, J. W. McClelland, A. I. Shiklomanov, R. G. M. Spencer, S. E. Tank, and A. V. Zhulidov, 2013: Climate change impacts on the hydrology and biogeochemistry of Arctic Rivers. *Global Impacts of Climate Change on Inland Waters*, edited by C. R. Goldman, M. Kumagai, and R. D. Robarts, Wiley, 3-26.

McClelland, J. W., S. J. Dery, B. J. Peterson, R. M. Holmes, and E. F. Wood, 2006: A pan-arctic evaluation of changes in river discharge during the latter half of the 20th century. *Geophys. Res. Lett*. 33, L06715, doi:06710.01029/02006GL025753.

McClelland, J. W., R. M. Holmes, K. H. Dunton, and R. Macdonald, 2012: The Arctic Ocean estuary. *Estuar. Coast.* 35, 353-368, doi:10.1007/s12237-010-9357-3.

Overeem, I., and J. P. M. Syvitski, 2010: Shifting discharge peaks in Arctic rivers, 1977-2007. *Geogr. Ann.*, 92a, 285-296.

Peterson, B. J., R. M. Holmes, J. W. McClelland, C. J. Vorosmarty, R. B. Lammers, A. I. Shiklomanov, I. A. Shiklomanov, and S. Rahmstorf, 2002: Increasing river discharge to the Arctic Ocean. *Science*, 298, 2171-2173.

Rawlins, M. A., et al. 2010. Analysis of the arctic system freshwater cycle intensification: observations and expectations. *J. Climate*, 23, doi: 10.1175/2010JCLI3421.1.

Shiklomanov A. I., and R. B. Lammers, 2009: Record Russian river discharge in 2007 and the limits of analysis. *Environ. Res. Lett.* 4, doi: 10.1088/1748-9326/4/4/045015.

Shiklomanov, A. I., and R. B. Lammers, 2011: River Discharge. In *Arctic Report Card: Update for 2011*, http://www.arctic.noaa.gov/report11/river_discharge.html.

Walruses in a Time of Climate Change

K. M. Kovacs[1], P. Lemons[2], J. G. MacCracken[2], C. Lydersen[1]

[1]Norwegian Polar Institute, Tromsø, Norway
[2]U.S. Fish and Wildlife Service, Anchorage, AK, USA

November 25, 2015

Highlights

- Sea ice deterioration due to global climate change is thought to be the most pervasive threat to ice-associated marine mammals in the Arctic, including walruses.
- Current population trajectories of some stocks of walruses are also influenced greatly by hunting levels, including those of the distant past in some areas, which results in a mosaic that includes an exponential increase in walruses in the region (Svalbard) that has experienced the fastest and most profound regional sea ice losses over recent decades.
- Habitat loss will be exacerbated for walruses by additional climate-change related factors such as ocean acidification, increased shipping and increasing development in the North, including oil and gas extraction, as well as increased disease and contaminant risks.

Introduction

Concern has been raised regarding the impacts of climate change on the conservation status of ice-affiliated marine mammals in the Arctic since the first suggestions that the planet's climate was warming. It is generally thought that global climate change is already the most pervasive threat to arctic pinnipeds (seals and walruses) (Hoffman 1995; Tynan and DeMaster 1997; Laidre et al. 2008, 2015; Huntington 2009; Kovacs et al. 2011, 2012; Jay et al. 2011; MacCracken 2012). But, there is significant regional variation in the rates of change of key environmental features within the Arctic, including the extent and seasonal duration of sea ice. Further, mammalian population trajectories are influenced by a host of factors, including a species' adaptive capacity (evolutionary potential, dispersal ability, genetic diversity, breadth of feeding niche, tolerance of various environmental conditions, behavioral plasticity, etc.; see Gilg et al. 2012 for a summary) and in the case of many marine mammals, human harvest levels past and present.

Walruses

Walruses make an interesting case study in this time of rapid climate change. They are broadly distributed in the Arctic but occur as two distinct subspecies within disparate ranges. *Odobenus rosmarus rosmarus* occurs in the North Atlantic Region (including the Barents Sea and adjacent seas to the east) while *O. r. divergence* occurs in the North Pacific region (Chukchi, Bering and western Beaufort seas) westward through to the Laptev Sea (Lindqvist et al. 2008). Both subspecies are benthic (bottom) feeders whose diet is dominated by bottom-dwelling invertebrates (e.g., Sheffield and Grebmeier 2009; Skoglund et al. 2010), so their foraging areas are located in shallow waters.

Walruses give birth on sea ice in the late spring and mate along ice edges in the drifting pack-ice during the winter. They also use ice extensively as a haul-out platform throughout much or all of the year, depending on sex, season and general availability of sea ice in areas that afford feeding opportunities. Sea ice also provides shelter from storms and from some predators. The rates of change in sea ice occurring in the ranges of the two subspecies are, in general terms, very different, with the rate of seasonal-ice-cover losses in the Atlantic region being faster than the rate in the Pacific region (Laidre et al. 2015). But, straightforward predictions for walrus trends on the basis of this important birthing, breeding and haul-out habitat do not work particularly well for assessing current or near-future states because varied hunting regimes in the distant past (100s of years ago), recent past (decades) and present, across the range of walruses heavily affect the population trajectories (**Fig. 9.1**). In addition geographic features - including the location of current summer sea ice margins compared to possible (shallow, benthic) feeding areas and also possible locations for terrestrial (summer) haul-out in comparison to feeding grounds - influence the energetics of accessing food differently on a regional basis.

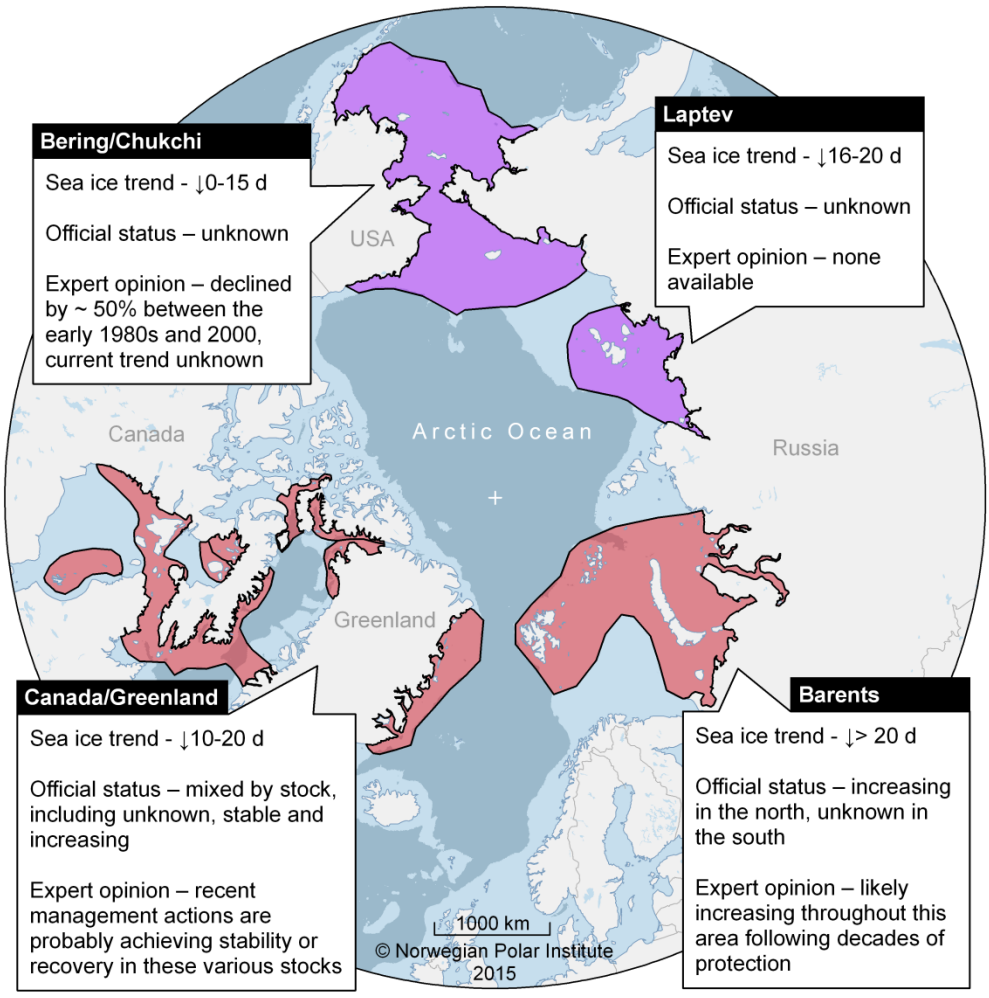

Fig. 9.1. Regional comparison of trends in sea ice (length of the summer season - number of days less coverage per decade) and walrus stocks according to Laidre et al. (2015) and expert opinion for Pacific (purple) and Atlantic walrus (red) by region. Stocks are identified by the black boundary lines.

Pacific Walrus Population

The latest research indicates that the Pacific walrus population in the Bering and Chukchi seas likely declined throughout the period from about 1980 to 2000 (MacCracken et al. 2014, Taylor and Udevitz 2015). The weight of evidence suggests that this population had actually approached the carrying capacity of their environment in the late 1970s - early 1980s, due to restrictions on subsistence harvests (Fay et al. 1989, 1997, Hills and Gilbert 1994). But, population models suggest a subsequent decline of approximately 50% (Taylor and Udevitz 2015), likely due to changes in vital rates associated with a population at or near carrying capacity. This decline has likely been exacerbated by declines in sea ice, which are associated with global climate change that are reducing the carrying capacity of the environment for walruses (Garlich-Miller et al. 2011, Taylor and Udevitz 2015). Hypothesized mechanisms include (1) the retreat of sea ice to a position over the deep Arctic Ocean basin, forcing walruses to use land-based haulouts where trampling events result in increased mortality to young animals (Jay and Fischbach 2008, Udevitz et al. 2012) and (2) the decline in sea ice reducing walruses' access to prey, which could affect adult female body condition, ultimately reducing calf survival and recruitment (Jay et al. 2011, Taylor and Udevitz 2015). While the use of land-based haulout areas is not novel for walruses, females with dependent young typically utilize sea ice for hauling out (Fay 1982), which allows them to avoid particularly large land-based haulouts where crowding and trampling events can result in large mortality events of dependent young (Fischbach et al. 2009). Unregulated subsistence harvests in the United States and subsistence and commercial harvests in the Russian Federation (commercial harvests ended in 1990) have contributed to declines of Pacific walruses in the past (Fay et al. 1989, Fay and Bowlby 1994). However, since 1992, harvest of this subspecies has been limited to subsistence takes by communities in Alaska and Chukotka (Garlich-Miller et al. 2006) and is currently not considered a threat to the population (USFWS 2011). However, a major remaining concern is the effects of declining sea ice on future energetics of females and young animals that must now make feeding trips from coastal haulouts to areas of high prey abundance (180 km one-way), rather than utilizing nearby ice edges for resting as they did in the past. Current research will hopefully soon shed light on this potential stressor. The status of the Pacific walrus stock in the Laptev Sea is currently unknown (Laidre et al. 2015).

Atlantic Walrus Population

Atlantic walrus abundance, similar to the situation in the Pacific, has largely been dictated in the past by hunting intensities through time (Stewart et al. 2014a, 2014b). Although some stock boundaries are still uncertain, seven eastern Canada/west Greenland stocks are generally recognized in addition to the east Greenland stock. The subpopulation that occupies the Barents Sea and adjacent areas to the south and east in Russia, are also included within the Atlantic subspecies range. The higher degree of population sub-structure in the Atlantic subspecies is likely a product of the extensive archipelago systems, continuous versus discontinuous regions of sea ice enhancing, or limiting connectivity, and a few deep water areas that promote isolation among groups.

Historically, walrus hunting increased as bowhead (*Balaena mysticetus*) whaling declined in both the northwest and northeast Atlantic. Accessible stocks were heavily depleted before protective measures came into place in the early- (Canada) and mid-1900s (Norway and Russia), and, in the case of Greenland, much more recently, with quotas being established in the early 2000s. Stewart et al. (2014b), Witting and Born (2014) and Gjertz et al. (1998) have explored Canadian, Greenlandic and Barents Sea hunting histories, respectively, within the limits of available data. All conclude that landed catches were far too high to be sustainable and

that depletions certainly occurred throughout most of the range of the Atlantic subspecies, even in isolated areas with heavy ice cover such as northeast Greenland and the Frans Josef Land Archipelago. A recent example of a significant reduction is the decline that took place in the west Greenland/Baffin Bay stock in the period 1900-1960, when this stock was reduced by 80%. But, management interventions (i.e., controlling human harvesting; see Wiig et al. 2014) have resulted in signs of recovery in this and some other previously depleted North Atlantic stocks (Witting and Born 2014). The total abundance of Atlantic walruses is not known, but it is likely that they number in excess of 25,000 animals when all of the various stock numbers are combined. This number is not markedly different from the estimates that have been made for this subspecies over several decades, though the dynamics of individual stocks have shown varied trends and some areas have never been surveyed. Protective measures recently put in place in Greenland are likely to go a long way towards ensuring more stable population numbers within the Atlantic subspecies.

A particularly noteworthy case with respect to trying to detect climate change impacts on arctic pinniped populations, among other stressors, is the situation for walruses in Svalbard, Norway. Svalbard is an Arctic hot-spot that is experiencing dramatic sea ice declines and warming ocean and air temperatures (Beszczynska-Möller et al. 2012; Nordli et al. 2014; Laidre et al. 2015), and yet walrus numbers in the archipelago are increasing exponentially (Lydersen et al. 2008; Kovacs et al. 2014). This situation arises because of the extreme historical overexploitation of the walruses in this area that took place over several hundred years up until the 1950s. When walruses did finally become protected in Svalbard in 1952, there were at best a few hundred animals occupying a few sites. But, after 60 years of complete protection from hunting, with some special no-go reserve areas, recovery is taking place. More females with calves are documented during surveys and historically used sites are being reoccupied as walruses continue to expand through the archipelago. These changes are occurring despite the fact that overall carrying capacity of the region for walruses is almost certainly declining because of sea ice declines. Studies are currently taking place to determine whether seasonal movement patterns are being affected by the changing sea ice conditions. This includes the use of remote cameras to study occupancy patterns at several haul-out sites, exploring the potential impacts of various sources of disturbance. For instance, the impact of rapidly expanding marine tourism activities is being investigated, via assessments at visited and non-visited sites.

Potential Threats to Walruses

Because walruses will make use of terrestrial sites for haul-out, extinction due to climate change impacts on sea ice is unlikely to occur for this species. But, it is certain that land-based sites alone will not support the same number of walruses that the mixed seasonal use of sea ice and land has permitted in the past (Jay et al. 2012; Kovacs et al. 2012). Additionally, documented indeclines in the northern Bering Sea among dominant clam populations that are critical prey for walruses, associated with reductions in sea ice declines (e.g., Grebmeier et al. 2010), provide cause for concern; such ecosystem changes are clearly important for walruses and other animals. It is also expected that other climate-change related factors such as acidification, increased shipping, increasing development in the North including oil and gas extraction, disease and contaminant risks, will all represent increasing threats to walruses in the future (e.g., Kovacs et al. 2012; MacCracken 2012, MacCracken et al. 2013).

Ocean acidification. Global warming has already led to increased acidification (lowered pH) of the world's oceans, particularly in the Arctic (AMAP 2013; Mathis 2011). Ocean acidification reduces the saturation state of carbonate ions in the water, which can affect the growth, development and survival of calcifying invertebrates that are the major prey of walruses.

However, the response of species to lowered pH is highly variable depending on the species, life stage, duration and level of exposure, adaptive capacity, and evolutionary history. To date, there is no evidence that ocean acidification is affecting walrus prey. It appears that carbonate saturation states are still adequate, though tipping points might be reached by as early as 2020 in the Arctic Ocean (Freely et al. 2009). This could have negative implications for bivalve populations, on which walruses feed.

Commercial shipping. Commercial shipping is increasing across the Arctic, especially through the Northern Sea Route as sea ice reductions have taken place. Associated with this increased activity is increasing noise and concerns about shipping accidents that might release oil or other contaminants. Most of this traffic within the range of the Pacific walrus has been confined to Russian waters. While no large accidents have been reported, oiled wildlife was found 2012 in the vicinity of St. Lawrence Island, albeit with no identified source. In the North Atlantic, fisheries are thriving, as is the tourist industry, adding to the movement of goods. Ships striking walruses appears to be a minor concern as they are able to avoid large vessels, but the disruption of subsistence hunts has been reported. The International Maritime Organization (IMO) recently adopted the voluntary Polar Code, which provides guidelines for safe operations in the Arctic. In addition, several groups, including the Arctic Council's PAME (Protection of the Arctic Marine Environment) team, are working to identify ecologically significant areas for incorporation into the IMO process and also working to identify sensitive areas for marine protected area planning (e.g. PAME 2015).

Oil and gas exploration/development. Oil and gas exploration in the Chukchi Sea in the range of the Pacific walrus population had a burst of activity starting around 2008, with numerous seismic surveys conducted in the US and Russia. This was followed by exploratory drilling, which occurred in 2012 and 2015 in the US. However, by 2015 several companies with leases in US waters had indefinitely suspended exploratory operations, eliminating this potential stressor for the foreseeable future for this subpopulation. In the North Atlantic, seismic surveys and plans for northward expansion of oil platforms continue. In waters of the Pechora and Kara seas development has already taken place in key walrus habitats in the southern parts of their range (Lydersen et al. 2012), with little or no impact assessment work related to marine mammals preceding development. These activities are deemed to be "highly hazardous" to walruses in the southeastern Barents Sea (Boltunov et al. 2010) and are likely to be a threat to this benthic feeding pinniped throughout its range if development is not well-managed.

Disease and contaminants. Increased disease risks associated with climate change have no direct elements that are specific to walruses. Instead, the risk is associated with the impact increased contact with temperate species might have on all of the ice-affiliated marine mammals that have lived in cold environments, with few disease vectors during recent evolutionary time frames (Altizer et al. 2013). Similarly, contaminants risks are likely to be associated with increased risks due to multiple stressors, rather than the actual contaminant burdens in walruses, given their generally low trophic feeding position in food webs (Robarts et al. 2009). However, possible trends toward increased seal predation by walruses (see Seymour et al. 2014) could dramatically alter the situation regarding contaminants exposure (Wolkers et al. 2006).

Walrus Harvesting and Management

Hunting has been the major source of mortality driving walrus population dynamics and distribution for the Atlantic and Pacific subspecies in the past (Garlich-Miller et al. 2006, Stewart et al. 2014b). The US Fish and Wildlife Service predicted a few years ago that sea ice losses

would eventually result in a Pacific walrus population decline and that the subsistence harvests of some 4,000-5,000 animals per year would become unsustainable. However, sea ice losses/conditions have restricted the ability of Alaskan hunters to harvest walruses, due to a variety of factors. Consequently, the US walrus harvest has declined to less than 1,400 animals per year in 2013 and 2014. Canadian hunts are on the order of only a few hundred animals per year over the last decade due to declining community dependence on this species. Greenlandic hunters have taken a few hundred walruses annually (range 121-404 in the last decade); quotas have recently been established in Greenland to attempt to achieve sustainable harvest levels (Wiig et al. 2014). The Russian harvest of Pacific walruses is the largest hunt currently, with approximately 1,800 and 1,500 animals harvested in 2013 and 2014, respectively (see Shadbolt et al. 2014 for summary statistics and sources). Although this level of harvesting is thought to be sustainable currently, there are concerns that if climate change induced alterations to the environment/ecosystem continue that this level of harvesting could pose a threat to Pacific walruses (USFWS 2011).

Accurate reporting of harvests, including struck and lost rates, as well as updated population estimates are essential tools for proper management of walruses given the additional risks faced by this species at this time related to climate change and concomitant ecosystem changes. Accurate assessment of risk is also dependent on an increased understanding of the effects that climate change is actually having on walruses. After all, climate change-driven alteration of the environment, caused by high levels of greenhouse gas emissions, is thought to be the ultimate driver of changes that will determine the future abundance of walruses. Mitigation via protection of terrestrial haul-out sites and other stressors are also likely going to be important conservation tools within the adaptive management system that will be required to sustain viable populations of this charismatic arctic endemic species.

References

Altizer, S., R. S. Ostfeld, P. T. J. Johnson, S. Kutz, and C. D. Harvell, 2013: Climate change and infectious diseases: from evidence to a predictive framework. *Science*, 341, 514-9.

AMAP, 2013: Arctic Ocean Acidification Assessment: Summary for Policy Makers. AMAP, Oslo, Norway.

Beszczynska-Möller, A., E. Fahrbach, U. Schauer, and E. Hansen, 2012: Variability in Atlantic water temperature and transport at the entrance to the Arctic Ocean, 1997-2010. *ICES J. Mar. Sci.*, doi:10.1093/icesjms/fss056.

Boltunov, A. N., S. E. Belikov, Y.A. Gorbunov, D. T. Menis, and V. S. Semenova, 2010: The Atlantic walrus of the Southeastern Barents Sea and adjacent regions: review of the present-day status. WWF Russia and the Marine Mammal Council, Moscow.

Fay, F. H., 1982: Ecology and Biology of the Pacific Walrus, *Odobenus rosmarus divergens* Illiger. North American Fauna, 74, 1-279.

Fay, F. H. and C. E. Bowlby, 1994: The Harvest of Pacific Walrus, 1931-1989. U. S. Fish and Wildlife Service Technical Report MMM 94-2.

Fay, F. H., B. P. Kelly and J. L. Sease, 1989: Managing the exploitation of Pacific walruses: A tragedy of delayed response and poor communication. *Mar. Mamm. Sci.* 5, 1-16.

Fay, F. H., L. L. Eberhardt, B. P. Kelly, J. J. Burns, and L. T. Quakenbush, 1997: Status of the Pacific walrus population, 1950-1989. *Mar. Mamm. Sci.*, 13, 537-565.

Fischbach, A. S., D. H. Monson, and C. V. Jay. 2009: Enumeration of Pacific walrus carcasses on beaches of the Chukchi Sea in Alaska following a mortality event, September 2009. U. S. Geological Survey Open-File Report 2009-1291.

Freely, F. A., S. C. Doney, and S. R. Cooley, 2009: Ocean acidification: present conditions and future changes in a high-CO_2 world. *Oceanography*, 22, 36-47.

Garlich-Miller, J. L., L. T. Quakenbush, and J. F. Bromaghin, 2006: Trends in age structure and productivity of Pacific walruses harvested in the Bering Strait region of Alaska, 1952-2002. *Mar. Mamm. Sci.*, 22, 880-896.

Garlich-Miller, J. L., J. G. MacCracken, J. Snyder, J. M. Wilder, M. Myers, E. Lance, and A. Matz, 2011: Status review of the Pacific walrus (*Odobenus rosmarus divergens*). U.S. Fish and Wildlife Service, Anchorage, Alaska, USA.

Gjertz, I., Ø. Wiig, and N. A. Øritsland, 1998: Backcalculation of original population size for walruses Odobenus rosmarus in Franz Josef Land. *Wildl. Biol.*, 4, 223-229.

Gilg, O., K. M. Kovacs, J. Aars, J. Fort, G. Gauthier, D. Gramillet, R. A. Ims, H. Meltofte, J. Moreau, E. Post, N. M. Schmidt, G. Yannic, and L. Bollache, 2012: Climate change and the ecology and evolution of Arctic vertebrates. *Ann. N. Y. Acad. Sci.*, 1249, 166-190.

Grebmeier, J. M., S. E. Moore, J. E. Overland, E. E. Frey, and R. Gradinger, 2010: Biological response to recent Pacific Arctic sea ice retreats. *EOS Trans. Am. Geophys. Union*, 91, No. 18, 4.

Hills, S., and J. R. Gilbert, 1994: Detecting Pacific walrus population trends with aerial surveys. *Trans. 59th N. Am. Wild. Natur. Resources Conf.*, 59, 201-210.

Hoffman, R. J., 1995: The changing focus of marine mammal conservation. *TREE*, 10: 462-465.

Huntington, H.P., 2009: A preliminary assessment of threats to arctic marine mammals and their conservation in the coming decades. *Marine Policy*, 33, 77-82.

Jay, C. V., and A. S. Fischbach, 2008: Pacific walruses response to Arctic sea ice losses. U. S. Geological Survey Fact Sheet 2008-3041.

Jay, C. V., B. G. Marcot, and D. C. Douglas, 2011: Projected status of the Pacific walrus (*Odobenus rosmarus divergens*) in the twenty-first century. *Polar Biol.*, 34, 1065-1084.

Jay, C. V., A. S. Fischbach, and A. A. Kochnev, 2012: Walrus areas of use in the Chukchi Sea during sparse sea ice cover. *Mar. Ecol. Prog. Ser.*, 468, 1-13.

Kovacs, K. M., S. Moore, J. E. Overland, and C. Lydersen, 2011: Impacts of changing sea-ice conditions on Arctic marine mammals. *Mar. Biodiv.*, 41, 181-194.

Kovacs, K. M., A. Aguilar, D. Aurioles, V. Burkanov, C. Campagna, N. Gales, T. Gelatt, S. Goldsworthy, S. J. Goodman, G. J. G. Hofmeyr, T. Härkönen, L. Lowry, C. Lydersen, J.

Schipper, T. Sipilä, C. Southwell, S. Stuart, D. Thompson, and F. Trillmich, 2012: Global threats to pinnipeds. *Mar. Mamm. Sci.*, 28, 414-436.

Kovacs, K. M., J. Aars, and C. Lydersen, 2014: Walruses recovering after 60+ years of protection at Svalbard, Norway. *Polar Res.*, 33, 26034.

Laidre, K. L., I. Stirling, L. Lowry, Ø. Wiig, M. P. Heide-Jørgensen, and S. Ferguson, 2008: Quantifying the sensitivity of arctic marine mammals to climate-induced habitat change. *Ecol. Appl.* 18, S97-S125.

Laidre, K. L., H. Stern, K. M. Kovacs, L. Lowry, S. E. Moore, E. V. Regehr, S. H. Ferguson, Ø. Wiig, P. Boveng, R. P. Angliss, E. W. Born, D. Litovka, L. Quakenbush, C. Lydersen, D. Vongraven, and F. Ugarte, 2015: Arctic marine mammal population status, sea ice habitat loss, and conservation recommendations for the 21st century. *Conserv. Biol.*, 29, 724-737.

Lindqvist, C., L. Bachmann, L. W. Andersen, E. W. Born, U. Arnason, K. M. Kovacs, C. Lydersen, A. V. Abramov, and Ø. Wiig, 2008: The Laptev Sea walrus *Odobenus rosmarus laptevi*: an enigma revisited. *Zool. Scripta*, 38, 113-127.

Lydersen, C., J. Aars, and K. M. Kovacs, 2008: Estimating the number of walruses in Svalbard from aerial surveys and behavioural data from satellite telemetry. *Arctic*, 61, 119-128.

Lydersen, C., V. I. Chernook, D. M. Glazov, I. S. Trukhanova, and K. M. Kovacs, 2012: Aerial survey of Atlantic walruses (*Odobenus rosmarus rosmarus*) in the Pechora Sea, August 2011. *Polar Biol.* 35, 1555-1562.

MacCracken, J. G., 2012: Pacific walrus and climate change: Observation and predictions. *Ecol. Evol.*, 2, 2072-2090.

MacCracken, J. G., J. Garlich-Miller, J. Snyder and R. Meehan. 2013. Bayesian belief network models for species assessments: an example with the Pacific walrus. *Wildl. Soc. Bull.*, 37, 226-235.

MacCracken, J. G., P. R. Lemons III, J. L. Garlich-Miller, and J. A. Snyder, 2014: An index of optimum sustainable population for the Pacific walrus. *Ecol. Indicators*, 43, 36-43.

Mathis, J. T., 2011: The extent and controls on ocean acidification in the western Arctic Ocean and adjacent continental shelf seas. In *Arctic Report Card: Update for 2011*, http://www.arctic.noaa.gov/report11/ocean_acidification.html.

Nordli, Ø., R. Przybylak, A. E. J. Ogilvie, and K. Isaksen. 2014. Long-term temperature trends and variability on Spitsbergen: the extended Svalbard Airport temperature series, 1898-2012. *Polar Res.*, 33, 21349.

PAME, 2015: Arctic Council Arctic Marine Strategic Plan 2015-2015. PAME International Secretariat, Akureyri, Iceland.

Robarts, M. D., J. J. Burns, C. L. Meek, and A. Watson, 2009: Limitations of an optimum sustainable population or potential biological removal approach for conserving marine mammals: Pacific walrus case study. *J. Environ. Manage.*, 91, 57-66.

Seymour, J., L. Horstmann-Dehn, and M. J. Wooler, 2014: Proportion of higher trophic-level prey in the diet of Pacific walruses (*Odobenus rosmarus divergens*). *Polar Biol.*, 37, 941-952.

Shadbolt, T., T. Arnbom, and E. W. T. Cooper, 2014: Hauling out: international trade and management of walrus. TRAFFIC and WWF-Canada, Vancouver, B. C.

Sheffield, G., and J. M. Grebmeier, 2009: Pacific walrus (*Odobenus rosmarus divergens*): differential prey digestion and diet. *Mar. Mamm. Sci.*, 25, 761-777.

Skoglund, E. G., C. Lydersen, O. Grahl-Nielsen, T. Haug, and K. M. Kovacs, 2010: Fatty acid composition of the blubber and dermis of adult male Atlantic walrus (*Odobenus rosmarus rosmarus*) in Svalbard, and their potential prey. *Mar. Biol. Res.*, 6, 239-250.

Stewart, D. B., J. W. Higdon, R. R. Reeves, and R. E. A. Stewart, 2014b: A catch history for Atlantic walruses (*Odobenus rosmarus rosmarus*) in the eastern Canadian Arctic. *NAMMCO Sci. Publ.*, 9, 219-314.

Stewart, R. E. A., K. M. Kovacs, and M. Acquarone, 2014a: Walrus of the North Atlantic. *NAMMCO Sci. Publ.*, 9, 7-12.

Taylor, R. L., and M. S. Udevitz, 2015: Demography of the Pacific walrus (*Odobenus rosmarus divergens*): 1974-2006. *Mar. Mamm. Sci.*, 31, 231-254.

Tynan, C. T., and D. P. DeMaster, 1997: Observation sand predictions of Arctic climate change: potential effects on marine mammals. *Arctic*, 50, 308-322.

Udevitz, M. S., R. L., Taylor, J. L. Garlich-Miller, L .T. Quakenbush, and J. A. Snyder, 2012: Potential population level effects of increased haulout-related mortality of Pacific walrus calves. *Polar Biol.*, 36, 291-298.

USFWS (United States Fish and Wildlife Service), 2011: Endangered and threatened wildlife and plants; 12-month finding on a petition to list the Pacific walrus as endangered or threatened. *Federal Register (U. S. A.)*, 76, 7634-7679.

Wiig, Ø, E. W. Born, and R. E. A. Stewart, 2014: Management of Atlantic walruses (*Odobenus rosmarus rosmarus*) in the arctic Atlantic. *NAMMCO Sci. Publ.*, 9, 315-344.

Witting, L., and E. W. Born, 2014: Population dynamics of walruses in Greenland. *NAMMCO Sci. Publ.*, 9, 191-218.

Wolkers, H., B. van Bavel, I. Ericson, E. Skoglund, K. M. Kovacs, and C. Lydersen, 2006: Congener-specific accumulation and patterns of chlorinated and brominated contaminants in adult male walruses from Svalbard, Norway: indications for individual-specific prey selection. *Sci. Total Environ.*, 370, 70-79.

Climate Change is Pushing Boreal Fish Northwards to the Arctic: The Case of the Barents Sea

M. Fossheim[1], R. Primicerio[2], E. Johannesen[1], R. B. Ingvaldsen[1], M. M. Aschan[2], A. V. Dolgov[3]

[1]Institute of Marine Research, Norway
[2]UiT, The Arctic University of Norway, Tromsø, Norway
[3]Knipovich Polar Research Institute of Marine Fisheries and Oceanography, Murmansk, Russia

December 16, 2015

Introduction

The biological impacts of climate change include shifts in population range and distributions, typically poleward (Doney et al. 2012, IPCC 2014). The pace of shifting populations reflects local climate velocities (Pinsky et al. 2013). In the Arctic, where warming is currently twice the global average (Hoegh-Guldberg and Bruno 2010), major shifts in species distribution are occurring (Cheung et al. 2009, Doney et al. 2012). In the marine environment, shifting species have been entering the Arctic Ocean from both the Atlantic Ocean and the Pacific Ocean (Grebmeier et al. 2010, Wassmann et al. 2011). Boreal (warm-water affinity) species of fish have shifted extensively northward into the Arctic domain (Mueter and Litzow 2008, Grebmeier et al. 2006, Rand and Logerwell 2011, Christiansen et al. 2013, Fossheim et al. 2015).

Here we present the case of the Barents Sea, the entrance point to the Arctic Ocean from the Atlantic Ocean. The results are based on a large-scale annual Ecosystem Survey that monitors the whole ice-free shelf of the Barents Sea in August-September, the season with the least sea ice. This cooperative survey between Russia (Knipovich Polar Research Institute of Marine Fisheries and Oceanography) and Norway (Institute of Marine Research) was initiated in 2004. The focus is on observations for the period 2004-2012, as they have been most thoroughly assessed.

The Barents Sea is Warming

In the sub-arctic Barents Sea, the present warming trend started in the late 1990s, with the temperature at the seafloor in late summer increasing by almost 1°C during the last decade alone (**Fig. 10.1b**). Sea surface temperature is also increasing (see **Fig. 5.1c** in the essay on *Sea Surface Temperature*). In addition, the sea ice in this region is retreating and sub-zero water masses in late summer have almost disappeared (**Figs. 10.1a** and **10.1c**).

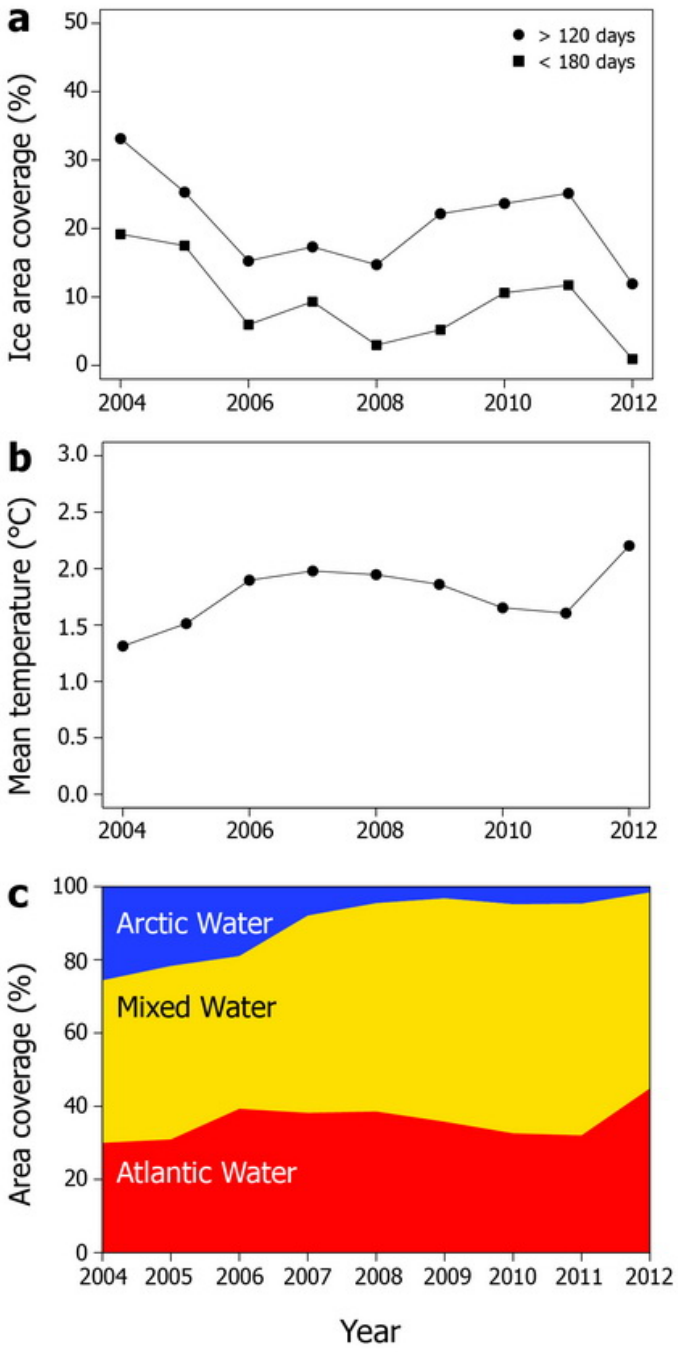

Fig. 10.1. The Barents Sea is a sub-arctic shelf sea bordering the Arctic Ocean. Since 2004 we surveyed bottom hydrography on the entire shelf area in fall, during seasonal minimal ice coverage. (a) Since 2004, sea ice presence (>120 days: circles, upper line; >180 days: squares, lower line) decreased from 33% to 12%, (b) the average bottom temperature of the shelf increased by approximately 1°C and (c) the Arctic water masses (<0°C) nearly disappeared (Atlantic Water (T>2°C, red), mixed water masses (0°C<T<2°C, yellow), and Arctic Water (T<0°C, blue)). (After Fig. S3 in Fossheim et al. 2015.)

Poleward Shift of Fish Communities

In association with the aforementioned warming, boreal (warm-water affinity) fish species, primarily from the southwestern Barents Sea, have entered the northern parts of the Barents Sea in large numbers. The movements of these fish species have led to a shift in communities: boreal communities are now found further north and the local Arctic (cold-water affinity) community has been almost pushed out of the shelf area (**Fig. 10.2**).

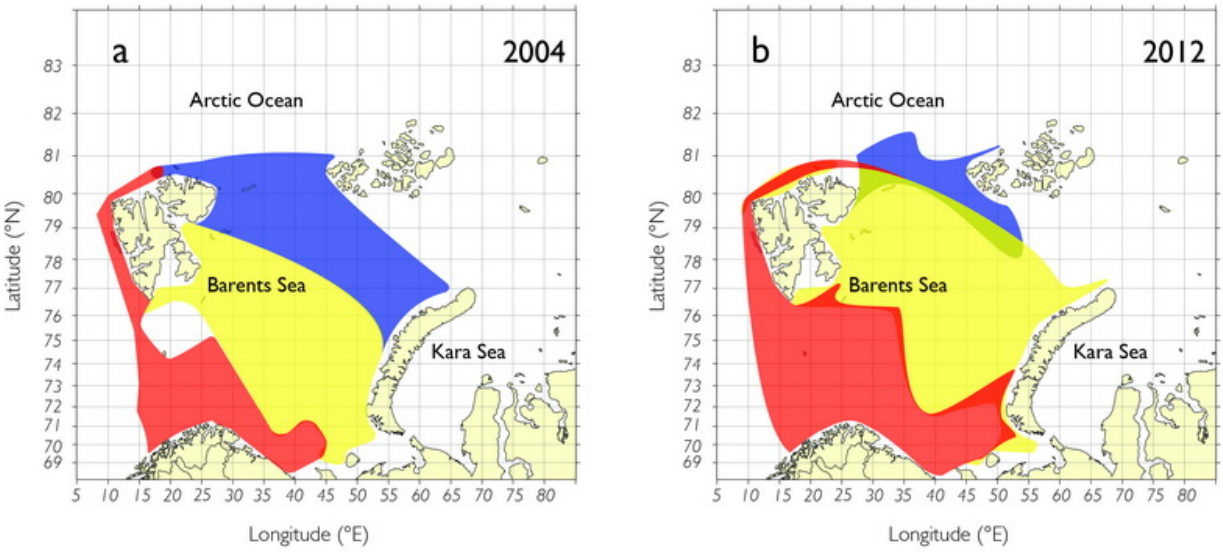

Fig. 10.2. A comparison of the fish communities between the beginning of the Ecosystem Survey taken in the Barents Sea in 2004 (a) and the survey in 2012 (b), indicates a significant change in distribution. The Atlantic (red) and central (yellow) communities (boreal fish species) have shifted north and east, taking over areas previously occupied by the Arctic (blue) community (arctic fish species). Data are available only for the shaded areas. (After Fig. 1 in Fossheim et al. 2015.)

Poleward-moving Fish are Boreal Generalists

Most of the fish species increasing in the north are large boreal fish predators such as cod (*Gadus morhua*), beaked redfish (*Sebastes mentella*) and long rough dab (*Hippoglossoides platessoides*) (**Fig. 10.3**). This is likely related to improved habitat conditions (both water temperature and food availability) for these fish species in the northern Barents Sea (Fossheim et al. 2015). The northward expansion of the thermal habitat for boreal species, increased productivity in a previously ice-covered area (Dalpadado et al. 2014), and increasing abundance and biomass of Atlantic zooplankton in the northern Barents Sea (Dalpadado et al. 2012), likely favour boreal over arctic fish species.

Cod, the main commercially important species, currently has reached a near record high population size (**Table 10.1**) not observed since the 1950s due to a combination of a favourable climate and lower fishing pressure (Kjesbu et al. 2014). Recently, high abundances have also been recorded for haddock (*Melanogrammus aeglefinus*) (**Table 10.1**), the other main commercial species, and for long rough dab, a very common and widespread species in the Barents Sea. A poleward expansion of cod and haddock, and a north-eastward displacement of beaked redfish (*Sebastes mentella*) have been suggested (Hollowed et al. 2013, Renaud et al. 2012) and are confirmed by Fossheim et al. (2015).

Table 10.1. Total Stock Biomass (TSB) and Spawning Stock Biomass (SSB, the total mass of all sexually mature fish in the stock) for cod (*Gadus morhua*) in 2013 and 2015, and SSB for haddock (*Melanogrammus aeglefinus*) in 2015, both in the northern Barents Sea. The 2013 values are the highest since the 1950s.

	TSB 2013 (10^6 tonnes)	TSB 2015 (10^6 tonnes)	SSB 2013 (10^6 tonnes)	SSB 2015 (10^6 tonnes)
Cod	3.590	2.963	1.943	1.139
Haddock	No data	No data	No data	0.769

Consequences for Arctic Fish Species and the Arctic Ecosystem

The Arctic fish community does not seem to cope with rising water temperatures as well as other communities (Fossheim et al. 2015). The Arctic fish community includes species within the families of snailfishes, sculpins and eel pouts (**Fig. 10.3**). Most arctic fish species are relatively small, stationary and benthivorous (i.e. feeding on benthic organisms living on or in the sediments). A shift in main energy pathways from benthic to pelagic habitats associated with sea ice retreat has been predicted for arctic shallow seas (Wassman et al. 2006, Cochrane et al. 2009), which would have a negative effect on arctic benthivore fish species. As arctic fish species have a more specialized diet (Planque et al. 2014, Kortsch et al. 2015), they are more vulnerable to climate change (Kortsch et al. 2015). In addition, these species are adapted to life on the shallow shelf of the Barents Sea. Since the central Arctic Ocean is much deeper, it is unlikely that these species will move further north. However, they can be found further to the east on the shelf (e.g., Kara Sea).

Large fish and marine mammals can move reasonably quickly over large distances, while other species, such as small arctic fish species and organisms that live on or near the seafloor, are more connected to one place. As a result, two previously separate communities are now mixing together (Fossheim et al. 2015). The larger fish species from the south will compete with the smaller arctic species for food, and even feed directly on these smaller fish species. Thus, the Arctic community is being pressured from two sides; the marine environment is changing as a result of the rising water temperature and new competitors and predators are arriving. It is anticipated that this could result in the local extinction of some arctic fish species, such as the gelatinous snailfish (*Liparis fabricii*) and even the most abundant arctic species, the Polar cod (*Boreogadus saida*), from the northern Barents Sea.

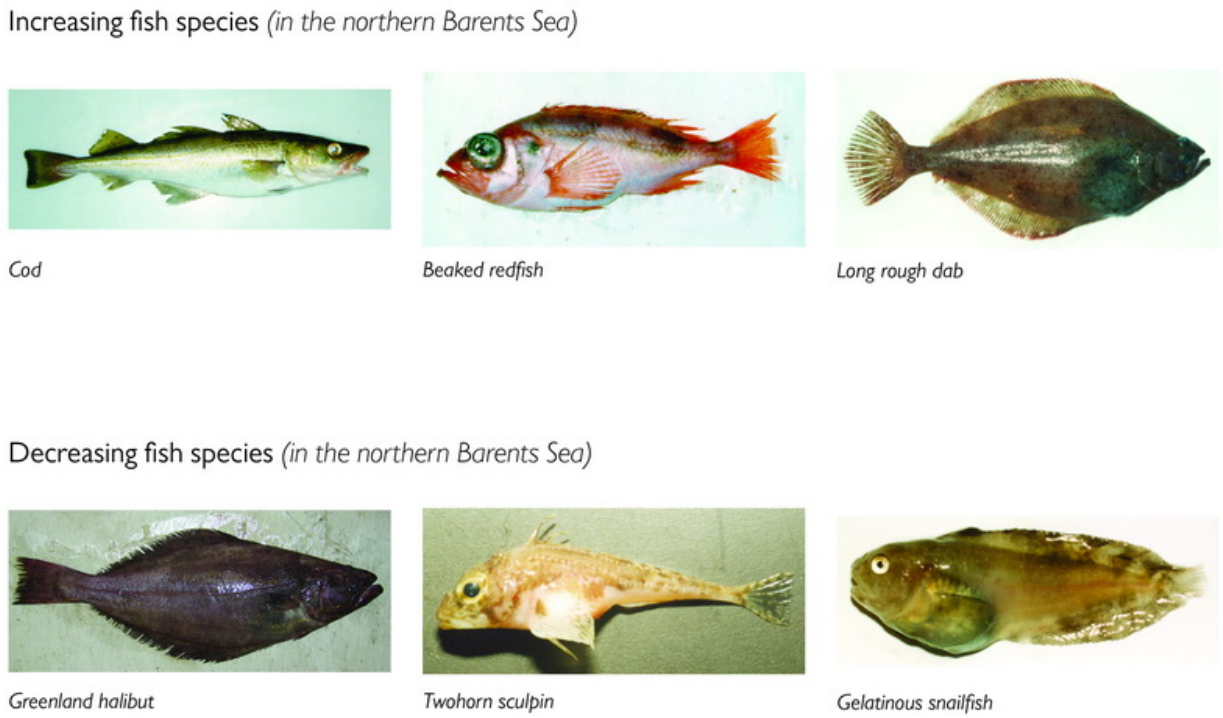

Fig. 10.3. In the northern Barents Sea, typical boreal species (cod - *Gadus morhua*, beaked redfish - *Sebastes mentella*, long rough dab - *Hippoglossoides platessoides*) increased in abundance from 2004 to 2012, while fish species with a more northern affinity or arctic species (Greenland halibut - *Reinhardtius hippoglossoides*; sculpins - e.g., *Icelus bicornis*; snailfishes - e.g., *Liparis fabricii*) displayed a lower mean abundance (Fossheim et al. 2015). All photographs by A. Dolgov.

As a consequence of the large boreal fish generalists moving north, many novel feeding links are established between incoming and resident species. Consequently, species in the Arctic community become more tightly connected and are no longer clearly separated into distinct food web compartments. In a more connected Arctic food web transfer of energy is faster and benthic and pelagic compartments are more tightly coupled (Kortsch et al. 2015).

References

Cheung, W. W. L., V. W. Y. Lam, J. L. Sarmiento, K. Kearney, R. Watson, and D. Pauly, 2009: Projecting global marine biodiversity impacts under climate change scenarios. *Fish. Fisheries*, 10, 235-251.

Christiansen, J. S., C. W. Mecklenburg, and O. V. Karamushko, 2013: Arctic marine fishes and fisheries in light of global change. *Glob. Change Biol.*, 20, 352-359.

Cochrane, S. K. J., S. G. Denisenko, P. E. Renaud, C. S. Emblow, W. G. Ambrose Jr., I. H. Ellingsen, and J. Skarðhamar, 2009: Benthic macrofauna and productivity regimes in the Barents Sea - Ecological implications in a changing Arctic. *J. Sea Res.*, 61, 222-233.

Dalpadado, P., R. B. Ingvaldsen, L. C. Stige, B. Bogstad, T. Knutsen, G. Ottersen, and B. Ellertsen, 2012: Climate effects on Barents Sea ecosystem dynamics. *ICES J. Mar. Sci.*, 69, 1303-1316.

Dalpadado, P., K. R. Arrigo, S. S. Hjøllo, F. Rey, R. B. Ingvaldsen, E. Sperfeld, G. L. van Dijken, L. C. Stige, A. Olsen, and G. Ottersen, 2014: Productivity in the Barents Sea - Response to recent climate variability. *PLoS ONE*, 9, e95273. doi:10.1371/journal.pone.0095273.

Doney, S. C., M. Ruckelshaus, J. E. Duffy, J. P. Barry, F. Chan, C. A. English, H. M. Galindo, J. M. Grebmeier, A. B. Hollowed, N. Knowlton, J. Polovina, N. N. Rabalais, W. J. Sydeman, and L. D. Talley, 2012: Climate change impacts on marine ecosystems. *Ann. Rev. Mar. Sci.*, 4, 11-37.

Fossheim, M., R. Primicerio, E. Johannesen, R. B. Ingvaldsen, M. M. Aschan, and A. V. Dolgov, 2015: Recent warming leads to a rapid borealization of fish communities in the Arctic. *Nature Clim. Change*, 5, 673-678.

Grebmeier, J. M., J. E. Overland, S. E. Moore, E. V. Farley, E. C. Carmack, L. W. Cooper, K. E. Frey, J. H. Helle, F. A. McLaughlin, and S. L. McNutt, 2006: A major ecosystem shift in the northern Bering Sea. *Science*, 311, 1461-1464.

Grebmeier, J. M., S. E. Moore, J. E. Overland, K. E. Frey, and R. Gradinger, 2010: Biological response to recent pacific Arctic sea ice retreats. *Eos*, 91, 161-163.

Hoegh-Guldberg, O., and J. F. Bruno, 2010: The impact of climate change on the world's marine ecosystems. *Science*, 328, 1523-1528.

Hollowed, A. B., B. Planque, and H. Loeng, 2013. Potential movement of fish and shellfish stocks from the sub-Arctic to the Arctic Ocean. *Fish. Oceanogr.* 22, 355-370.

ICES, 12 June 2015: Latest Advice (for cod: *Gadus morhua* and haddock: *Melanogrammus aeglefinus* in the Barents Sea ecoregion) [http://www.ices.dk/community/advisory-process/Pages/Latest-advice.aspx].

IPCC, 2014: Summary for policymakers. *Climate Change 2014: Impacts, Adaptation, and Vulnerability*, Field, C.B. et al., eds., Cambridge University Press, 1-32.

Kjesbu, O. S., B. Bogstad, J. A. Devine, H. Gjøsæter, D. Howell, R. B. Ingvaldsen, R. D. M. Nash, and J. E. Skjæraasen, 2014: Synergies between climate and management for Atlantic cod fisheries at high latitudes. *PNAS*, 111, 3478-3483.

Kortsch, S., R. Primicerio, M. Fossheim, A. V. Dolgov, and M. Aschan, 2015: Climate change alters the structure of arctic marine food webs due to poleward shifts of boreal generalists. *Proc. R. Soc. B*, 282, 20151546.

Mueter, F. J., and M. A. Litzow, 2008: Sea ice retreat alters the biogeography of the Bering Sea continental shelf. *Ecol. Appl.*, 18, 309-320.

Pinsky, M. L., B. Worm, M. J. Fogarty, J. L. Sarmiento, and S. A. Levin, 2013: Marine taxa track local climate velocities. *Science*, 341, 1239-1242.

Planque, B., R. Primicerio, K. Michalsen, M. Aschan, G. Certain, P. Dalpadado, H. Gjøsæter, C. Hansen, E. Johannesen, L. L. Jørgensen, I. Kolsum, S. Kortsch, L. M. Leclerc, L. Omli, M. Skern-Mauritzen, and M. Wiedmann, 2014: Who eats whom in the Barents Sea: a food web topology from plankton to whales. *Ecol. Archives* E095-124.

Rand, K. M., and E. A. Logerwell, 2011: The first demersal trawl survey of benthic fish and invertebrates in the Beaufort Sea since the late 1970s. *Polar Biol.*, 34, 475-488.

Renaud, P. E., J. Berge, Ø. Varpe, O. J. Lønne, J. Nahrgang, C. Ottesen, and I. Hallanger, 2012: Is the poleward expansion by Atlantic cod and haddock threatening native polar cod, *Boreogadus saida*? *Polar Biol.*, 35, 401-412.

Wassmann, P., M. Reigstad, T. Haug, B. Rudels, M. L. Carroll, H. Hop, G. W. Gabrielsen, S. Falk-Petersen, S. G. Denisenko, E. Arashkevich, D. Slagstad, and O. Pavlova, 2006: Food webs and carbon flux in the Barents Sea. *Prog. Oceanog.*, 71, 232-287.

Wassmann, P., C. M. Duarte, S. Agusti, and M. K. Sejr, 2011: Footprints of climate change in the Arctic marine ecosystem. *Glob. Change Biol.*, 17, 1235-1249.

Community-based Observing Network Systems for Arctic Change Detection and Response

L. Alessa[1,2,3], A. Kliskey[1,2], D. Forbes[4], D. Atkinson[5], D. Griffith[1], T. Mustonen[6], P. Pulsifer[7]

[1]Center for Resilient Communities, University of Idaho, Moscow, ID, USA
[2]International Arctic Research Center, University of Alaska Fairbanks, Fairbanks, AK, USA
[3]Department of Homeland Security Arctic Domain Awareness Center, Anchorage, AK, USA
[4]Geological Survey of Canada, Natural Resources Canada, Dartmouth, NS, Canada
[5]University of Victoria, Department of Geography, Victoria, BC, Canada
[6]Snowchange Cooperative, Selkie, Finland
[7]National Snow and Ice Data Center, University of Colorado Boulder, Boulder, CO, USA

November 25, 2015

An Anatomy of Community-based Monitoring

Community-based monitoring (CBM) is a broad set of approaches that engage the capacity of community residents in observing and monitoring of a region, e.g., the Arctic (Arctic Council 2015; Johnson et al. 2015). CBM encompasses a continuum of approaches from community-based observing network systems (CBONS), citizen science and observer blogs (**Table 11.1**).

Table 11.1 . Comparison of community based monitoring types (CBONS: community-based observation networks and systems; CBM: community-based monitoring)

	CBONS	Citizen Science	Generic CBM	Observer Blog
Pre-determined variables	Yes	Yes	Yes	No
Observer types	Domain experts	General population	General population	General population
Observers trained - instruments	Yes	Sometimes	Sometimes	No
Observers trained - scientific method	Yes	Sometimes	No	No
Observers trained - QA-QC	Yes	No	Sometimes	No
Standardized intakes	Yes	No	Often	No
Context based application	Yes	No	Sometimes	Sometimes
Systems based approach	Yes	No	Sometimes	Sometimes
Coordinated / networked	Yes	Sometimes	Sometimes	Yes
Interoperable	Yes	Yes	Sometimes	No
Validated	Yes	No	Sometimes	No
Archived	Yes	Yes	Yes	Yes
Quality assured	Yes	No	Sometimes	No

CBONS consist of distributed networks of skilled residents in communities throughout a region who systematically observe and document their environment on a regular basis in the context of hunting, fishing or other livelihood activities (Alessa et al. 2015a). A key feature of CBONS is that data collection protocols and the resulting observing data are quality-assured and quality-controlled (QA-QC).

Citizen science is the engagement of volunteers from the public in the systematic measurement or observation of specified phenomena, typically using physical instrumentation or a standard scientific protocol (Alessa et al. 2015a). Citizen science provides important opportunities for the participation of the general public in scientific data collection leading to valuable educational outcomes. Many citizen science projects attempt to include quality assurance, although in some cases observer bias can be difficult to control.

Observer blogs are online portals that provide a two-way communication mechanism for members of the public to report environmental observations from their local area and to receive reciprocal feedback from the portal manager. Such observer blogs have the benefit of being open conduits for anyone to report observations. Observer blog entries may be vetted by a moderator, but there is little or no QA-QC. Examples of observer blogs include the Local Environment Observer (LEO) Network facilitated by the Alaska Native Tribal Health Consortium, and CitizenSky hosted by the American Association of Variable Star Observers.

CBONS are built on a strategic network of communities where the observations from multiple groups can be scaled up to provide a regional-level perspective and inter-community sharing on, for example, changes in common species or issues. Citizen science projects vary widely in scale and in the nature of the phenomena observed or measured. Some citizen science project efforts may involve a network of individuals or a sampling network of multiple individuals who coordinate observations by their community, although this is a feature of the sampling protocol rather than an explicit effort to network communities or observers. Observer blogs receive observations via an open, self-selected range of individuals leading to the possibility of regional coverage and two-way communication.

Both citizen science and CBONS involve observers who have received some professional development or training in the use of specific equipment. For citizen science this might include training in the use of instrumentation and the application of a measurement or observing protocol. CBONS is based on full partnerships with communities who internally select and support a cohort of specialized observers, i.e., long-term residents whose awareness of the environment and quality of observing is high. In this type of observing network the community is a key driver of the variables to be monitored, complete with co-developed protocols and data protections under their control. Observer blogs are open to any interested individual with access to the portal or social media; training is not necessary.

Each system has its individual strengths and weaknesses (false positives, false negatives, predictive capability, timeliness, relevance to need, costs, etc.), but a diversity of systems (different approaches) can enhance the overall strength of the suite of arctic observing efforts.

Place-based and Local Knowledge

Traditional ecological knowledge (TEK) has been defined as:

> … a systematic way of thinking and knowing that is elaborated and applied to phenomena across biological, physical, cultural and linguistic systems.

> Traditional Knowledge is owned by the holders of that knowledge, often collectively, and is uniquely expressed and transmitted through indigenous languages. It is a body of knowledge generated through cultural practices, lived experiences including extensive and multigenerational observations, lessons and skills. It has been developed and verified over millennia and is still developing in a living process, including knowledge acquired today and in the future, and it is passed on from generation to generation. (Arctic Council 2015)

TEK and its more generic form, traditional local knowledge (TLK), typically refer to Indigenous societies and communities. The counterpart to this type of knowing among multi-generational, though transplanted, people is local knowledge (LK). Collectively these are referred to as place-based local knowledge (PBLK): the cumulative and transmitted knowledge, experience and wisdom of human communities with a long-term attachment to the land and sea (Kliskey et al. 2009). The expression of PBLK through CBM generally, and CBONS more specifically, represents one way in which collective cultural histories enable environmental change to be placed into societal contexts. However, while this form of knowledge is particularly essential in arctic communities, where rapid economic, climatic and technological changes require adaptive responses unique to place, it is critical that it be place, not race, bound.

A Snapshot of Current Networks

The Community-based Observation Network for Adaptation and Security (CONAS) is an example of a long-standing, quality-assured and effective CBONS. CONAS, and its predecessor the Bering Sea Sub Network (BSSN, www.bssn.net), was created in 2007 as a partnership between Arctic indigenous communities and scientists. CONAS, an official project under the Arctic Council's Conservation of Arctic Flora and Fauna (CAFF) program, utilizes distributed human observers as intelligent sensors across the Bering Sea (**Fig. 11.1**) in both Alaska and the Russian Far East to systematically observe and document over 40 factors of Arctic environmental and globalization changes through co-developed surveys and questionnaires (Alessa et al. 2015b; Arctic Council 2015). All observations, ranging from weather to marine traffic, are subject to QA-QC, meaning they are verified, validated and vetted by community and academic practitioners and scientists.

a.

b.

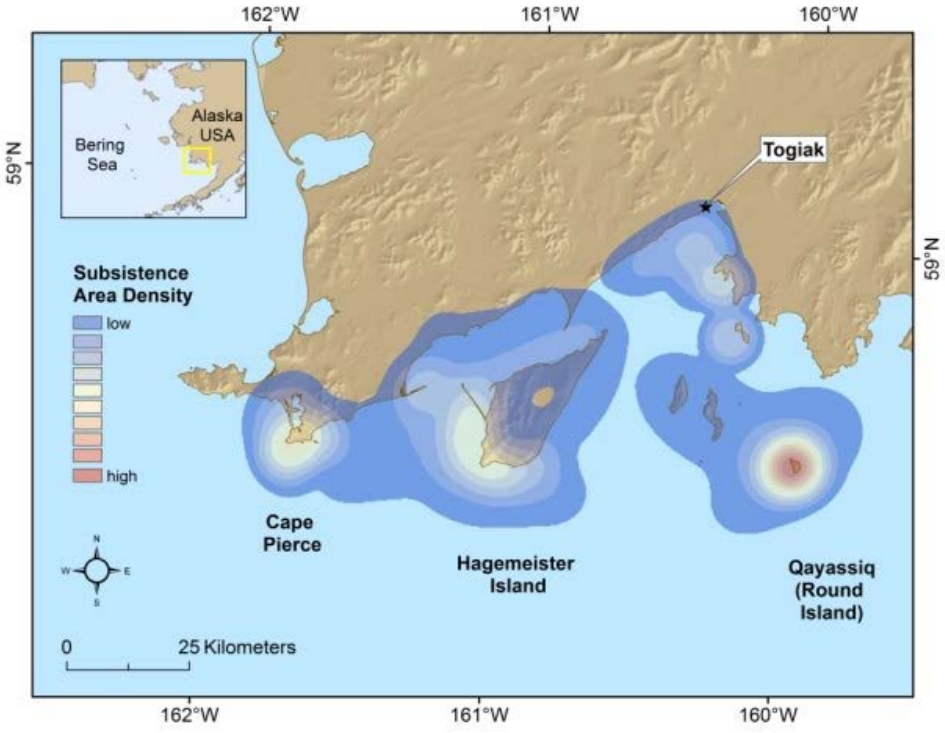

Fig. 11.1. (a, top) Map showing the eight Bering Sea communities that comprise CONAS (Community-based Observing Network for Adaptation and Security), an example of an operational CBON. (b, bottom) Example of community-based observing network data, in this case from CONAS and the village of Togiak, used to support decision-making with respect to walrus habitat.

The Inuvialuit Settlement Region Community-based Monitoring Program (ISR-CBMP) is a CBM effort that supports environmental monitoring linked with Inuvialuit knowledge of Arctic wildlife, environment and biological productivity (Johnson et al. 2015). The objective of ISR-CBMP is to inform and support decisions by resource managers, Inuvialuit organizations and co-management boards.

The Snowchange Cooperative is a network of Saami, Yukaghir and Chukchi communities across Finland, Norway and the Russian North that documents oral history archives of the traditional knowledge, stories, handicraft and fishing and hunting traditions (Roop et al. 2015). The Circumpolar Arctic Coastal Communities Observatory Network (CACCON) is a pan-Arctic network of community-engaged, integrative coastal community observatories with a focus on environmental and social change. These represent a collection of CBM programs, including several CBONS, with pan-Arctic coverage.

Data Management and Interoperability: A Critical Aspect of Community-based Observing

CBONS data range from numerical, quantified values, open-ended interview questions that provide qualitative data, and location surveys that generate geospatially explicit data. To derive an integrated understanding of arctic social-ecological systems, CBONS data need to be synthesized. This, by necessity, requires addressing data interoperability and developing approaches for synthesizing qualitative, quantitative and spatial data (**Fig. 11.2**). To support the co-production of knowledge it is essential to have established data management protocols, e.g., those established by the Exchange for Local Observations and Knowledge of the Arctic (ELOKA: Pulsifer et al. 2014). CBONS data are interoperable with geospatial frameworks such as NOAA's Emergency Response Management Application (ERMA).

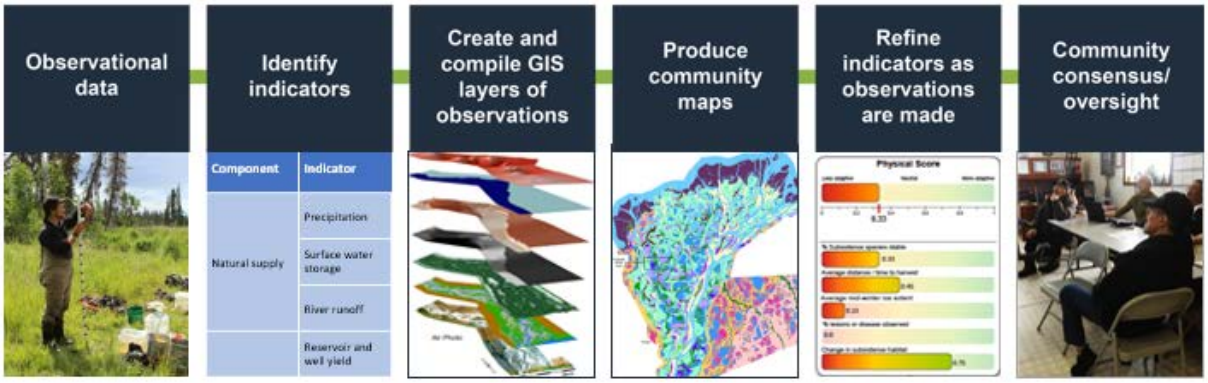

Fig. 11.2. Diagram showing the process of co-development of a community-centered, regional early warning and response system based on interoperable data from community-based observing networks and systems.

The premise for CBONS data is that the network communities, via community research associates (CRAs), in consultation with science and data management members of the network, decide on and approve data sharing protocols. CBONS data management aims to maintain and share observational data, to protect the cultural property rights and confidentiality of participant individuals and communities, and to share metadata, summarized data and raw data (following community approval) with the broader scientific community. Since data are viewed as community-controlled or community-owned this involves a constant balance between maintaining data access and protecting sensitive data. As important is ensuring the integrity of

data and knowledge when they are applied and used in a policy-making or decision-making arena (**Fig. 11.3**); control of and responsibility for ensuring the validity of the interpretation of knowledge needs to be articulated.

Community-based Observing and a Systems Approach for Responding to Change

When considering a framework for responding to change it is necessary to integrate social components, including policies, laws and governance, the biogeophysical components (including the inherent types and rates of change in ecosystems), and the technological components, which include the range of technologies that are both driving socio-environmental change as well as available to respond to them. To do this, there must be systematic observation of change, placement of these observations of change in both a situational and anticipatory context for forecasting critical events, and then targeted preparedness such that response actions can occur quickly with the best likelihood of success (**Figs. 11.2** and **11.3**). CBONS are essential to this systems approach to responding to change.

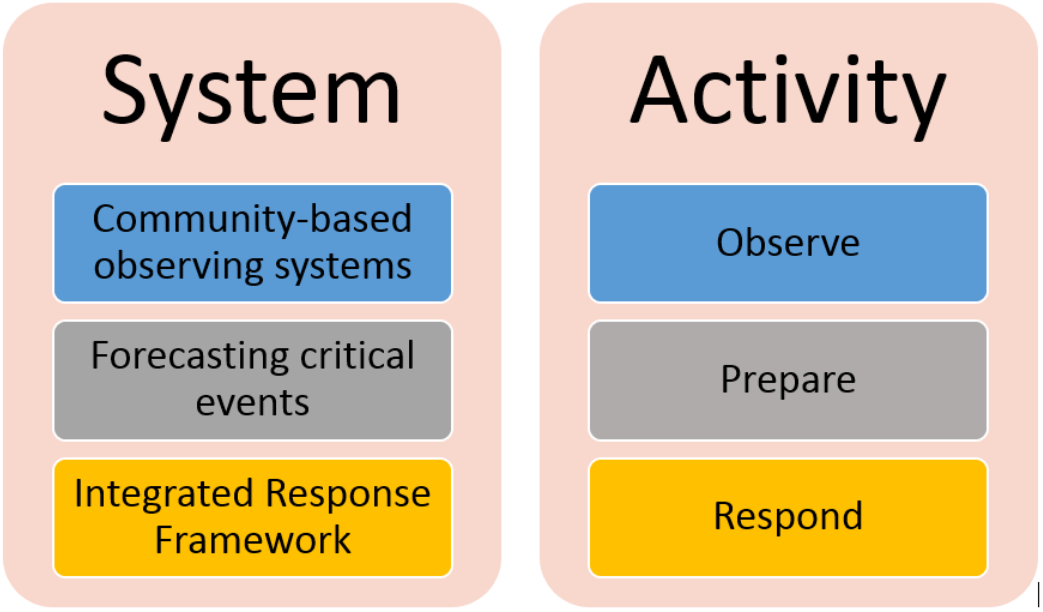

Fig. 11.3. Diagram showing the relationship between observation, preparation, and response activities, in the context of early-warning systems, with corresponding system components for the Arctic: CBONS allow observations to be placed in a situational context; arctic natural and social sciences provide input to the forecasting system, and; an integrated response framework allows targeted preparedness, training and equipment to be mobilized.

Ultimately, CBONS allow observations to be placed in a situational and social context best suited to the locale in which observations, and responses, are made. The vast array of arctic natural and social sciences can provide input to a forecasting system, and an integrated response framework allows targeted preparedness, training and equipment to be mobilized in partnership with responding agencies (Alessa et al. 2015c). Such a framework could better enable local and regional responses around an "Observe-Prepare-Respond" paradigm, ensuring that communities on the ground gain control of not only anticipating change as it happens but also responding successfully to it.

References

Alessa, L., G. Beaujean, L. Bower, I. Campbell, O. Chemenko, M. Copchiak, M. Fidel, U. Fleener, J. Gamble, A. Gundersen, V. Immingan, L. Jackson, A. Kalmakoff, A. Kliskey, S. Merculief, D. Pungowiyi, O. Sutton, E. Ungott, J. Ungott, and J. Veldstr, 2015a: *Bering Sea Sub-Network II: Sharing Knowledge, Improving Understanding, Enabling Response - International community-based environmental observation alliance for a changing Arctic*. Conservation of Arctic Flora and Fauna, 61 pp.

Alessa, L., A. Kliskey, J. Gamble, M. Fidel, G. Beaujean, and J. Gosz, 2015b: The role of Indigenous science and local knowledge in integrated observing systems: Moving toward adaptive capacity indices and early warning systems. *Sustainability Science*. doi: 10.1007/s11625-015-0295-7.

Alessa, L., A. Kliskey, P. Williams and G. Beaujean 2015c: Incorporating Community Based Observing Networks and Systems: Toward a Regional Early Warning System For Enhanced Responses to Marine Arctic Critical Events. *Washington J. Environmental Law and Policy*, in press.

Arctic Council, 2015: Ottawa Traditional Knowledge Principles. Arctic Council NCR#6642168, 3 pp.

CAFF (Conservation of Arctic Flora and Fauna), 2015: Traditional Knowledge and Community-based Monitoring. Conservation of Arctic Flora and Fauna, 4 pp.

Johnson, N., L. Alessa, C. Behe, F. Danielsen, S. Gearhead, V. Gofman, A. Kliskey, E. Krummel, A. Lynch, T. Mustonen, P. Pulsifer, and M. Svoboda, 2015: The contributions of community-based monitoring and traditional knowledge to Arctic observing networks: Reflections on the state of the field. Arctic, 68, doi: http://dx.doi.org/10.14430/arctic4447.

Kliskey, A., L. Alessa, and B. Barr, 2009: Integrating local and traditional ecological knowledge for marine resilience. *Managing for resilience: New directions for marine ecosystem-based management*, K. McLeod and H. Leslie, Eds., Island Press Publishers, 145-161.

Pulsifer, P., H. Huntington, and G. Pecl, 2014: Introduction: local and traditional knowledge and data management in the Arctic. *Polar Geog.*, 37, 1-4, doi: 10.1080/1088937X.2014.894591.

Roop, S., L. Alessa, A. Kliskey, M. Fidel, and G. Beaujean, 2015: "We didn't cross the border; the border crossed us": Informal Social Adaptations to Formal Governance and Policies by Communities across the Bering Sea Region in the Russian Far East and United States. *Washington J. Environmental Law and Policy*, 5, 69-96.

Greenland Ice Sheet Surface Velocity: New Data Sets

T. Moon[1], I. Joughin[2]

[1]Department of Geological Sciences, University of Oregon, Eugene, OR, USA
[2]Polar Science Center, Applied Physics Laboratory, University of Washington, Seattle, WA, USA

November 17, 2015

Ice loss from the Greenland Ice Sheet (see **Fig. 3.4** in the essay on the *Greenland Ice Sheet*) is a principal source of sea level rise. During 2009-2012, the Greenland Ice Sheet lost ~380 Gt of ice per year, contributing ~1.05 mm yr^{-1} to sea level rise (Enderlin et al. 2014), compared with a global mean sea level rise of ~3.2 mm yr^{-1} during 1993-2010 (IPCC 2013). Ice loss occurs through two primary processes: (1) surface melt and runoff from across the ice sheet, and (2) calving of icebergs into the ocean from marine-terminating outlet glaciers. The rate and magnitude of discharge of icebergs is determined by glacier ice thickness and velocity. Here, we review the most current results on annual ice surface velocities for fast-flowing Greenland glaciers, and highlight several additional new and updated datasets that provide velocity measurements at higher resolution time scales (roughly seasonal) or provide supporting data valuable for studying ice sheet mass changes. All datasets discussed are currently or will be available shortly through the NASA Making Earth System Data Records for Use in Research Environments (MEaSUREs) project or the Greenland Mapping Project (GIMP), hosted at the National Snow and Ice Data Center (NSIDC).

For this review of marine-terminating glacier velocity observations (see also the essay on the *Greenland Ice Sheet*), we focus on glaciers on the west and southeast coasts of Greenland. These regions have shown significant, and sometimes rapid, changes in ice velocity and associated mass loss in the past (Moon et al. 2012). We use interferometric synthetic aperture radar (InSAR) and speckle tracking techniques to measure ice sheet surface velocity from SAR data, acquired via the RADARSAT-1, ALOS and TerraSAR-X satellites (Joughin et al. 2010). With these measurements we have created annual ice-sheet-wide winter velocity maps for 2000-2001 and 2005-2006 through 2009-2010. In 2009, improved satellite coverage began to support increased sampling rates (weekly to seasonal), allowing study of seasonal as well as annual and multi-year velocity changes. We use winter (November through February) data to review the long-term and most recent annual velocity variations. While seasonal changes in glacier velocity do occur across Greenland (Moon et al. 2014), regular sampling during winter is considered a good indicator of the longer-term velocity trend.

Starting with short-term changes, **Fig. 12.1** shows the velocity difference between winter 2013-2014 and winter 2012-2013 for 65 Greenland glaciers. During the year, 23 glaciers slowed, but only 14 slowed more than 50 m yr^{-1}, with 3 slowing more than 200 m yr^{-1}. In contrast, the speed of 42 glaciers increased, with 26 speeding up more than 50 m yr^{-1}. The increase in speed of 12 glaciers exceeded 200 m yr^{-1}, with 4 speeding up more than 750 m yr^{-1} during this single year. Despite a few large changes, the speed of most glaciers increased or slowed down by less than 250 m yr^{-1}, roughly similar in magnitude to seasonal velocity changes, with substantial local variability. High local variability in glacier behavior is well documented across Greenland (e.g., Moon et al., 2012), so it is helpful to examine longer-term records as well.

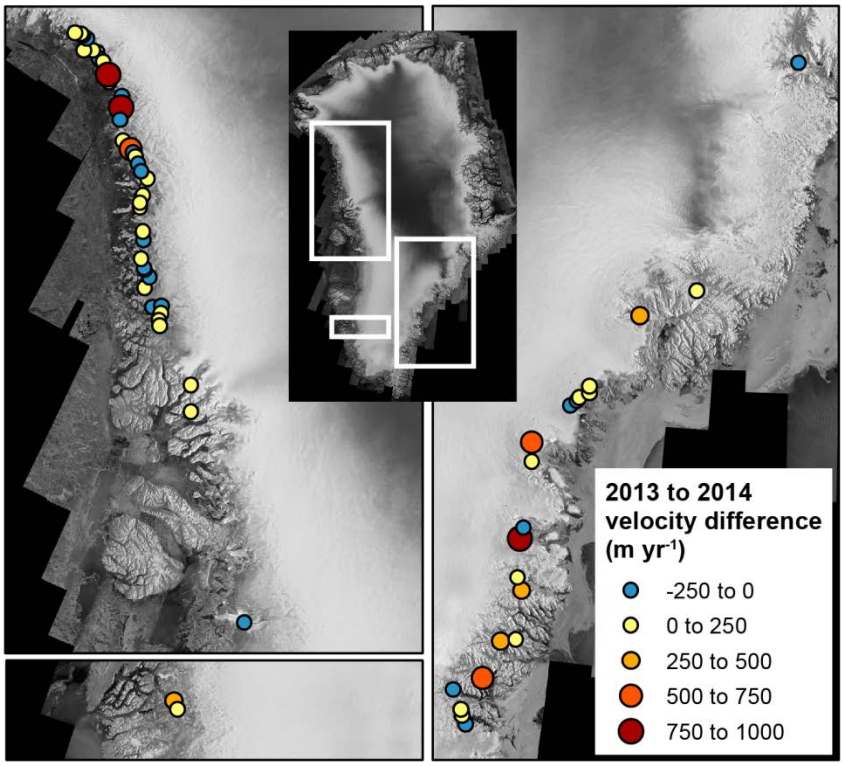

Fig. 12.1. Velocity difference (m yr^{-1}) between winter 2012-2013 and winter 2013-2014 measurements for marine-terminating outlet glaciers along the western and southeastern coasts of the Greenland Ice Sheet. The background image is a 20-m resolution RADARSAT-1 SAR mosaic.

Figure 12.2 uses the full time span of velocity data posted through the NASA MEaSUREs project to show winter velocity differences between 2000-2001 and 2013-2014 for 63 outlet glaciers. Over the 14-year period, 13 glaciers slowed but only 8 slowed more than 100 m yr^{-1}. Increasing speed is much more common, with 50 glaciers speeding up, 45 speeding up >100 m yr^{-1}, and 17 reaching speeds in 2013-2014 that are at least 1,000 m yr^{-1} faster than 2000-2001.

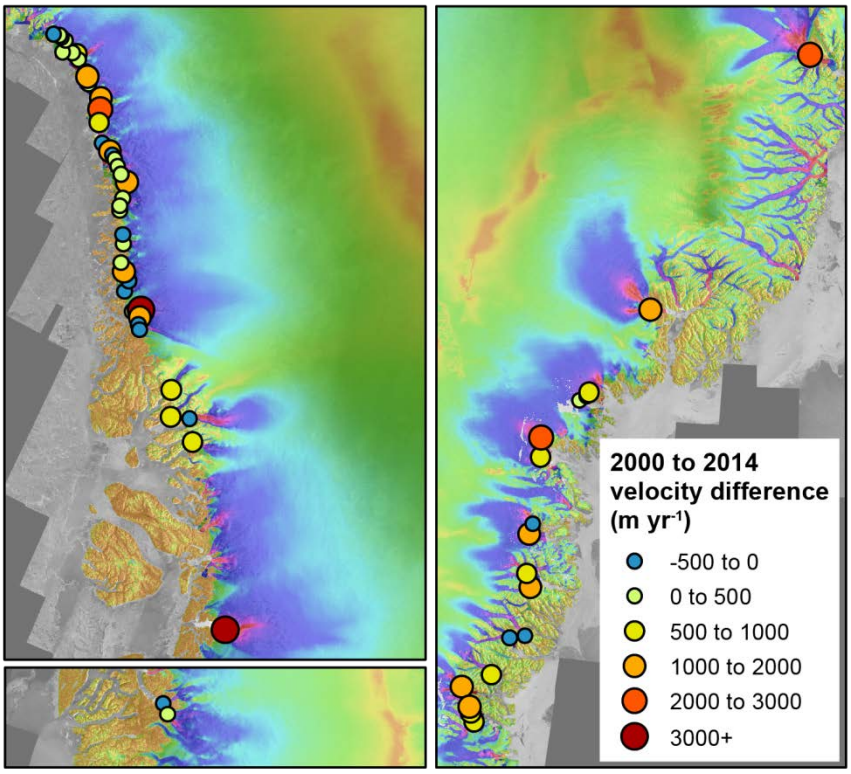

Fig. 12.2. Velocity difference (m yr^{-1}) between winter 2000-2001 and winter 2013-2014 measurements for marine-terminating outlet glaciers along the Greenland Ice Sheet western and southeastern coasts. The background image is a composite velocity map derived from InSAR and speckle tracking measurements using the datasets discussed here.

Both the long- and short-term trends in velocity, showing an overall increase in speed across the ice sheet, are consistent with modeling studies examining the influence of the warming ocean and air temperatures on the Greenland Ice Sheet (Nick et al. 2013). The new glacier terminus position dataset (details about these datasets are included in **Table 12.1**) shows that glacier retreat is widespread (also see the essay on the *Greenland Ice Sheet* here and in previous Arctic Report Cards), and the increase in speed is consistent with glacier retreat into deeper waters. We emphasize, however, that for some glaciers, particularly those that retreat into shallower water, a decrease in speed is an expected response to retreat and may not indicate stabilization, especially if the glacier flows fast enough to discharge mass.

Along with the velocity data highlighted in the results in **Figs. 12.1** and **12. 2**, several related data products are now available or were updated during 2015; they are summarized in **Table 12.1** (dataset also available through NASA MEaSUREs). Updates to these data continue and are posted at NSIDC as soon as they are available.

Table 12.1. New and updated NASA MEaSUREs datasets for the Greenland Ice Sheet.

Data Type	Time Period	Description
Image mosaics	Winters: 2000-2001, 2005-2006 to 2008-09, 2012-2013	Synthetic aperture radar (SAR) image mosaics of the full Greenland Ice Sheet
Glacier terminus positions	Winters: 2000-2001, 2005-2006 to 2009-2010, 2012-2013	Digitized glacier terminus positions created from SAR image mosaics
Annual velocity data	Winters: 2000-2001, 2005-2006 to 2009-2010	Updated ice surface velocity maps derived from SAR data, with near-complete coverage of the Greenland Ice Sheet. This includes the first release of an ALOS velocity map (for 2009-2010).
Weekly to seasonal velocity data	2009-2014	Velocity maps for Greenland outlet glacier areas derived from TerraSAR-X image pairs.
Surface elevation	2007 (including data from 2003-2009)	The Greenland Mapping Project (GIMP) Digital Elevation Model (DEM).

The spatial coverage of the Greenland Ice Sheet MEaSUREs data, along with their extended annual and growing weekly to monthly temporal coverage, provide an unprecedented record of ice sheet motion and its evolution over the last decade and a half. Additional data (elevation, terminus position, image mosaics) deliver critical complimentary records that also support analysis of ice sheet change. Together, these datasets have enabled local characterization of glacier behavior in concert with ice-sheet-wide analysis, supported the first multi-region assessments of seasonal to multiyear velocity change, and provided observational data for full ice sheet modeling. With the data freely available to the scientific community, we can expect their research use and value to continue to grow.

References

Enderlin, E. M., I. M. Howat, S. Jeong, M. J. Noh, J. H. Angelen, and M. R. Broeke, 2014: An Improved Mass Budget for the Greenland Ice Sheet. *Geophys. Res. Lett.*, doi:10.1002/(ISSN)1944-8007.

IPCC, 2013: *Climate Change 2013: The Physical Science Basis. Contribution of Working Group I to the Fifth Assessment Report of the Intergovernmental Panel on Climate Change*. T. F. Stocker et al., Eds. Cambridge University Press, Cambridge, United Kingdom and New York, NY, USA, 1552 pp.

Joughin, I., B. E. Smith, I. M. Howat, T. A. Scambos, and T. Moon, 2010: Greenland flow variability from ice-sheet-wide velocity mapping. *J. Glaciol.*, 56, 415-430.

Moon, T., I. Joughin, B. Smith, and I. Howat, 2012: 21st-Century Evolution of Greenland Outlet Glacier Velocities. *Science,* 336, 576-578, doi:10.1126/science.1219985.

Moon, T., I. Joughin, B. Smith, M. R. van den Broeke, W. J. van de Berg, B. Noël, and M. Usher, 2014: Distinct patterns of seasonal Greenland glacier velocity. *Geophys. Res. Lett.*, 41, 7209-7216, doi:10.1002/2014GL061836.

Nick, F. M., A. Vieli, M. L. Andersen, I. Joughin, A. Payne, T. L. Edwards, F. Pattyn, and R. S. W. van de Wal, 2013: Future sea-level rise from Greenland's main outlet glaciers in a warming climate. *Nature*, 497, 235-238, doi:10.1038/nature12068.